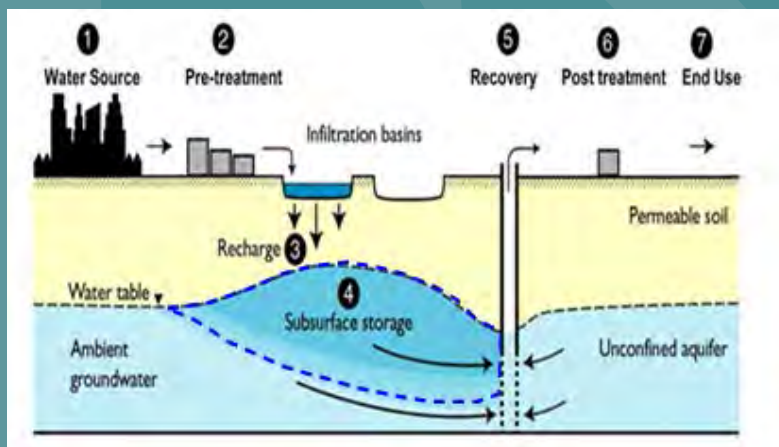**EPA**

United States
Environmental Protection
Agency

Decision Support System for Aquifer Recharge (AR) and Aquifer Storage and Recovery (ASR) Planning, Design, and Evaluation - Principles and Technical Basis

Decision Support System for Aquifer Recharge (AR) and Aquifer Storage and Recovery (ASR) Planning, Design, and Evaluation – Principles and Technical Basis

Prepared By

Y. Jeffrey Yang[1]
Chelsea Neil[2]

and
Jill Neal[1], James A. Goodrich[3], Michelle Simon[1],
Youngshin Jun[4],
Daniel K. Burnell[5], Robert Cohen[5],
Donald Schupp[6], and Rhoda Krishnan[6]

1. U.S.EPA, Office of Research and Development, National Risk Management Research Laboratory, Water Supply and Water Resources Division, 26 West Martin Luther King Drive, Cincinnati, Ohio 45268

2. U.S.EPA, Office of Research and Development, National Risk Management Research Laboratory, ORISE Fellowship Program, 26 West Martin Luther King Drive, Cincinnati, Ohio 45268

3. U.S.EPA, Office of Research and Development, National Homeland Security Research Center, Water Infrastructure Protection Division, 26 West Martin Luther King Drive, Cincinnati, Ohio 45268

4. Washington University in St. Louis, Department of Energy, Environmental and Chemical Engineering, One Brookings Drive, St. Louis, Missouri 6313—4899

5. Tetra Tech Inc., 45610 Woodland Road, Suite 400, Sterling, Virginia 20166

6. CB&I Federal Services LLC, 5050 Section Avenue, Cincinnati, OH 45212

Prepared For

The U.S. Environmental Protection Agency (EPA), through the Office of Research and Development (ORD) National Risk Management Research Laboratory (NRMRL), conducted research and development on aquifer storage and recovery (ASR), a commonly used practice to store water in the subsurface for later recovery and beneficial use. Research and development activities were implemented by ORD technical personnel, contractors, and cooperative organizations. One product of the research is an ASR Decision Support System (DSS) for ASR planning and site evaluation. This report (EPA 600-R-16-222) discusses the research results, and describes the principles and technical basis of the DSS.

The report has been peer-reviewed, and administratively reviewed and approved for publication as an EPA document. It is intended for informational use only. Any opinions contained in the reports are those of the authors, and should not be construed to represent the position of EPA. Mention of trade names or commercial products does not constitute endorsement or recommendation for use of a specific product.

Abstract

Aquifer recharge (AR) is a technical method being utilized to enhance groundwater resources through man-made replenishment means, such as infiltration basins and injections wells. Aquifer storage and recovery (ASR) furthers the AR techniques by withdrawal of stored groundwater at a later time for beneficial use. It is a viable adaptation technique for water availability problems. Variants of the water storage practices include recharge through urban green infrastructure and the subsurface injection of reclaimed water, i.e., wastewater, which has been treated to remove solids and impurities. In addition to a general overview of ASR variations, this report focuses on the principles and technical basis for an ASR decision support system (DSS), with the necessary technical references provided.

The DSS consists of three levels of tools and methods for ASR system planning and assessment, design, and evaluation. Level 1 of the system is focused on ASR feasibility, for which four types of data and technical information are organized around: 1) ASR regulations and permitting needs, 2) Water demand projections, 3) Climate change and water availability, and 4) ASR sites and technical information. These technical resources are integrated to quantify water availability gaps and the feasibility of using ASR to meet the volume and timing of the water resource shortages. A systemic analysis of water resources was conducted for sustainable water supplies in Las Vegas, Nevada for illustration purposes. The Level 2 components of the ASR DSS are intended to support ASR planning and assessment, while the Level 3 components are intended to assist in the design and evaluation. Quantitative tools in the DSS include analytical and numerical models capable of examining four key attributes of an ASR system: 1) ASR-Need in water availability, 2) Hydraulic control and rate of recovery, 3) Contaminant fate and transport, and 4) Geochemical change and arsenic mobilization. The principles and technical basis in each of these areas are described and illustrative examples are provided.

Acknowledgments

Executive Summary

Aquifer storage and recovery (ASR) is a widely used technical method for the storage of water in a groundwater aquifer for later withdrawal and beneficial use. ASR application and sustainability are judged by the rate of recovery, system efficiency, and benign environmental impact. Practices without intentional recovery is generally called as aquifer recharge (AR). Examples include recharge through urban green infrastructure and the subsurface injection of excess water such as treated wastewater (i.e., reclaimed water). Over the past few years, the Safe and Sustainable Water Resources (SSWR) research on ASR practice has focused on developing an ASR decision support system (DSS) for planning and assessment, design, and evaluation. The research results are contained in two reports. This report provides an overview of ASR, AR, and other subsurface activities, with a focus on the ASR technique, its principle, and technical basis. The second report will describe the DSS software and its applications.

The DSS tools and methods are structured in three levels with the goal to facilitate ASR system design and related permitting. Level 1 tools and methods are focused on ASR need and feasibility as they are related to four types of data and technical information: 1) ASR regulations and permitting needs, 2) Water demand projections, 3) Climate change and water availability, and 4) ASR sites and technical information. These technical resources are useful to users in assessing water availability gaps and evaluating whether ASR can be used to address volume shortages or flow imbalances in local water supplies. For illustration, a system-scale analysis in master-planning was conducted for sustainable water supplies in Las Vegas, Nevada. The results are presented in this report.

Levels 2 and 3 of the DSS can be used to assist ASR planning and assessment, design, and evaluation at specific sites. During the planning and assessment, the ASR site characterization and the analysis of water treatment needs prior to injection are two major elements of investigation. The Level 3 analysis consists of engineering design and evaluation, for which detailed hydrogeological and geochemical characterization is conducted, including contaminant mobilization analysis. Together, the analyses are intended to produce technical data necessary to answer the following questions:

- *What is the likely recovery rate of injected water?* This planning question is pertinent for water storage operations that are intended to address temporal or chronic water shortages. Poor recovery rates can also negatively affect the economics of an ASR project.

- *What hydrological changes occur during ASR operation?* Vertical hydraulic conductivity and soil-clogging in the vadose zone are important considerations for ASR operations that utilize spreading basins and soil infiltration. For ASR wells into saturated zones, aquifer permeability and near-well clogging from biological growth and inorganic precipitation are key assessment factors.

- *Can geochemical reactions between the injected water and native groundwater and/or the geological formation deteriorate the groundwater quality?* During ASR operation, the injected water forms a "bubble" by displacing the native water closest to the point of introduction and mixing with native water for some distance away from the injection point. The point at which only native groundwater is present in pore space defines the edge of the injection bubble. The cycle of injection-withdrawal operations will encourage geochemical reactions and, in some cases, mobilize contaminants within the bubble.

- *Given the analysis, what type of site-specific monitoring program should be used to monitor potential water quality changes?* Water quality can be impacted by both geochemical reactions and hydrological changes. The water quality impacts must be monitored to ensure that ASR operation is not endangering the groundwater source.

- *Would treating the water prior to injection decrease or eliminate the likelihood of adverse geochemical interactions at an ASR site?* For example, can the injected water be treated to prevent arsenic mobilization from an aquifer formation where arsenic mobilization may otherwise occur?

Level 1 DSS for ASR Feasibility Analysis

The first level of DSS consists of databases and user inputs for the ASR-Need and feasibility analysis. One database contains state ASR regulations promulgated under the Safe Drinking Water Act (SDWA) and web links to the EPA Underground Injection Control (UIC) program's guidelines in permitting and developing ASR applications. From the DSS database, users can review specific parameter limits of state water quality criteria. Another database contains the location and purpose of application (e.g., aquifer recharge, potable reuse, etc.) of existing ASR sites across the contiguous U.S. This database will help user assess whether the local geological strata at a proposed site are suitable for an ASR operation. Hydrological investigations often aim to determine formation properties and groundwater flow fields under ambient and ASR operation conditions. Spatial distribution of faults and fault networks, along with geotechnical instability at or near the ASR site, are also important considerations. It has been reported that fluid injection in the vicinity of pre-existing faults can trigger seismic activity in the form of local earthquakes (Ellsworth, 2013). In the DSS Level 1 analysis, the site-specific geological and hydrogeological data can be analyzed in the context of other ASR operations in the database. This technical information is organized in a geographic information system (GIS) graphical user interface (GUI), allowing the browsing of existing ASR example sites for reference in the feasibility analysis.

Location-specific ASR-Need analysis also consists of two other components – climate change and water availability, and water demand projections. Factors this analysis includes are precipitation projections using climate change modeling, and projected water demand for socioeconomic development and land use change scenarios. Alternatively, local master planning documents in economic developments, land use zoning, and population projection are the preferred basis for water demand projections. Model-generated projections can be used when socioeconomic data is not available. Suitable models include the U.S. Census Bureau's projection of population changes, EPA's Integrated Climate and Land-Use Scenarios (ICLUS) projections, and the Cellular Automata (CA) – Markov land use model projections. The land use projection methods were systematically reviewed in the *National Water Infrastructure Adaptation Assessment, Part II: Characterize Climatic Change and Impacts for Water Adaptation Planning and Engineering* (U.S. EPA, 2015a).

Projecting climate change for master planning purposes typically involves defining precipitation intensity and variation over a period of at least 30 years. Data collected from an ensemble of global circulation models (GCMs) and downscaled regional climate models (RCMs) are commonly used to project a future climate condition. Due to large uncertainties in the projection for local watershed applications, climate downscaling results are often used and the model is validated against long-range local precipitation data. The U.S. EPA (2015a) report describes the datasets and precipitation projections of climate models for local water resource engineering. The models determined appropriate were included in the ASR DSS.

Estimated water availability gaps and water shortage durations are the essential variables that define ASR needs and scale requirements. This quantitative analysis, which involves of the determination of water availability and water demand at a given location, is often a core component of water resource master planning.

Water resource master planning activities within a municipality are commonly based on water resource inventory and water demand projections alone. The inability of available water resources to provide enough water to meet current or future water demand is referred to as a water availability gap. Gap analysis in master planning determines when and how much water should be stored and used to meet water demands. For many municipalities, the total water management concept can be used in more comprehensive ASR-Need analysis. This analysis includes quantifying the water demand, water availability gap, water reuse, and economics, along with consideration of climate and land use changes, and their impacts on local hydrology and water usage. Equations used in the water budget analysis are provided in Section 3.2.1 and a description of the analysis can be found in Section 3.3.3. A practical example for the Las Vegas water district is described in Section 3.3.

The Las Vegas example

To illustrate the total water management concept, the quantitative water budget gap in an ASR-Need analysis for the Las Vegas metropolitan area were analyzed. The Las Vegas Valley in southern Nevada faces chronic water shortages due to both drought conditions related to climate change and a growing water demand from the increasing population (SWNA, 2009; USGS, 2000). The water level of Lake Mead, the only surface water source for the region, has dropped over 130 feet from 2000 to 2014 in response to seasonal precipitation changes, decreasing snowmelt-derived water flow, water diversions from the Colorado River, and chronic droughts (SWNA, 2015). To reduce the water availability gap in water supplies, the Southern Nevada Water Authority (SWNA) has operated a large ASR facility since 1985. Operation of this "water bank" relies on water from Lake Mead. Water withdrawn from the Lake during high flow periods, such as in the spring when snowmelt occurs, is stored in the aquifer for use during dry seasons.

The total balance between water supply and water demand from 2004 to 2050 was quantified using the methodology adopted in this DSS. By comparing the time-evolution of major fixed fresh water supplies with the total demand estimated using population projections, it was determined that the existing sources supplying the Las Vegas Valley system – Lake Mead and the ASR facility – would provide adequate water supply through the early 2020s. After 2024, the demand will exceed the total amount of water available, and the system will need to find alternative sources of fresh water to meet the future demand. Planning how to address a potential deficit after 2024 can be a challenge. The total water deficit is projected to increase up to nearly 2.46×10^8 m^3 per year by 2050, accounting for a 39% increase in water demand from 9.55×10^8 m^3 per year in 2024 to 1.33×10^9 m^3 per year in 2050. Four options to augment the water supplies were evaluated: 1) Draw water from other groundwater resources in Clark, Lincoln, and White Pine Counties, 2) Transfer groundwater through a massive pipeline from the Great Basin aquifer system about 482.8 km (300 miles) north of Las Vegas, 3) Promote water conservation to reduce the per capita water use by 0.753 m^3 per day by 2035, and 4) As described in this research, increase the volume of water stored through ASR by capturing the reclaimed water returning to Lake Mead and storing more water in Lake Mead during peak flow conditions. Quantitative analysis indicates that the ASR and water reclamation option may increase the long-term water supply resilience for the city.

Level 2 DSS for ASR planning and assessment

The second phase of planning and assessment (Level 2) involves the site characterization and the determination of necessary water treatment and/or conditioning prior to injection or infiltration. For these purposes, less-intensive computational tools are used for the analysis of groundwater flow, contaminant fate and transport, and groundwater geochemistry. Contaminants of interest include both residual contaminants, such as endocrine disrupting compounds (EDC) which may not be removed completely by conventional activated sludge wastewater treatment, and contaminants mobilized through geochemical reactions during ASR operation.

The DSS provides a step-by-step guide to site characterization. Geological data, hydrological data, and site information are gathered to answer three major questions regarding site storage capacity, the fate and transport of residual and mobilized contaminants in injected water, and the mobilization of contaminants from aquifer formation. Mobilized contaminants can include arsenic, uranium, gross alpha, and gross beta, while residual contaminants can include EDCs, nitrosamines and other disinfection by-products (DBPs). Nitrosamines and DBPs are of particular interest because the carcinogenic compounds can form in disinfection of reclaimed water before injection. It is difficult to remove nitrosamines once they are introduced into groundwater aquifers. The site assessment can also be used to determine any treatment requirements for water prior to injection operations. This analysis is focused on two major investigative components: the flow paths of injected water and the geochemical compatibility of injected water with both native groundwater and the storage aquifer formation. Based on analysis results, one can assess the treatment needs and determine the injected water composition that has the least groundwater impact.

Modeling and assessment tools are described in this report. Groundwater flow modeling tools include: 1) Hantush (1967), a 2-D transient groundwater mounding model in an Excel spreadsheet, 2) SuperQ, a 2-D

transient well hydraulics superposition model in an Excel spreadsheet, 3) WhAEM2000 version 3.2.1, a 2-D analytical and semi-numerical model, and 4) A variant Visual AEM released in February 2009. For water quality variation, the quantitative models include: 1) 2-D AT123D-AT mode for fate and transport of residual contaminants in injected water, and 2) Analytical multi-species sequential first-order reaction model over the AT123D-AT codes.

These models yield approximate solutions, but are quick and appropriate in the planning and assessment stage. This analysis relies on simplified model simulations for groundwater systems and ASR operations. Therefore, Level 3 tools are recommended for actual ASR site engineering design and system evaluation.

Level 3 Tools for ASR Design and Evaluation

Level 3 of the DSS is intended for engineering design and evaluation of ASR systems to achieve the planning objectives in both recovery rate and water quality impact control. Technical analysis is necessary to maximize accuracy and precision of the quantitative results for the following three system performance criteria:

- *Residence time of injected water in storage.* Many states, such as Washington, California, Florida, and Hawaii, have established minimum residence times that injected water must spend in groundwater storage to ensure biological safety. The criterion is often specified in an ASR operational permit. The minimum residence time for biological safety is generally determined based on the inactivation rates of pathogens in the aquifer. It is also noted that actual residence time varies among ASR projects. Through the DSS' particle tracking functions, the water residence time can be calculated from simulation results. For aquifer recharge operations with no water recovery, particle tracking provides valuable information for evaluating the long-term recharge performance and location-specific groundwater management objectives.

- *Flow field simulation and evaluation.* The ambient groundwater flow field and its changes during ASR operation are used to assess hydraulic control of the injected volume. Capture zone analysis is often accomplished through modeling of groundwater head distributions and particle tracking. In the DSS, three-dimensional groundwater simulation packages using MODFLOW are recommended.

- *Contaminant fate and transport simulation.* Water quality simulation can help characterize the residual and mobilized contaminant distribution in the injected water and the aquifer to assess groundwater impacts. Customized, site-specific field pilot testing and demonstration, a common engineering practice used for groundwater remediation programs, can be used as the alternative. The transport simulation relies on site-specific hydrological parameters and requires greater precision than the assessment used in the planning phase (Level 2). In such engineering analysis, available tools include semi-analytical models such asWhAEM2000 or VisualAEM, and numerical packages such as MODFLOW or PHAST.

Evaluations of the groundwater chemistry change and contaminant mobilization are assessed stepwise in the DSS. First, the simulation package PHAST is used to assess water chemistry change in the injection "bubble," including the perimeter mixing zones. This investigation may utilize the results from site hydrogeology and groundwater chemistry investigations in the Level 2 analysis. Second, the quantitative data on water chemistry changes are used along with hydrogeological information to evaluate the likelihood of contaminant mobilization and to estimate contaminant concentration distributions under the existing or proposed ASR design and operational options.

Arsenic is one notable contaminant that can be mobilized in groundwater during ASR. The arsenic mobilization evaluation was developed from an extensive literature review and experimental studies on arsenic mobilization. Experimental studies of ASR operation were carried out using reclaimed wastewater and arsenopyrite, a common arsenic-bearing accessory minerals in aquifer materials. Appendix A contains details of the review, experimental investigation, and the technical conclusions. In summary, arsenic mobilization depends on a combination of site hydrology, injected water chemistry, aquifer petrologic composition, and the resulting groundwater geochemistry at an ASR site. The influential factors are: 1) Water chemistry (e.g., pH, Eh, ORP) differences between injected water and native groundwater, 2) Presence of natural organic matter

(NOM), S, microbiota, and nutrients in the injected water that may promote biological activities in the subsurface, and 3) Cyclic operation resulting in groundwater fluctuation and oxygenation in the subsurface.

Table of Contents

List of Tables

List of Figures

Abbreviations/Acronyms

AR	Aquifer Recharge
ASR	Aquifer Storage and Recovery
BLM	Bureau of Land Management
BOD_5	5-day Biological Oxygen Demand
CA	Cellular Automata
CERCLA	Comprehensive Environmental Response, Compensation, and Liability Act of 1980
CFR	Code of Federal Register
CMIP5	Coupled Model Intercomparison Project Phase 5
DOC	Dissolved Organic Carbon
DOM	Dissolved Organic Matter
DSS	Decision Support System
EDC	Endocrine Disrupting Compounds
ENSO	El Nino Southern Oscillation
ET	Evapotranspiration
GCM	Global Circulation Models
GIS	Geographic Information System
GUI	Graphical User Interface
HSPF	Hydrological Simulation Program in Fortran
ICLUS	Integrated Climate and Land Use Scenarios
IPCC	Intergovernmental Panel on Climate Change
NCAR	National Center for Atmospheric Research
NLCD	National Land Cover Dataset
NOM	Natural Organic Matter
NPDES	National Pollution Discharge Elimination System
NRMRL	EPA National Risk Management Research Laboratory
ORP	Oxidation Reduction Potential
ORD	EPA Office of Research and Development
RCRA	Resource Conservation and Recovery Act
RCM	Regional Climate Model
SDWA	Safe Drinking Water Act
SNWA	Southern Nevada Water Authority
TN	Total Nitrogen
TOC	Total Organic Carbon
TP	Total Phosphorus
TSS	Total Suspended Solid
UIC	Underground Injection Control
USBR	U.S. Bureau of Reclamation
USCCSP	United States Climate Change Science Program
USDW	Underground Source of Drinking Water
USEPA	U.S. Environmental Protection Agency
USGCRP	U.S. Global Change Research Program
USGS	U.S. Geological Survey
USHCN	U.S. Historical Climate Network

1.0 Introduction

Aquifer storage and recovery (ASR) is the technological means to enhance natural groundwater recharge through man-made infiltration basins or injection wells for the purpose of recovering the water at a later date. Without the recovering operation, the practice is often referred as aquifer recharge (AR). ASR practices are widely used in the U.S. to improve water availability during droughts and to counter chronic water shortage. Climate change and continuous socioeconomic development are compounding factors that make water availability a pressing challenge in many parts of the country (e.g., Barsugli et al., 2009; Mearns et al., 2009, 2015). One approach to adapt to these challenges is the reuse and storage of water to make up for water volume deficits. This technical method has two essential components: water reuse to expand water availability, and water storage to overcome temporal water budget deficits and imbalances. It is worthy to note, however, that the ASR operation can result in changes in water quality and water chemistry in the injected water and the native groundwater aquifer. Thus, sustainable and effective ASR practice requires management and reduction of negative environmental impacts through proper planning, operation and monitoring.

Currently, ASR with wastewater is being implemented or is under consideration around the world as a means to combat water deficits. In 2002, the total wastewater reuse reached 6.4×10^6 m^3/d (U.S. EPA, 2004), prompting the U.S. EPA (2001, 2004) to publish guidelines for this practice. These developments were summarized in Miller (2006), which articulated the need for an integrated wastewater reuse program to systematically address technological, regulatory and public perception difficulties. As of 2015, ASR operations involving water and wastewater reuse are used in 27 states (Bloetscher, 2015). Elsewhere in the Middle East, North Africa and Southern Europe, Angelakis et al. (1999) evaluated water demand statuses and described the need for wastewater reuse as an unconventional resource. Qadir et al. (2007) further analyzed water demand and supply imbalance in water scarce countries, mostly in the Middle East, and related sustainable wastewater reuse to food security. Such analysis and conclusions about the need for widespread wastewater reuse are echoed in a number of publications (Haruvy, 1998; Angelakis et al., 1999; Thomas and Durham, 2003; Pasch and Macy, 2005; and Khan et al., 2006).

Water availability is also a particular concern as it relates to the impacts of global climate change. The United States Climate Change Science Program (USCCSP) (2001) and the Intergovernmental Panel on Climate Change (IPCC) (2013) provided strong evidence that future climates will be characterized by increased precipitation extremes, leading to increased rainfall and flooding in some areas and prolonged droughts in others. These changes will likely induce water availability stress in many parts of the U.S. and the world. ASR can be implemented to mitigate stress related to this precipitation variability because it allows for the storage of water during periods of increased rainfall for later use during periods of drought.

Adequate water storage capacity is critical to the sustainability of water resource development, and is essential to minimizing the impacts of large changes in water availability and demand. In response, the EPA Office of Research and Development (ORD) has conducted systematic research through the National Risk Management Research Laboratory (NRMRL) to evaluate ASR technical feasibility, regulatory implications, and engineering techniques for field applications. The study covers three areas: 1) Need for ASR to mitigate water budget imbalances, 2) Environmental impacts and potential regulatory implications, and 3) Adaptation techniques and engineering guidelines for sustainable ASR development.

This research has led to the development of a decision support system (DSS) for ASR planning, design, and evaluation. ASR has been widely used in the U.S. and other parts of the world. However,

there are widespread reports of ASR-related water quality concerns and technical challenges in ASR siting, planning, design, and operation, which makes the need for a DSS apparent. The desire for sustainable ASR demands for a systematic investigation into ASR viability and engineering requirements.

This report describes the scientific basis of the ASR DSS. The DSS computer program, software functionality, and application examples will be provided in a separate EPA report and software manual. The report describes the three levels of analysis which will be used to develop ASR. Level 1 tools are focused on ASR feasibility as it pertains to regulations and permitting needs, water demand and availability, and climate change impacts. Level 2 of the DSS can be used to assist ASR planning and assessment to characterize ASR sites and analyze pre-injection water treatment options. Level 3 analysis consists of engineering design and evaluation using detailed hydrogeological and geochemical characterization. This report consists of four main sections to cover these three levels:

1) Section 2.0 describes ASR practice and applications in the U.S., including state regulations and the EPA UIC programs that manage ASR operations;

2) Section 3.0 discusses the factors controlling ASR practice and sustainability. A focus is placed on water availability needs in both quantity and quality, climate change, and socioeconomic factors. This section further introduces the ASR DSS framework in levels of feasibility analysis, planning and assessment, and design and evaluation (Level 1).

3) Section 4.0 describes the theoretical basis and models for ASR planning and assessment (Level 2) along with illustrative examples.

4) Section 5.0 describes the theoretical basis and models for ASR design and evaluation (Level 3) along with illustrative examples.

2.0   ASR Practice and Applications

2.1   ASR Types and General Considerations

2.1.1   *Storage and recovery operation*

Water storage operations in typical hydrological engineering include reservoirs, above-ground storage facilities, and underground ASR operations. Comparatively, ASR is often preferred for large-scale, long-term and economic water storage and recovery. It has been long practiced in the U.S. and other parts of the world such as the Middle East (See U.S. EPA, 2004; Weeks, 2002; Shelef and Azov, 1996). Groundwater injection wells, spreading basins, and infiltration galleries are major mechanisms for water injection into suitable aquifers. Two major types of ASR operations exist, differing based on the type of geological strata into which injection takes place (Figure 1):

- *Injection into a confined aquifer*. In this case, water from secondary sources, such as treated wastewater or collected rainwater, is pre-treated and injected into a confined geological unit. The water can then be recovered from the same well, or designated recovery well(s), and treated for a specific end use. The water piezometric surface changes in accordance with pressure changes induced during injection and withdrawal. Components of this ASR type are shown in Figure 1A.

- *Injection into an unconfined aquifer*. For many applications, water is injected into an unconfined aquifer. Injection through a spreading basin, infiltration basin (or gallery), or well can result in

mounding of the groundwater table under these conditions. These practices are considered AR rather than ASR if there is no recovery component. Components of this ASR type are shown in Figure 1b.

In both cases, injected water occupies an "injection bubble" within the formation. The injected water fills formation voids in the core of an injection bubble and mixes with native groundwater on the periphery. Regional groundwater flow outside of the injection bubble can change both direction and velocity due to ASR injection effects on the hydraulic field.
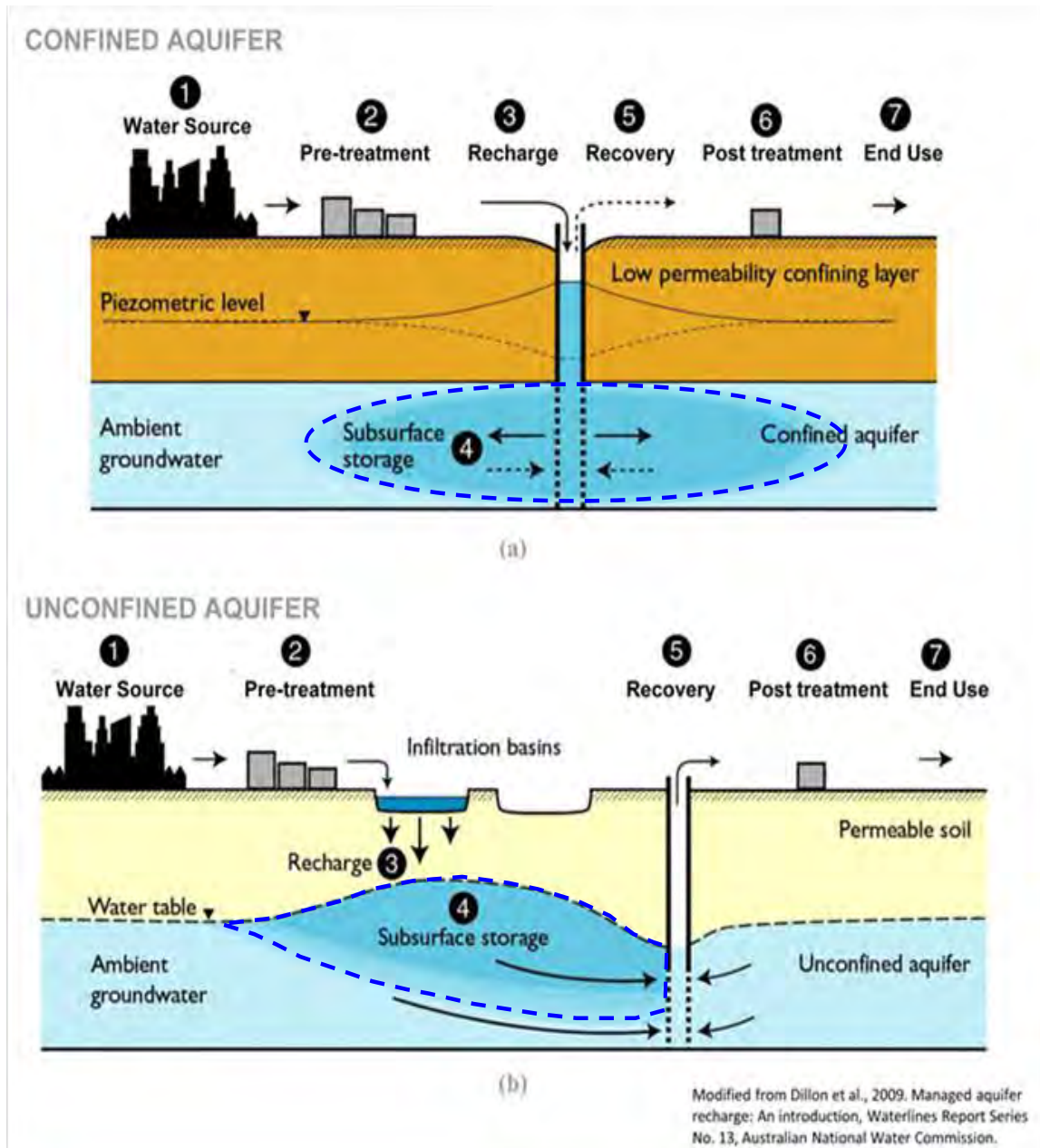
Figure 1   Major types of ASR operations for water storage and reclamation. A) Injection into a confined aquifer; B) Injection into an unconfined aquifer. The dotted blue lines indicate the outer edge of the ASR bubble.

An ASR system consists of components for water injection into the aquifer and components for water recovery. Groundwater injection may utilize several engineering means including injection wells, infiltration basins, and infiltration galleries. The EPA's UIC program regulates AR and ASR injection wells, but not infiltration basins or galleries (U.S. EPA, undated). Infiltration basins, also known as spreading basins, are commonly used such as those by the Water Replenishment District of Southern California.[1] The volume of water stored is maximized by inducing infiltration over a large area. In the case of an infiltration gallery, multiple installations of infiltration media are completed deep in the vadose zone, commonly arranged as linear features in map view. Green infrastructure infiltration systems (e.g., rain gardens, grass swales, and permeable pavements) function in much the same way. However, these systems are not a focus of this report because they cannot be used to inject high enough volumes of water to meet growing water demands, but for the purpose of groundwater replenishment

The groundwater recovery process is relatively straight forward. Recovery wells can be used for both confined and unconfined aquifers. Intercept trenches are also commonly used for shallow unconfined groundwater due to high water yield and economic efficiency. An intercept trench is physically similar to an infiltration gallery, but is trenched into an unconfined aquifer as opposed to being completed in the vadose zone. It is also important that the UIC and drinking water programs coordinate to discuss site specific ASR projects, as there may be special testing and treatment requirements that must be addressed prior to recovering the water for various beneficial uses.

Table 1 shows the potential injection and withdrawal pairs in ASR operations and their objectives. For example, injection and withdrawal in a confined aquifer can be accomplished by a single well in a sequential injection-storage-recovery operation (Figure 1A). Storage and recovery can also be accomplished by using a pair of wells for injection and withdrawal, respectively. Unconfined aquifers have seen more combinations in practice. Depending on combinations of injection-withdrawal system pairs, ASR operations can lead to diverse types of groundwater flow fields and geochemical changes within the injection bubble, where reactions with both aquifer formation minerals and native groundwater may occur.

The difference in AR and ASR operation types is related to the end use purpose (See subsequent Section 2.1.2). They differ in the volume injected, aquifer depth, and injection rate of an operation. For example, most green infrastructure installations are intended to facilitate low-rate infiltration over a large area. Green infrastructure uses vegetation, soils, and other practices to augment the natural processes by promoting water infiltration downward into surficial aquifers, thus reducing overland runoff, enhancing groundwater recharge, and creating healthier urban environments. Other examples of low rate systems include decentralized wastewater treatment operations such as individual household septic tanks and drain fields. By comparison, large water volumes are generated from municipal and industrial wastewater treatment plants. Natural infiltration in green infrastructure installations are typically inefficient in handling the large reclaimed water volumes generated by these operations. Therefore, direct injection into aquifers is the more common solution.

In considering these variations, ASR and AR operations are generalized into four major categories for analysis in this report:

a) *Confined aquifer – Case (a)*. The injection-withdrawal operation is carried out either by a single well or a pair of injection-withdrawal wells (Figure 1A). Injected water forms an injection bubble around the well screen and influences local groundwater flow at the ASR site. The injection bubble core is nearly pure injected water, while mixing occurs at the bubble perimeter. The water residence time

---

[1] http://www.wrd.org/engineering/groundwater-replenishment-spreading-grounds.php

Table 1. Possible ASR operation types for water storage (and recovery).

Water Source	Injection Zone		
	Vadose Zone	Aquifer	Combination*
	Objective	Objective	Objective
Treatment effluent			
Municipal wastewater plants		Reuse	Reuse
Storm water runoff		Reuse	Reuse
Mining water**		Disposal/recharge	
Industrial wastewater		Disposal/recharge	
Green infrastructure			
Permeable pavements	Replenshment		
Rain garden#	Replenshment	Potential recharge	
Green roof / Ciston	Replenshment		Replenshment
Runoff swales, etc.			Replenshment
Decentralized treatment			
Community septic tanks	Replenshment		Reuse
Household dainfield	Replenshment		

Note: * - Operation involves vadose zone and underlying aquifer.

** - Large water volumes generated from mining operations such as hydraulic fracturing.

\# - Rain gardens may or may not have gravel water trenches for deep infiltration.

(average time that injected water spends in storage) and capture zone (region of water extracted by the withdrawal well) are two basic hydraulic planning parameters.

b) *Unconfined aquifer without vadose zone treatment – Case (b)*. This operation is a variation of Case (a). Wells are used for injection and withdrawal, while intercept trenches can be used when the groundwater table is shallow. As for Case (a), the capture zone and residence time are two basic hydraulic planning parameters.

c) *Unconfined aquifer with vadose zone treatment – Case (c)*. As shown in Figure 1B, infiltration water from a spreading basin or infiltration gallery passes through the oxygen-rich vadose zone, where several geochemical processes may occur including soil adsorption, ventilation (i.e., the drawing of air into the space between soil particles), and biodegradation. Water infiltration rate is determined by native soil in the vadose zone. The water is recovered through the use of a withdrawal well or an intercept trench. The basic hydraulic parameters in this case include the infiltration rate through the vadose zone, hydraulic control, and residence time.

d) *Unconfined aquifer with no withdrawal operations (i.e., AR) – Case (d)*. Groundwater recharge comes from infiltration processes (e.g., spreading basins or green infrastructure, such as a green garden or gravel infiltration layer connected to a roof rain water collection system). Case (d) is hydraulically similar to Figure 1B, but with no groundwater withdrawal operations. The basic hydraulic parameters in this case include infiltration rate and receiving aquifer properties (e.g., permeability, porosity, etc.).

2.1.2 Water sources and end use

AR and ASR processes have been applied to store various water sources, including wastewater treatment plant effluent for recycling and reuse, storm water runoff, household and commercial greywater, and reclaimed industrial water such as treated cooling tower blowdown. A previous EPA report (U.S.EPA, 2004) on water reuse describes the characteristics of the various water sources. Major types of AR and ASR applications include:

- *Groundwater storage and recovery for beneficial use (ASR)*. Examples include mitigation of seasonal or chronic water shortages, crop and landscape irrigation, and industrial usage. This end use variation is shown schematically in Figure 2, and involves storing water in an aquifer for later recovery. Understanding the different combinations of water sources and potential reuses can help to identify important aspects related to ASR sustainability and regulatory programs.

- *Groundwater recharge (AR)*. This category of end use includes replenishment of depleted aquifers, augmentation of stream flows through natural aquifer-to-stream discharge, development of a groundwater barrier against salt water intrusion, and long-term storage of excess water such as drilling fluids in mining operations. However, because AR and ASR wells are considered Class V injection wells, in order for this drilling fluid to be injected it must first be proven to not endanger the underground source of drinking water (USDW). Thus, advanced water treatment of injected water is common (Figure 2), in order to protect groundwater sources at an ASR site. Due to this important regulation, pre-injection water treatment and water quality requirements are a focus of this study, and will be discussed in later sections.
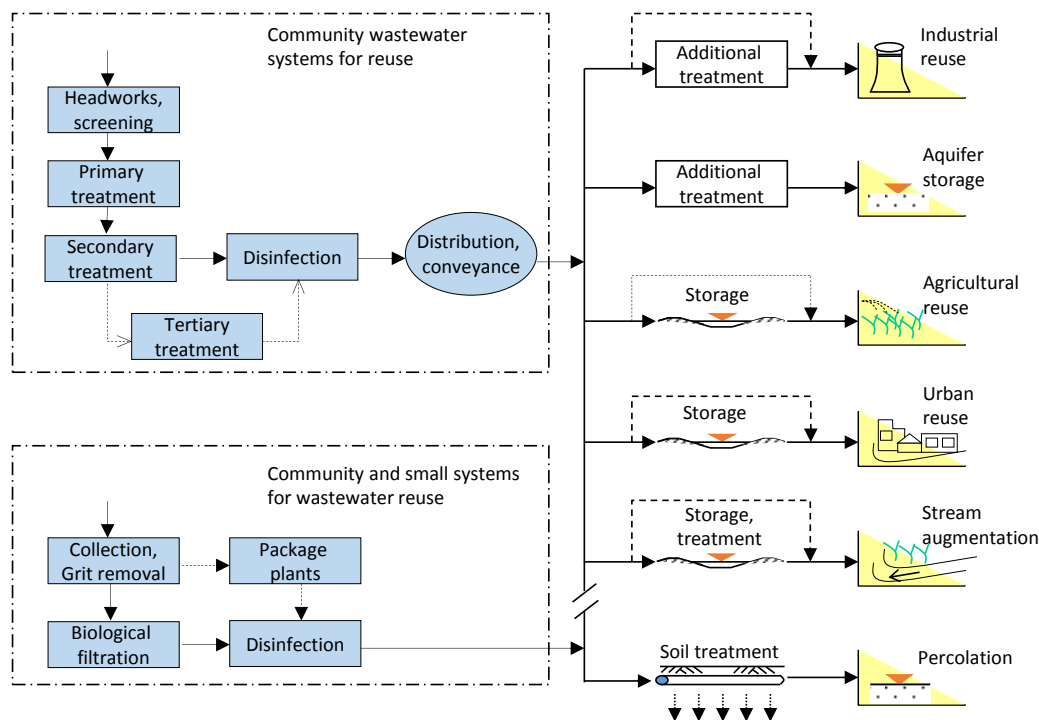
Figure 2   Potential scenarios of municipal wastewater reuse involving in ASR and other types of storage operations. Note the last scenario for percolation is the form of uncontrolled aquifer recharge.

6

- Groundwater recharge by enhanced infiltration (AR). Unlike centralized injection in the above two categories, engineered process units are used to increase infiltration for the purpose of replenishing soil moisture and shallow groundwater. Examples include infiltration basins and infiltration galleries.

Figure 2 shows a variety of end use scenarios for wastewater, a common source of reclaimed water. For many communities, wastewater and storm water are collected and conveyed to a central location for treatment before discharge. Some of these centralized wastewater treatment systems are increasingly engaged in water reuse, including water utilities in California, Texas, and Florida, as well as in other water-stressed regions. Centralized systems in the U.S. are generally equipped with a secondary wastewater treatment system (Figure 2), consisting of head works with screening of large debris, a primary clarifier, activated sludge process and secondary clarifier in secondary treatment, followed by disinfection before discharge under a National Pollution Discharge Elimination System (NPDES) permit. These systems are generally capable of achieving treatment standards. EPA regulations on wastewater treatment effluent commonly include limits on the 5-day biological oxygen demand (BOD_5), N, P, and biological plate counts. Typical standards are 45 mg/L BOD_5, 45 mg/L total suspended solids (TSS), and 400 per 100ml fecal coliform in 7-day averages. Many states have stricter discharge standards particularly on total phosphorus (TP) and total nitrogen (TN). Groundwater standards can also vary by region. For example, the standards that are complied with in Region 8 are background concentrations of natural groundwater above maximum contaminant levels, national drinking water standards and water standards that EPA toxicologists have found to be appropriate for regional conditions.

A tertiary treatment process can be employed in the interest of water reuse safety (Figure 2). The purpose varies; for example, further removal of nitrogen and phosphorus may be necessary to protect sensitive environments in stream augmentation. The reclaimed water is then conveyed to the application site for reuse. Some typical end use types are shown in Figure 2, including direct industrial reuse, agriculture reuse, urban reuse (e.g., landscape irrigation), and stream augmentation. These operations do not require long-term, large-volume storage. Large-volume storage involves the use of storage options such as ASR. This report is only focused on operations involving long-term ASR, uncontrolled aquifer recharge through infiltration, or Case (d) AR operations.

Small-scale wastewater treatment systems are often used for communities and individual households (U.S.EPA, 2004). These systems normally have a limited wastewater treatment capacity; for example, inadequate or no unit process for nitrification and denitrification. As a consequence, micronutrient management in small-system wastewater effluent is often a concern. The challenges for decentralized, small-system management have been well documented in states such as Maryland, Virginia, and other states where septic tank systems are prevalent (Katz et al., 2011). Some additional N and macronutrient removal from small system effluent occurs during infiltration in systems such as drain fields. This type of end use, as in Case (d), recharges local aquifers.

2.1.3 *Water quality changes in ASR processes*

The quality of injected water and native groundwater is subject to change during ASR operation. Figure 3 schematically shows a conceptual model of such changes during a paired injection and recovery ASR operation. In the schematic, a constituent of concern has a concentration C_{WW-GW} in the injected water. Geochemical changes in the vadose zone are accounted for by ΔC_{ST} to become C_{ST} at the groundwater table for ASR operations involving infiltration (Figure 3).

The injected water is mixed with native groundwater, which has a concentration of C_{gw}°. Resulting concentrations in the core and perimeter of the injection bubble are subject to compliance with groundwater standards, $\{C_{GW}^{std}\}$. The injected water enters the aquifer formation at the original concentration C_{WW-GW} when direct injection through a well occurs. Subsequently, the injected water

A.

Effluent → Treatment & Conditioning → $\{C_{WW-GW}\}$

Spreading basin   Infiltration gallery   Monitoring well   Production well   Monitoring well

$\{C_{WW-GW}\}$ ↓↓↓↓

Δh

ΔC_{ST}

Injection well

$\{C_{min}\}\{C_{DW}^{std}\}$

$\{C_{ST}\}$ $\{C_{WW-GW}\}$

$\{C_{gw}^{0}\}$ $\{C_{GW}^{std}\}$ $\{C_{GW}^{std}\}$ $\{C_{GW}^{std}\}$

ΔC_{GW}

$\Delta x\ (\Delta t)$

B.
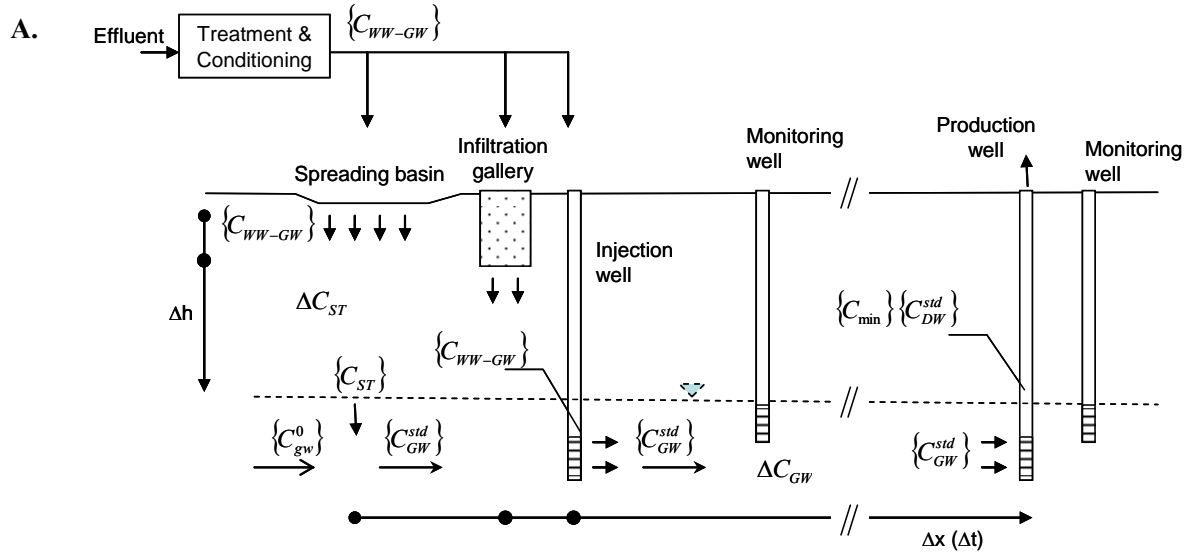
Concentrations		Variable Changes		Standards	
C_{WW-GW}	Injected water concentration	ΔC_{ST}	Change in water concentration due to geochemical interactions in vadose zone	$\{C_{GW}^{std}\}$	Groundwater standard
C_{gw}°	Native groundwater concentration	ΔC_{gw}	Change in water concentration due to mixing with native groundwater and transport to recovery wells	$\{C_{DW}^{std}\}$	Drinking water standard
C_{ST}	Injected water concentration after geochemical changes in vadose zone	Δt	Residence time of injected water in the groundwater	$\{C_{min}\}$	Permit minimum concentration
C_{gw}	Injected water concentration after mixing with native groundwater and transport to recovery wells	Δx	Distance travelled by injected water during its residence time		

Figure 3   (A) Process schematic of flow and water quality changes to consider in ASR design and operation. The dotted line indicates the location of the water table. The end-use water quality requirements are first determined to define the requirement for effluent composition after treatment/conditioning, the soil treatment, ΔC_{ST}, and change in groundwater, ΔC_{GW}. (B) Definitions of variables included in the process schematic.

transports and resides in groundwater for a period of time (Δt). Geochemical changes that occur during transport to recovery (production) wells are accounted for by ΔC_{GW}. The resulting groundwater concentration, C_{gw}, should be in compliance with the groundwater standards, and the water quality in the recovery well is required to meet drinking water standards, $\{C_{DW}^{std}\}$, or a minimal water quality threshold in accordance with the site permit, $\{C_{min}\}$ (Figure 3). The major geochemical processes leading to water quality change include:

1) *Residual contaminants in reclaimed water for ASR operations*. Some recalcitrant contaminants like endocrine disrupting compounds (EDC) may not be removed during conventional activated sludge

treatment processes. As a result, these contaminants can persist in reclaimed water. In many cases, the contaminants can be removed by implementing appropriate treatment processes before injection. The impact of these contaminants on groundwater depends on initial concentrations in the injected water and geochemical processes in the vadose zone and/or in the aquifer formation.

2) *Leaching from vadose zone*. The literature (e.g., Pitt et al., 1999) indicates that contaminant transport can be retarded in the vadose zone during infiltration, resulting in contaminant accumulation in the root zone and/or top soil. When geochemical conditions change, these previously immobilized contaminants, along with contaminants native to the soil, may become mobilized and transported into the underlying groundwater.

3) *Mobilization of multi-valent transition metals from native aquifer formation minerals*. Introduction of oxygen-rich injected water and additional organic matter may change the groundwater conditions; for example, the reduction potential (E_h) of groundwater can increase, i.e. become more oxidative. The change in E_h, and perhaps pH, of groundwater can lead to the oxidation of some native minerals such as arsenic (As)-bearing pyrite and arsenopyrite. Oxidation of these minerals can lead to the release of arsenic and other contaminants into the groundwater. The resulting contaminant concentrations depend on the presence and abundance of native contaminant-bearing minerals, geochemical condition changes, and reaction rates.

These general geochemical processes have been investigated using laboratory soil column studies, field investigations, and computer modeling (Bouwer et al., 1981; Yates and Ouyang, 1992; Westerhoff and Pinney, 2000; Lo et al., 2002; Sen et al., 2005; Scheytt et al., 2006). However, knowledge gaps exist with respect to the geochemical interactions between injected water and native groundwater during ASR operation. This limitation can lead to negative public perception and uncertainty in regulatory oversight (Friedler, 2001; WHO, 2006; and Weber et al., 2006). For example, some studies suggested that most contaminants are removed from injected water in the upper 1-1.5 m of soil (Westhoff and Pinney, 2000; Greskowiak et al., 2005). However, toxic organic contaminants, organic matter, emerging contaminants, inorganic compounds, and pathogens have been observed entering the groundwater during laboratory and field studies (Bouwer et al., 1981; Manka and Rebhun, 1982; Lucho-Constantino et al., 2005; Scheytt et al., 2006).

The inconsistent findings potentially result from varying soil and groundwater conditions, organic carbon content, the contaminant matrix in wastewater effluent, and AR engineering and operations. These variables and engineering factors can affect contaminant adsorption, biological and abiotic degradation, transport in unsaturated and saturated soils, and geochemical conditions in the soil and groundwater, which may promote or suppress re-dissolution of contaminants into the water phase. For this reason, ASR system planning and evaluation may consider the following factors that can affect water quality changes:

▪ *Fate and transport of emerging and recalcitrant contaminants in ASR operations*. Scheytt et al. (2006) described the mobility of pharmaceutical compounds in soil at wastewater reuse sites, and Toze (2004) listed these contaminants along with endocrine disrupting compounds and pathogens as a concern in reuse applications.

▪ *Long-term changes in the receiving aquifers*. Sheng (2005) showed that there had been no substantial impact to the storage characteristics and groundwater quality at El Paso, Texas ASR sites after 20 years of operation. However, significant impacts have been observed at other locations. DeSimone et al (1997) determined that alteration of geochemical properties had occurred due to ASR operation in Cape Cod, MA, where an aquifer of glacial deposits was contaminated with partially treated effluent. ASR impacts have also been observed in the Central groundwater basin in Los Angeles after 40 years

of operation (Schroeder, 2002). Apparently the nature and extent of long-term changes in water quality and aquifer properties can differ by location and operation.

- *Hydrogeological impacts on contaminant attenuation*. Aquifer properties and groundwater composition can impact chemical and biological contaminant attenuation at an ASR site (e.g., Greskowiak et al., 2005). The impact is a function of aquifer hydrogeology and ASR operation characteristics, which provides the basis for a thorough and systematic investigation.

The occurrence and magnitude of these negative impacts are functions of a number of variables. Therefore, site-specific groundwater assessment and ASR evaluation are important. Quantitative analysis and water quality modeling are useful and often necessary to address potential complications at a given location. Such analyses normally take place in two steps. Based on site investigation results, hydrological modeling is conducted, followed by contaminant fate and transport analysis. The ASR DSS framework outlines these procedures in Section 2.3. This report also describes the hydrological assessment component. Based on the hydrological and water quality analysis results, one can assess the minimum injected water composition requirements for different soil and hydrological site conditions. This is important for engineering control over virus, bacteria, and protozoa viability in soil profiles.

2.2   ASR Practice in the U.S.

2.2.1   *ASR Applications in water stressed regions*

ASR practice is increasingly used to manage water resources and mitigate water shortages in the U.S. Long-term precipitation measurements across the contiguous U.S. show uneven precipitation distribution and changes through the time. The details of these long-term changes and regional distributions are provided in a recent EPA report (U.S. EPA, 2015a). Based on historical precipitation measurements, Oregon and Washington received the greatest average monthly precipitation (up to 5.5 in/month), while much of the Great Plains region and California received the least (less than 1.5 in/month) (U.S. EPA, 2015a). Existing ASR projects are mostly located in the water-stressed states, including Florida, California, and the Southwest (Figure 4). There are also a number of active ASR sites in New Jersey and South Carolina (Bloetscher et al., 2014). By 2002, at least 27 states had water reclamation facilities and associated water reuse guidelines, and nine states (Wisconsin, South Carolina, Texas, Iowa, Missouri, Wyoming, Oregon, North Carolina, and Colorado) had enacted strict regulations over ASR practices according to the UIC program. In early national assessment, U.S. EPA (2004) reported that ASR facilities in the U.S. emplaced a total of 6.4×10^6 m^3 of reused water into the subsurface, with Florida and California accounting for 34% and 31% of this total, respectively. The ASR operation is expected to expand for the increasing water availability gap. For example, in a recent focus report for the Texas House of Representatives, the House Research Organization expected a large increase of water storage in ASR practice nearly by three times from 2012 to estimated 152,000 acre-feet per year by 2070[2]. According to the U.S. EPA's *2012 Guidelines for Water Reuse*, the U.S. population uses 121 million m^3 of water per day. Currently only 7-8% of this water is reused, while the NRC Water Science & Technology board reports that one-third of the total water being used could potentially be reused (U.S. EPA, 2012a).

ASR operation can be adjusted in response to water demand and demographic changes. The U.S. population has increased since 1900 and the rate of increase has accelerated since the 1970s. This rapid

---

[2] House Research Organization report "Addressing Water Needs Using Aquifer Storage and Recovery". July 12, 2016.   http://www.hro.house.state.tx.us/pdf/focus/asr.pdf

A.

States with water reuse and groundwater recharge rules (as of 2007)

Legend

State with water reuse regulations

State with water reuse guidelines

B.

Elevated Arsenic Concentration
- $\geq 10 - 25$ ppb
- $> 25 - 50$ ppb
- $> 50 - 75$ ppb
- $> 75 - 100$ ppb
- > 100 ppb

ASR/AR Well Status
- Active
- Inactive
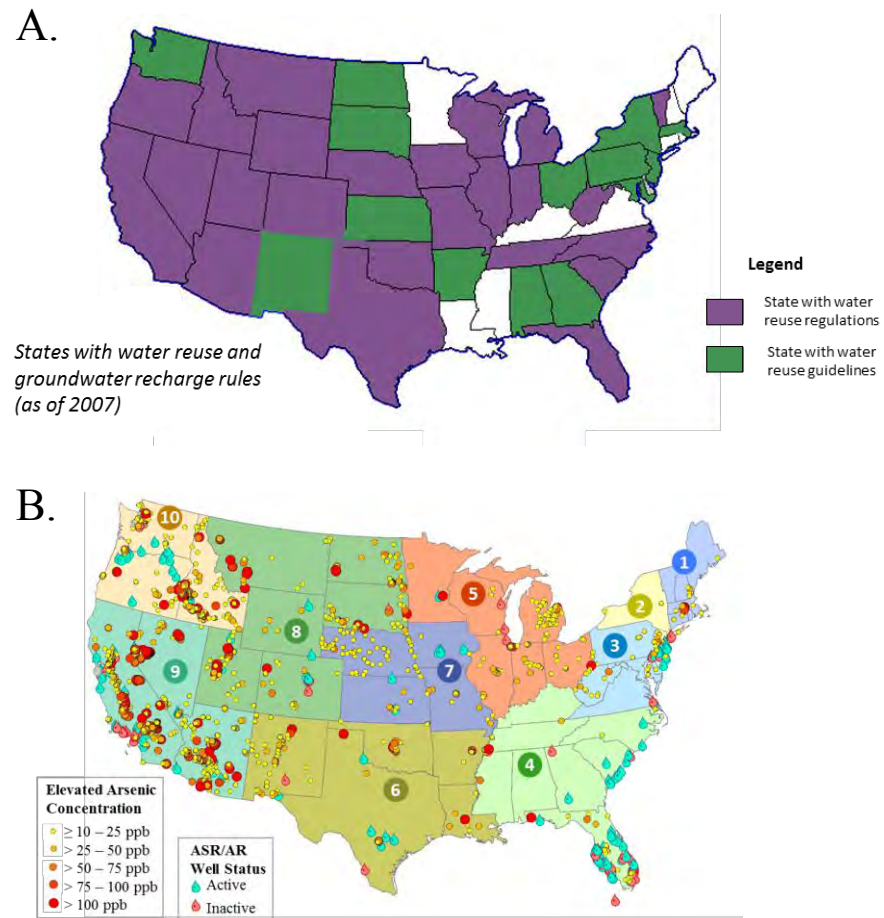
Figure 4   (A) The states with water reuse and ASR rules (Yang et al., 2007 and references therein), and (B) a map of arsenic-contaminated wells and ASR/AR wells in the 10 EPA regions of the contiguous United States (created with Ersi® ArcMap™ 10.3)

population growth has increased water demand, necessitating the implementation of techniques such as ASR to supplement natural water supplies. It is worthwhile to note that the largest increases in population have occurred in 5 water-poor states: Nebraska, Arizona, Utah, Nevada, and Florida with population growth particularly concentrated in the southern region (See Figure 8B later in Section 3.2.2). It is important to consider these population growth projections in the larger context of industrial and agricultural water demands, as well as precipitation variability. For example, in the case of Nebraska, the population growth rate is expected to level off by 2030 (Yang et al., 2007). However, like other Great Plains states, Nebraska has high fresh water usage per capita, largely due to agriculture irrigation. Yet more than 50% of Nebraska's fresh water is derived from groundwater aquifers that are vulnerable to overdrafting. The extensive use of groundwater resources can lead to overdrafting where groundwater pumping exceeds natural recharge rates. Similar observations on the imbalance can be found in many other areas of the Great Plains region (U.S. EPA, 2015a).

Therefore, unless steps are taken to mitigate stresses to the water supply, population/agriculture-induced water shortages are likely to occur in the future. ASR using wastewater can be a means of addressing these shortages by supplementing non-potable agricultural irrigation. The water budget can be assessed using numerical modeling techniques, such as the neural network model described in Chen et al. (2003). Many ASR applications in the U.S. are intended for non-potable water and wastewater reuse in irrigation, industrial, and urban landscape applications (Figure 2) (Asano and Levine, 1996). However, ASR application for indirect potable water reuse is increasing (Miller, 2006). Reported field-scale indirect potable examples include the spreading basins in the Southern California Groundwater Replenishment program, wastewater reuse for aquifer recharge in Las Vegas, Nevada (Ranatunga et al., 2014), and ASR applications in master planning for water supplies in Manatee County, Florida (Chang et al., 2012).

2.2.2   Water quality standards in ASR operations

There are 1185 aquifer recharge and ASR wells documented in the U.S., which were counted in a state and U.S. EPA Regional survey as part of a Class V Underground Injection Control Study. The total number is estimated to be between 1695 and 2000, since not every ASR well is documented due to variations in the permitting and reporting requirements for Class V wells on a state-by-state basis (U.S. EPA., undated). As of 1999, approximately 89% of documented wells were located in ten states: FL (488, including storm drainage and connector wells), ID(48), NV(110), TX(67), SC(55), ID(48), OK(44), OR(16), WA(12), and CO(9). For these and future ASR sites, regulatory oversight at the U.S. EPA is administrated by the Underground Injection Control (UIC) program[3]. ASR wells are regulated as Class V injection wells in the regulatory framework. The EPA may directly implement a program, or a state may have primary enforcement authority, or "primacy". ASR system owners and operators need to submit basic inventory information to the primacy enforcement agency prior to constructing the well. In many states, the state's regulating department, for primacy states, or the EPA, for states without primacy, will require a permit for a Class V well. In some states, the operation can be authorized by rule if the owner or operator submits the inventory information for a fresh water source and demonstrates that the well will operate in a manner that does not endanger an underground source of drinking water (USDW).

Minimum water quality standards have been promulgated under the Safe Drinking Water Act (SDWA) to protect groundwater and surface water sources in the United States. Table 2 lists water quality criteria in ASR, urban reuse, and agricultural reuse for food crops. Florida regulates fecal, TSS and nitrate concentrations for ASR operations (Table 2). As of 2015, states that require individual ASR permits include Florida, Idaho, Nevada, Oregon, South Carolina, New Jersey, and Washington. Five states (CA,

---

[3] http://water.epa.gov/type/groundwater/uic/aquiferrecharge.cfm#uicregulations

CO, ID, OK and TX) require permits that satisfy groundwater rules. Other states do not have state-specific water quality criteria, but generally follow the federal drinking water standards.

Regulations adopted by primacy states for ASR wells vary. As of 2007, nine states (Wisconsin, South Carolina, Texas, Iowa, Missouri, Wyoming, Oregon, North Carolina, and Colorado) require that water used for ASR injection be potable water or drinking water treated to national or state Drinking Water Standards or state ground water standards. Potable water is defined differently in each state but generally refers to water that is high quality and poses no immediate or long term health risk when consumed. Some states require that the injected water not exceed the background levels of natural groundwater, while other primacy states allow additional types of water to be used in ASR, including treated effluent, untreated surface and ground water, and reclaimed water subject to state recycled water criteria. Nevada also allows "any" injected water. However, these state-specific ASR regulations do not supersede the prohibition of movement of contaminated fluid into a U.S. drinking water source. Specifically, EPA regulations provide that "no owner or operator shall construct, operate, maintain, convert, plug, abandon, or conduct any other injection activity in a manner that allows the movement of fluid containing any contaminant into underground sources of drinking water, if the presence of the contaminant may cause a violation of any primary drinking water regulation under 40 CFR part 142 or may otherwise adversely affect the health of persons." (40 CFR 144.12).

2.3   ASR Decision-Support Framework

ASR development at a municipality often involves several consecutive planning and engineering actions. These include ASR-Need analysis, feasibility studies, planning and assessment, and ASR design, construction, and operation. A technical evaluation may also involve many of these elements for existing ASR facilities. In this research, an ASR DSS framework was developed to support ASR planning, design, and evaluation. The DSS can be applied to assist technical investigation and management analysis in three levels: 1) ASR feasibility analysis; 2) ASR planning and assessment; and 3) ASR design and evaluation.

2.3.1   ASR Decision-Support Framework

These levels of technical and engineering investigations are interrelated and can provide a structured analysis for ASR development, permitting, and evaluation. The DSS principles, tools and methods are presented in the remainder of this report along with illustration examples.

Level 1: Feasibility analysis

Level 1 of the DSS framework consists of databases and user inputs. One database contains state ASR regulations promulgated under the SDWA and weblinks to the EPA UIC program. Users can review specific parameter limits such as those in Table 2. Another database contains the location and purpose of application (e.g., aquifer recharge, portable reuse, etc.) for existing ASR sites across the contiguous U.S. which will be kept current. Technical information on ASR example sites is provided in a GIS GUI for planning and design reference purposes.

Additional components of feasibility analysis are location-specific ASR site information and ASR-Need analysis (Figure 5). Factors considered in the ASR-Need analysis include projections of climate change, water demand for projected socioeconomic development, and land use changes. Local master planning documents for economic developments, land-use zoning, and population projection, are preferably used as the basis for the water demand projections. Model-generated projections, such as those from the U.S. Bureau of Census projections on population or the Cellular Automata (CA) – Markov land use projections, can be used in the absence of local master planning data. Land use projection methods were systematically reviewed by the U.S. EPA (2015a), which recommended the CA-Markov modeling

End-use	US EPA (2004)*	Arizona	California	Florida	Nevada	Texas
Urban Reuse						
Turbidity	2 NTU	2 (5) NTU (Class A)	2 (5) NTU (1-D avg, max)		NS	2 NTU (1-D avg) 5 NTU (max)
Fecal coliform	ND/100 ml	ND 4/7-D (Class A) 23/100ml, Max (Class A) 200 (800)/100 ml (Class B)	2.2/100 ml (7-D mean) 23/100 ml (30-D max) 240/100 ml (max)	ND at 75% samples 25/100 ml (30-D, max)	2.2/100 ml (30-D avg) 23/100 ml (30-D max)	14/100 ml 200/100 ml (7-D avg) 800/100 ml (max)
Biochemical oxygen demand (BOD_5)	10 mg/L			20 mg/L (yr avg)	30 mg/L	5 mg/L (10 mg/L) 30 (20) mg/L, Type II
Total suspended solids (TSS)	<2 mg/L			5 mg/L	Not specified	Not specified
pH	6-9			6 - 8.5		6 - 9
Free chlorine	1.0 mg/L			1.0 mg/L		1.0 mg/L
Agriculture, flood crops						
Turbidity		2 (5) NTU (Class A)	0.5 - 2 NTU (1-D max)		Not specified	3 NTU (1-D avg)
Fecal coliform	<200/100 ml	ND 4/7-D (Class A) 200 (800)/100 ml (Class B)	2.2/100 ml (7-D mean) 23/100 ml (30-day max)	25/100 ml (30-D, 75%)	200/100 ml (avg) 400/100 ml (30-day max)	20/100 (75/100) ml 200/100 ml (7-D avg) 800/100 ml (max)
BOD_5	30 mg/L	Not specified	Not specified	20 mg/L (yr avg)	30 mg/L	5 mg/L (10 mg/L) 30 mg/L (Type II)
TSS	30 mg/L		Not specified	5 mg/L	Not specified	3 NTU
pH	6-9			6 - 8.5		
Free chlorine	1 mg/L			1.0 mg/L		
Aquifer recharge						
Turbidity	Site specific and use dependant	Not regulated	Case-by-case	Not specified	Case-by-case	Case-by-case
Fecal coliform	Site specific and use dependant	Not regulated	Case-by-case	200/100 (yr avg) 800/100 (max)	Case-by-case	Case-by-case
Carbonaceous BOD_5	Site specific and use dependant	Not regulated	Case-by-case	Not specified	Case-by-case	Case-by-case
TSS	Site specific and use dependant	Not regulated	Case-by-case	10 mg/L	Case-by-case	Case-by-case
pH	Site specific and use dependant	Not regulated	Case-by-case		Case-by-case	Case-by-case
Free chlorine	Site specific and use dependant	Not regulated	Case-by-case		Case-by-case	Case-by-case
Nitrate	Site specific and use dependant	Not regulated	Case-by-case	12 mg/L	Case-by-case	Case-by-case

Note: Data source - US EPA (2004)

* Suggested guidelines for various types of wastewater reuse.
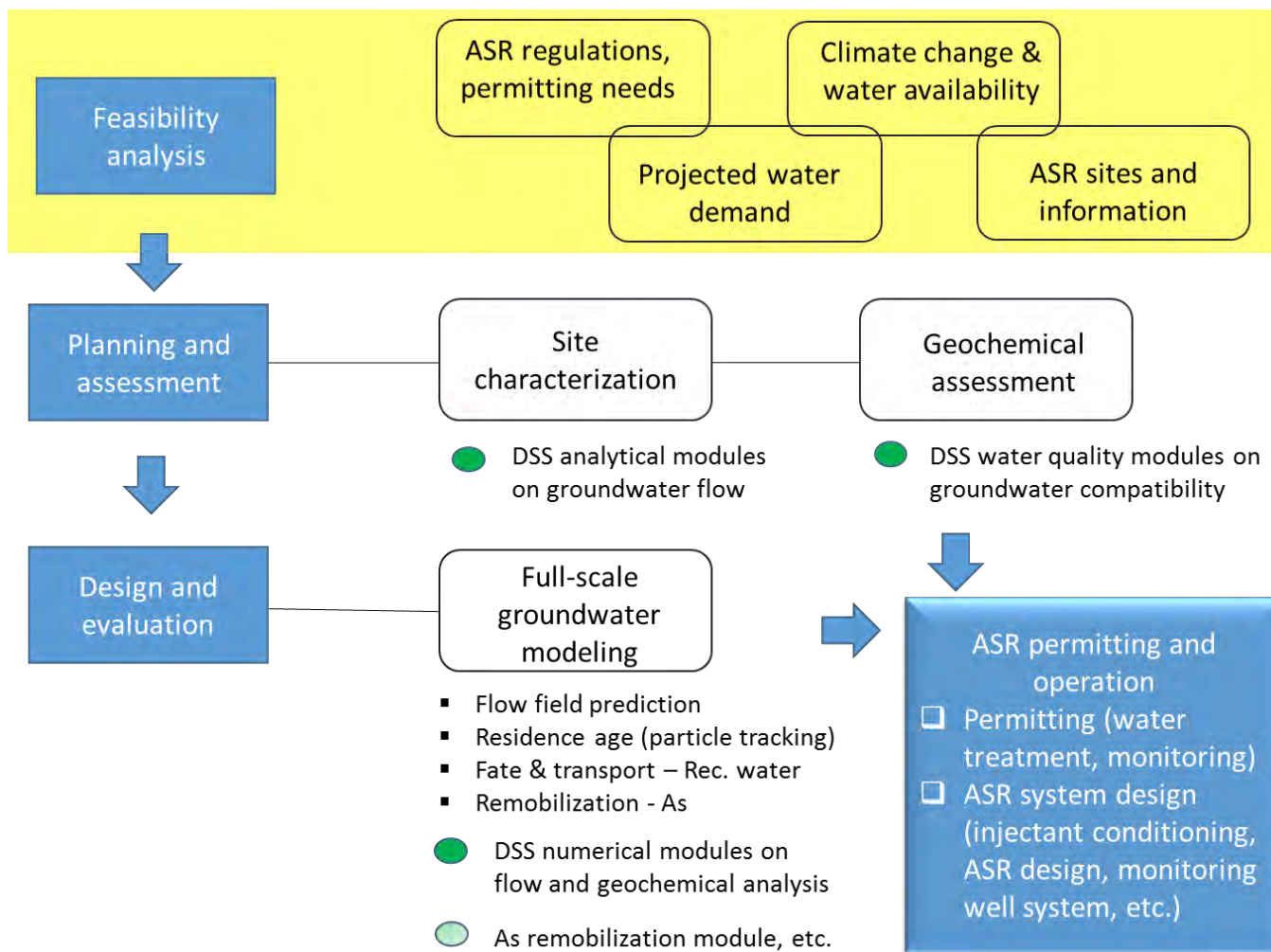
Figure 5   Layout of the ASR DDS framework, consisting of programs in three levels: 1) Feasibility analysis; 2) Planning and assessment; and 3) Design and evaluation.

method to predict dynamic urban land changes. Climate change analyses typically projects precipitation changes over a period of ~30 years. As described by the U.S. EPA (2015a), future climate considerations are commonly projected based on climate data, an ensemble of global circulation models (GCMs), or the RCM downscaling data. These models are validated against historical precipitation data. However, climate down-scaling results are often used for projection of local watershed applications due to the large uncertainties that are inherent in the science. The EPA (2015a) describes the datasets and precipitation projections of climate models for local water resource engineering.

Feasibility analyses are used to determine the magnitude of water availability gaps and durations of water shortages, and are used to define ASR need and scale requirements. The quantitative analysis is a core component of water resource master planning, and involves detailed assessment of water availability and demand. A practical example for the Las Vegas water district is given in Section 3.2.4.

The feasibility analysis portion of the DSS is used to answer key questions about geological strata suitability for ASR operation. Hydrological investigations are conducted to obtain aquifer transmissivity or formation permeability, porosity, and geochemical characteristics, and to determine groundwater flow fields under ambient and ASR operation conditions. Spatial distribution of faults and fraction networks, along with geotechnical instability at or near the ASR site, are also important considerations. It has been reported that fluid injection in the vicinity of pre-existing faults can trigger seismic activity in the form of local earthquakes. In the DSS Level 1 analysis, the site-specific geological and hydrogeological data can be analyzed in the context of other ASR operations in the database. This may lead to a preliminary assessment of the ASR feasibility at a given location.

Level 2: ASR planning and assessment

Site characterization and analysis of water treatment prior to injection are two major components in engineering investigation at the planning and assessment level (Figure 5). Hydrogeological characterization is necessary to obtain, at a minimum, the technical parameters necessary to answer the following questions:

1) What is the likely recovery rate of injected water? This planning question is pertinent for temporary storage operations that are intended to address temporal or chronic water shortages. Poor recovery rates can also negatively affect the economics of an ASR project.

2) What hydrological changes occur during ASR operation? Vertical hydraulic conductivity and soil-clogging in the vadose zone are important considerations for spreading basin and soil infiltration operations. Aquifer permeability and near-well clogging from biological growth and inorganic precipitation are parameters assessed in the planning phase for wells that inject into saturated zones.

3) Is there potential for adverse geochemical reactions between the injected water and native groundwater and/or geological formations? During ASR, the injected water forms a "bubble" by displacing the native water closest to the point of introduction and mixing with native water for some distance away from this point. The point at which only native groundwater is present in pore space defines the edge of the injection bubble. This spatial distribution of injected water defines the nature and extent of geochemical reactions and contaminant mobility during injection and withdrawal operations. These geochemical reactions can be simulated for anticipated geochemical conditions (e.g., Eh, pH, cation and anion species, etc.).

In the DSS's step-by-step site characterization, geological data, hydrological data, and site information are gathered to answer the three major questions listed above. The assessment can also be used to define injected water treatment requirements prior to recharge operations. In this analysis, geochemical compatibility of the injected water with aquifer materials and the flow paths of injected

water are two major investigative components. Based on treatment scenario analysis, one can determine the treatment options and the injected water composition that has the least impact on groundwater.

Level 3: ASR design and evaluation

Level 3 of the DSS framework is designed to aid in engineering design and evaluation of ASR systems to achieve the planned objectives in recovery rate and water quality impact control (Figure 5). Engineering analysis and groundwater modeling are necessary to determine the following three system performance variables:

- Residence time of injected water in storage. Many states, such as Washington, California, Florida, and Hawaii, have established minimum residence times to ensure biological safety. The required residence time is specified for water flow from injection to recovery, which varies among ASR projects. Water residence times are calculated by applying particle tracking functions in model simulations. For AR operations with no water recovery, such as groundwater replenishment, particle tracking provides valuable information for evaluating long-term AR performance and location-specific management objectives.

- Flow field simulation and evaluation. The ambient groundwater flow field and ASR operation criteria are used to assess hydraulic control of the injected water volume. Capture zone analysis is often accomplished through modeling of groundwater head distributions and particle tracking. In the DSS, 3-D groundwater simulation packages using MODFLOW are recommended.

- Contaminant fate and transport simulation. Characterization of the distribution of residual contaminants in injected water and mobilized contaminants in the aquifer is used to assess groundwater impacts. The alternative is customized, site-specific field pilot testing and demonstration, a common engineering practice used during CERCLA or RCRA programs. For ASR design and evaluation, the water quality simulation requires site-specific hydrological parameters and a higher degree of precision than during the planning and assessment phase (Level 2).

Field pilot tests are an important aspect of ASR planning and will help to determine the hydraulic parameters used in modeling. However, this DSS does not deal directly with field pilot testing and cannot recommend one procedure. Instead, each region implementing ASR must develop their own region-specific procedure. Nevertheless, the results in design and evaluation can lead to a technical basis for the design of monitoring programs and permitting requirements to meet the ASR objectives and performance criteria. Therefore, site investigations must produce detailed, accurate, and site-specific hydrogeological and engineering parameters.

2.3.2   *Technical models in hydrological and geochemical simulations*

The DSS models for the Level 2 and 3 analyses are listed in Figure 6, with technical descriptions provided in Appendix A. These hydrological and geochemical simulators can be applied for ASR planning, design, and evaluation purposes. The software is organized and executed through a custom-designed GUI interface for model interoperability.

ASR planning models

The models in the first row of Figure 6 are the least data-intensive, but are appropriate for ASR planning purposes. These models provide fairly accurate two-dimensional analyses of groundwater flow under ambient or ASR operation conditions. Hantush (1967) and SuperQ are Excel spreadsheet programs that are simple to use while preserving essential groundwater hydraulics. SuperQ utilizes the Theis and Hantush-Jacob equations to determine groundwater flow fields, and uses superposition principles to

calculate groundwater flow effects from multiple wells with different pumping rates. It can be used for estimating and assessing the groundwater hydraulic response from ASR injection and recovery wells.

WhAEM2000 (U.S. EPA, 2007) and a variation, Visual AEM (Craig and Matott, 2009), are better suited for simulating 2-D, steady-state groundwater flow under complex aquifer conditions such as multilayer aquifers, irregular recharge boundaries, and aquifer heterogeneity. The program can be augmented to perform 3-D flow simulations (Kraemer, personal communication). Visual AEM is capable of analytically and numerically simulating contaminant transport in vertically averaged water flow. This capability is valuable for assessing ASR operations when residual contaminants are of concerns.

The 1-D multi-species semi-analytical model and the semi-analytical AT123D-AT (Burnell et al., 2012) model in the ASR DSS can be used to assess contaminant fate and transport for ASR planning purposes. These two programs include simplifying assumptions with respect to groundwater solute transport. For example, the 1-D multi-species transport model yields steady-state longitudinal dispersion of parent and daughter contaminants from a continuous point source. The semi-analytical AT123D-AT, on the other hand, is more computationally complex because of its improved numerical solver and the new use of Green's function for a finite-depth aquifer, and thus is more versatile. However, by simplifying the hydrological conditions through model assumptions, outcomes from these models are limited in their usefulness. For example, while these steady-state solutions can be used for planning purposes, such as to predict the potential for arsenic contamination, steady-state solutions must be combined with more complex 3-D groundwater flow models to be used for engineering design.

ASR design and evaluation models

As compared to planning analysis, system design and evaluation analyses require models with a greater fidelity. Important engineering parameters include injection rate and hydraulic control, as well as recovery rate and residence time when recovery is involved. These design considerations are described in Section 4.1.

The DSS utilizes 3-D groundwater flow and geochemical models to analyze the groundwater system and the 1-D AT123D-AT model for vadose zone analysis. These models are chosen due to the physical condition of water injection. As shown in Figure 1, ASR water injection can cause groundwater mounding at the injection location. Water injection or spreading through the vadose zone further complicates the model simulations because, while vertical water infiltration and contaminant transport can be simulated using 1-D models, groundwater mounding is superimposed on a regional flow field. As a result, the 3-D variation in flow and solute transport is difficult to quantify using 1-D or 2-D groundwater models.

MODFLOW is a widely used and verified modeling package for groundwater simulation. The modular structure of MODFLOW has provided a robust framework for the integration of additional simulation capabilities since it was originally introduced in 1984. The current MODFLOW-related family of programs are capable of simulating 3-D steady or transient flow fields in confined and/or unconfined aquifers. In addition, the MODPATH module allows for tracking of particle pathways using a semi-analytical particle-tracking scheme. The results are useful to evaluate the residence time of injected water and to calculate the rate of recovery. MODFLOW and MODPATH technical details are provided in Appendix A.

MT3DMS is a multi-species transport model. The numerical model, originally developed by the U.S. Army of Engineers (Zheng, 2010), considers advection, dispersion, matrix diffusion, and chemical reactions. Simulation results can provide contaminant concentration distribution at an ASR site, along with time-series pressure and chemical concentrations at observation wells for a variety of hydrologic

Hantush (1967): 2-D Water Table Mounding Model	SuperQ: 2-D Well Hydraulics Superposition Model	WhAEM2000: 2-D Groundwater Flow and Particle Tracking Model	Visual AEM: Groundwater Flow, Particle Tracking, & Transport Model	AT123D-AT: Semi-Analytical Transport Model	1-D Multi-Species Semi-Analytical Transport Model
• The USGS (Carleton, 2010) developed an Excel spreadsheet to calculate transient water table mounding beneath a rectangular recharge basin based on the Hantush (1967) equation. An Excel-based spreadsheet program.	• Uses the Theis and Hantush-Jacob equations and superposition to evaluate transient effects of multiple wells, variable rate pumping, and simple boundary conditions on hydraulic heads in a uniform 2-D aquifer. SuperQ is an Excel-based spreadsheet program.	• USEPA (2007) public domain Analytical Element Model (AEM) code simulates 2-D steady flow caused by pumping wells, hydrologic boundaries (river, recharge, and no-flow conditions), and inhomogeneity zones. Easy-to-use Graphical User Interface (GUI).	• Visual AEM (Craig and Mattott, 2009) is a GUI for single and multi-layer AEM modeling of steady-state groundwater flow particle-tracking, and numerical/ analytical modeling of vertically-averaged contaminant transport. Incorporates an easy-to-use GUI.	• Simulates advection, hydrodynamic dispersion, linear sorption, and first order reaction of 1-D, 2-D, or 3-D dissolved pollutants in groundwater from an Instantaneous, continuous, pulse, or time-dependent source mass flux. Incorporates an easy-to-use GUI.	• Simulates advection, hydrodynamic dispersion, linear sorption, and sequential degradation reactions of multiple pollutants along uniform or variable velocity flow path for use in risk assessment. Incorporates an easy-to-use GUI.

MODFLOW: 3-D Groundwater Flow Model	MODPATH: 3-D Particle-Tracking Pathline Model	MT3DMS: 3-D Particle-Tracking Pathline Model	SEAWAT: 3-D Particle-Tracking Pathline Model	PHREEQC: Geochemical Model	PHAST: 3-D Reactive Geochemical Transport Model
• The USGS MODFLOW (Harbaugh, 2005) finite-difference code (with its family of compatible programs) is used to simulate 3-D groundwater flow, groundwater/ surface-water interactions, etc. ModelMuse is a Windows GUI for MODFLOW and other model codes.	• MODPATH is a USGS (Pollock, 2012) post-processing program that computes 3-D flow paths and travel times of groundwater particles and retarded solutes using MODFLOW output. ModelMuse is a GUI for MODPATH.	• Links with MODFLOW to simulate variable velocity from injection/pumping, hydrodynamic dispersion, linear sorption, and first order sequential reactions of multiple pollutants in groundwater. No free Windows GUI is available.	• The USGS SEAWAT code (Langevin et al., 2007) is a generic MODFLOW/ MT3DMS-based computer program designed to simulate 3-D variable-density groundwater flow coupled with multi-species solute and heat transport. No free Windows GUI is available.	• The USGS PHREEQC (Parkhurst and Appelo, 2013) geochemical program performs (1) speciation and saturation-index calculations, (2) batch reaction and 1-D transport calculations with reactions, and (3) inverse modeling. PHREEQC-I is a Windows GUI for PHREEQC.	• Using PHREEQC to handle equilibrium and kinetic geochemical reactions, the USGS PHAST code (Parkhurst et al., 2010) can simulate multicomponent, reactive solute transport in 3-D groundwater flow systems. ModelMuse is a Windows GUI for PHAST.

Figure 6   Groundwater and vadose zone simulation programs involved in the ASR decision support system.

conditions and well configurations. MT3DMS is used to simulate the fate and transport of residual miscible contaminants, mostly organic trace constituents, in injected water.

SEAWAT is a coupled version of MODFLOW and MT3DMS designed to simulate 3-D, variable-density, saturated groundwater flow. Although MT3DMS and SEAWAT are not explicitly designed to simulate heat transport, temperature can be simulated a chemical species by using a mathematical analog to Fickian diffusion with appropriate transport coefficients. Thus, the SEAWAT module allows simulation of various "unusual" ASR applications, including the injection of oil field brine water after treatment, or water injection into a saline aquifer.

Design and evaluation models for aquifer recharge

On the other end, the AR operations do not include recovery components. As these represent simplified cases, the models listed above are capable of providing accurate simulation results for design and evaluation. This approach is applicable for groundwater recharge through green infrastructure applications, water percolation from septic tank to drain fields, and water injection using wells and trenches (Figure 2).

2.3.3   *Groundwater chemistry changes and arsenic mobilization*

An ASR operation introduces water into the aquifer that is geochemically different from native groundwater, forming an injected water bubble of different water composition. This condition is schematically illustrated in Figure 1. Displacement of native groundwater at the core and mixing at the peripheries of the bubble are the processes that lead to potentially detrimental geochemical reactions. One example is arsenic mobilization from formation minerals into groundwater (Jones and Pichler, 2007; Neil et al., 2012; 2014; Wallis et al., 2010). ASR-induced mobilization has also been reported for other metallic constituents (e.g., Pb, Cr, U, Fe, etc.) (Arthur et al., 2002).

PHAST is a 3-D groundwater flow and geochemical package that is used to characterize transient changes of geochemical parameters (e.g., pH, Eh, etc.) (See Figure 6). PHAST combines the geochemical program PHREEQC and the 3-D groundwater flow program, HST3D, both from the USGS. PHREEQC is designed to simulate cation and anion speciation and saturation index, transport of species with reversible and irreversible reactions, as well as inverse modeling from field measurements. This allows PHAST application for a diverse set of geochemical conditions in fate and transport analysis.

Arsenic-bearing minerals, such as arsenopyrite (FeAsS), can be present in aquifer formations under anoxic conditions. However, when conditions become oxic due to the introduction of injected water, arsenic becomes soluble in groundwater (Jones and Pichler, 2007; Wallis et al., 2010; Neil et al., 2012). Principle reactions governing arsenic mobility involve arsenopyrite oxidation (an arsenic source) and iron (hydr)oxide mineral formation (an arsenic sink) (Neil et al., 2014):

$FeAsS + 1.5H_2O + 2.75O_2(aq) \rightarrow Fe^{2+} + H_3AsO_3 + SO_4^{2-}$

$Fe^{2+} + 3H_2O \rightarrow Fe(OH)_3 + 3H^+ + e^-$
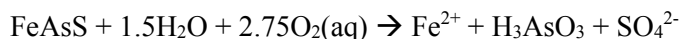
PHREEQC is capable of simulating arsenic mobilization in groundwater under various geochemical conditions (e.g., Appelo et al, 2002; Zheng et al., 2009; Tabelin et al., 2012; Keeting et al., 2010; Wallis et al., 2010). Arsenic mobilization assessment is achieved using the following steps:

- Define environmental conditions using PHREEQC;

- Identify arsenic mobilization potential by comparing arsenic mineral phase diagrams with existing mineral phases in the aquifer.

- Perform PHAST simulation to determine dissolved arsenic concentrations in groundwater.

3.0   ASR-Need Analysis in Planning

3.1   ASR Assessment and Evaluation

3.1.1   *Water quantity, quality and water availability*

Water master planning for municipalities is conducted to assure adequate water supply for domestic, industrial, and environmental needs. ASR operation is necessary in many water-stressed regions to augment available water resources and meet water demand. Major criteria involved in water budget analysis include water quantity, water quality, and economics:

- *Water quantity*. This factor includes both water volume and flow. In many cases, temporary or seasonal water shortages occur due to an imbalance in the flow requirements for consumptive and environmental flow demand. This can occur even when an adequate volume of water is available due to precipitation being underutilized. A common mitigation strategy is to have sufficient storage capacity (e.g., ASR or reservoirs) to capture all available water and use it to mitigate seasonal shortages.

- *Water quality*. Naturally available water resources at a location may be not suitable for intended consumptive or environmental use. For example, brackish water is not potable unless advanced water treatment is applied to decrease the salt concentration.

- *Economics*. Water availability is a function of economics for local managers and water resource management. Water can be made available from inter-basin or inter-watershed transfers, desalination, rainwater harvesting, or through storage of different forms (e.g., reservoirs, impoundment, storage tanks, and ASR). Each option is associated with a set of costs and economic/environmental benefits. The first step in master planning is often a feasibility analysis of different technical and management options.

Water master planning involves analysis of water budget and flow components to determine water availability and water demand for the master planning period. Master planning technical details and an application example are provided in Section 3.2. A technical feasibility analysis is needed after determining the need for water storage through ASR operations. ASR operations designated for water injection must demonstrate that there will be no adverse impacts to native groundwater resources. This criterion applies to residual contaminants in the injected water, as well as the consequences of any geochemical reactions between the injected water and native aquifer materials. Other criteria to consider for water injection are the storage capacity of the formation, and the operational economics in comparison to other alternatives.

3.1.2   *Technical feasibility analysis*

ASR feasibility depends on several technical conditions, including formation suitability for storage and recovery, injected water and native groundwater quality, injection and recovery system engineering, and economic comparisons among alternatives. The analysis results often serve as the basis for planning and subsequent detailed engineering design. They can also be part of existing ASR evaluations.

Not all locations have geological formations that are a potable groundwater resource, and/or are otherwise suitable for ASR operation. A hydrogeological investigation must be conducted to determine important attributes such as:

- *Aquifer storage characteristics.* The permeability, porosity, and spatial boundaries of the aquifer will determine injection/extraction rates and the injection bubble geometry for storage. The location of boundaries such as aquitards, faults, and surface water bodies influence the long-term pressure distributions and injection/extraction rates. Aquifer depth is also an important consideration from an economic perspective.

- *Petrology and mineralogy of the aquifer formation.* Mineral composition often determines geochemical compatibility with injected water, and thus the potential for groundwater contamination at an ASR site. For example, formations composed of sandy sediments tend to have high permeability and porosity, making them good ASR candidates. However, these geological formations can contain accessory minerals such as arsenic-bearing pyrite, which contain arsenic or other heavy transition metals that can leach out from rocks, leading to groundwater contamination. Another potential issue is precipitation of minerals during geochemical reactions with injected water leading to plugging and reduction in aquifer permeability.

- *Geologic structures and water recoverability.* Preferential groundwater flow occurs along faults and fractures, which have important impacts on hydraulic control and recovery of injected water at a storage site. Furthermore, water injection under pressure can generate hydraulic fractures in the geologic formations. This type of secondary permeability has been reported numerous times and is the main mechanism for hydraulic fracturing engineering.

In addition, ASR operation is only one of many storage options in addressing water deficits. Other options include surface impoundment, reservoirs, storage tanks, inter-basin or inter-watershed water transfer, and even water credit trading. Each option has its own advantages and disadvantages. A compromising optimization technique, for example, was used for option evaluation in water infrastructure master planning in Manatee County, Florida (Chang et al., 2012). More details can be found in EPA (2015b).

Investigation focus should be placed on system hydraulic control and water quality when conducting ASR evaluation and design analyses. Section 3.3 provides an overview of ASR evaluation and design, and the rest of the report illustrates tools and methods.

3.2　　　Water Availability in ASR Feasibility Investigation

Water availability and climate change can significantly affect estimates of ASR needs for a given location. This component of the Level 1 DSS is further discussed here.

3.2.1　*Water availability analysis*

<u>Current Practice</u>

Water resource master planning is focused on water resource inventory and water demand projections. A quantitative analysis is used to determine the current water availability gap, and to make projections for future conditions. Water gap mitigation options are identified that either increase water availability, such as water reuse and ASR practice, or reduce water demand, such as residential and agricultural conservation practices (e.g., Wang et al., 2013; Chang et al., 2012). This type of water resource management is well documented in literature and planning guidelines.

<u>Total water management analysis</u>

ASR need for a municipality can be defined using a more comprehensive approach, which treats ASR operation as a storage unit process and quantifies the parameters necessary to meet water demand. ASR is especially needed to address large seasonal and time variations in water demand or supply,
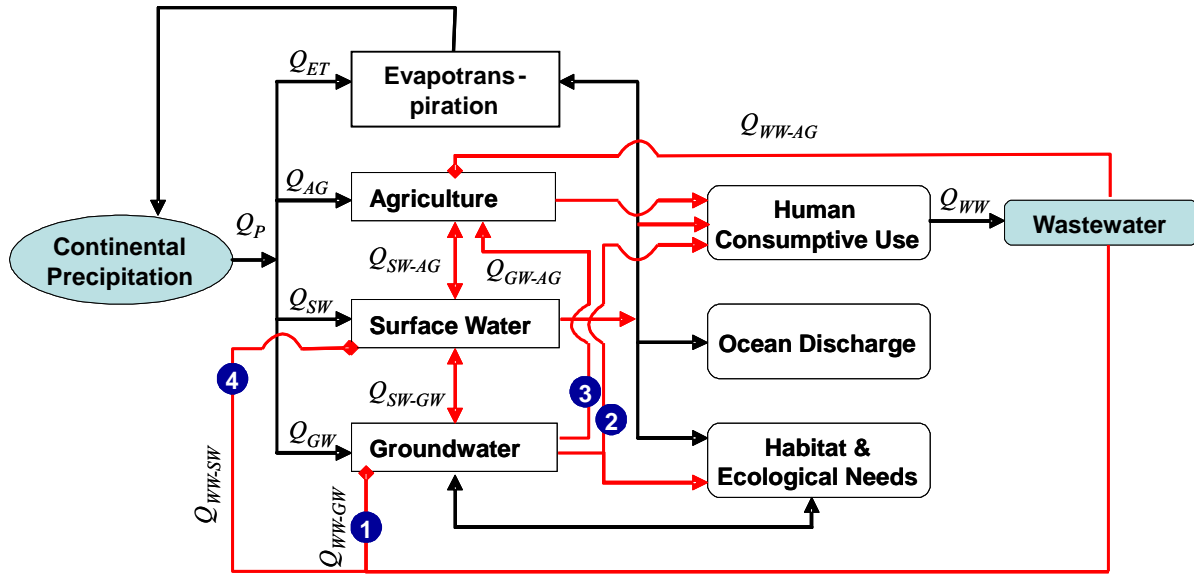
Figure 7   Conceptual schematic showing water distributions among major and secondary water process units. Also shown as red lines are possible flow vectors for water reclamation and re-distribution. Reclaimed water reuse options are labeled: (1) Groundwater recharge; (2) ASR for human reuse; (3) ASR for agricultural reuse; and (4) Surface water in ecological flow augmentation.

resulting in temporal water shortages. Total water management is necessary in this case to identify which components of water usage affect downstream environments and human activities.

Figure 7 illustrates a conceptual schematic showing water distributions. In this schematic, the water input of continental precipitation is partitioned into four primary water unit processes: evapotranspiration, net surface water storage, net groundwater storage, and net agriculture consumption. The balance defines water resource abundance and availability. In this evaluation, the unit processes are balanced in terms of volumes and flow rates. Water flow into each unit must equal the outflow to secondary processes. These secondary processes include human consumption, habitat and ecological needs, and oceanic discharge, each of which have specific water quality requirements (Figure 7). These principles form a basis to evaluate water resource sustainability and to optimize management techniques to achieve objectives. Water transfer and water quality interactions among the process units are considered in addition to flow balance during the optimization process. An example can be found in the quantitative analysis of water resource master planning in Manatee County, Florida (Chang et al., 2012; Board of County Commissioner, 2008; and references therein).

Water resource imbalance for a municipality or watershed occurs when the flow rates in Figure 7 are mismatched. Under reduced precipitation, $Q_p \downarrow$, and increased evapotranspiration, $Q_{ET} \uparrow$, which can occur in some regions due to global climate change, the water unit processes can become imbalanced based on the current state of agriculture, surface water and groundwater, leading to water shortages. This imbalance can be managed by water redistribution among end water uses. Examples include the reuse of wastewater in groundwater recharge and ASR for agricultural reuse. Agricultural practices use a significant amount of fresh water and nutrients. Agricultural irrigation in water-poor regions can account for volumes of potable water comparable to human consumption.

23

A systemic analysis of the water budget components in Figure 7 can produce a technical basis in master planning for water reuse and ASR needs. There are variations in the principle sources of reclaimed water among municipalities. The most predominant volumetric sources are centralized water treatment facilities, which are listed in the first category of Table 1. The volumetric flow rate injected during ASR operation (Figure 7) can be written as:

$$Q_{RW \to GW}(T, Y) = Q_{RW} - Q_{RW \to SW}(T) - Q_{RW \to DR}(T, Y, C, A, ET) - Q_{GW \to AG}(T, Y, C, A), (1)$$

where subscript RW is reclaimed wastewater; GW, SW, and DW are groundwater, surface water, and drinking water, respectively. Variables T, Y, C, A, ET are time (season), geographic location, crop types, acreage, and evapotranspiration, respectively. Flow vectors are indicated by paired subscript; for example, $Q_{RW \to SW}$ is the flow rate of reclaimed water to surface water.

The water quality limitations are set by groundwater standards (C_{GW}^{std}), drinking water standards (C_{DW}^{std}), or requirements for specific uses such as landscape water use (C_{min}). Often times, water recovered from ASR operations is further treated for potable drinking water, urban, or agricultural reuse; ΔC_{WT} in the following equations represents the change in concentrations due to these treatments.

$$C_{RW \to SW} \equiv \left. \begin{array}{c} \bar{C} \\ C_{max} \end{array} \right. \tag{2}$$

$$C_{RW \to DR} \equiv C_{min} \tag{3}$$

$$C_{RW \to GW} \equiv \begin{cases} C'_{GW} + \Delta C_{ST} \equiv C_{GW}^{std} \\ C'_{GW} + \Delta C_{ST} + \Delta C_{WT} \equiv C_{min} \\ C'_{GW} + \Delta C_{ST} + \Delta C_{WT} \equiv C_{DW}^{std} \end{cases} \tag{4}$$

The injection rate during ASR operation depends on the reclaimed water flow rate, $[Q_{RW} - Q_{RW \to SW}(t)]$, agriculture use of recovered water in ASR storage, $[Q_{GW \to AG}(t, Y, C, A, \Psi)]$, and the direct usage of reclaimed water in agricultural and urban landscaping, $[Q_{GW \to AG}(t, Y, C, A, ET)]$. Water quality requirements for these end use scenarios are incorporated as variables into Eqs.2-4. Operation criteria and secondary treatment systems are tailored during the design phase to ensure that effluent water quality ($C_{RW \to GW}$) meets the drinking water standards (C_{DW}^{std}), agricultural irrigation requirements (C_{min}), or groundwater standards (C_{GW}^{std}), depending on the end use of the effluent. Effluent treatment (ΔC_{WT}) accounts for water quality changes that occur during the ASR process (ΔC_{ST}). In compliance with NPDES permits, effluent quality must comply with effluent concentration limits in monthly average ($\bar{C}$) and maximum (C_{max}) values (Eq.2). Effluent water quality (C_{min}) is defined in consideration of crop type, long-term soil salinity and sodicity management, and pathogen dispersion when used for direct irrigation. Reverse engineering in the quantitative analysis is used to optimize process assemblies among $C_{WW \to GW}$, ΔC_{ST}, ΔC_{GW}, and engineering economics.

Applications and data needs

The total water management concept and analytical framework (Figure 7) have been applied to analyze water resource components, evaluate component interactions, and develop optimal solutions through ASR operations (Thomas and Durham, 2003; Al-Zubari, 1998; Friedler, 2001). Water distribution and redistribution through human activities and natural processes are treated as unit processes. This allows quantitative evaluation of management and engineering options and in depth characterization of water quantity and quality interrelationships. Wastewater reuse was often overlooked in conventional resource development in the past, but is now viewed as a viable component in water supply deficiency mitigation conceptually (Pereira et al., 2002; Thomas and Durham, 2003), in Texas

(Sheng, 2005), in China (Chu et al., 2004), in Europe (Angelakis et al.., 1999), and in water-stressed Gulf countries and the Mediterranean region (Georgopoulou et al., 2001; Friedler, 2001; Al-Zubari, 1998).

Variations exist between the current practice and the comprehensive total water analysis discussed above. The ASR-Need analysis is designed to determine water supply gaps, in total volume or flow rate, over the master planning period. Ranatunga et al (2014) reported an example water budget analysis for the Las Vegas Valley region in Nevada, which is described in Section 3.2.4. In a similar approach, Chang et al (2012) analyzed the engineering costs and environmental footprints of 21 engineering options including components of ASR operations in water supply master planning in Manatee County, Florida. This type of water availability analysis involves characterization of the following technical dimensions:

- Land use and population projections to estimate future water demand;
- Water resource inventory and water availability changes with time;
- Management options to reduce water demand
- Options to increase water availability, including water reuse and ASR operation, water credit trading, water harvesting, etc.

3.2.2   *The climate change consideration*

Master water resource planning typically involves temperature and precipitation projection over a period of 30 years, a time frame over which significant climate change may occur (Yang and Goodrich, 2014). Therefore, it is important to consider potential climate change impacts on water availability during master planning. The U.S. Southwest, Florida, Southern California, and parts of the Basin and Range physiographic province, will very likely experience further decreases in precipitation and temperature-induced increases in evapotranspiration (IPCC, 2001, 2013; U.S. EPA, 2015a). As a result, the water availability gap and general water stress will likely increase.

Precipitation projection to analyze climate change impacts

There are two major precipitation projection approaches available for master planning. One uses historically observed precipitation data in the analysis. A comprehensive statistical analysis of historical climatic records was conducted by the EPA (U.S. EPA, 2015a). The analysis utilized >100 years of precipitation data from 1084 monitoring stations in the contiguous U.S. Precipitation data from each station was characterized by time-series spectrum analysis to reveal the time dependence of inter-annual, decadal, and multi-decadal variability. The results lead to the delineation of major hydroclimatic provinces with unique precipitation variability characteristics (Figure 8).

On a national average, precipitation changes in the historical measurement period are relatively small. While the average temperature and precipitation in recent decades have increased in the U.S. and worldwide, precipitation has only increased ~ 6% in the lower 48 states and nearly 2% worldwide since 1901. Climate models project that changes in the national precipitation average through 2100 will be small (IPCC, 2007, 2013), however, large variability is expected among and within different geographic regions (Figure 8A). This has practical significance to watershed-scale water resource adaptations.

Changes in precipitation rates with time also were determined using linear regressions. Figure 9 shows the mean and spread of determined precipitation change rates for stations within each hydroclimatic province. The approximate boundaries of the provinces are shown in Figure 8. There are many stations with persistent precipitation increase or decrease over the term represented in the historical data. Areas characterized by large changes in precipitation rate are defined as congregate areas with
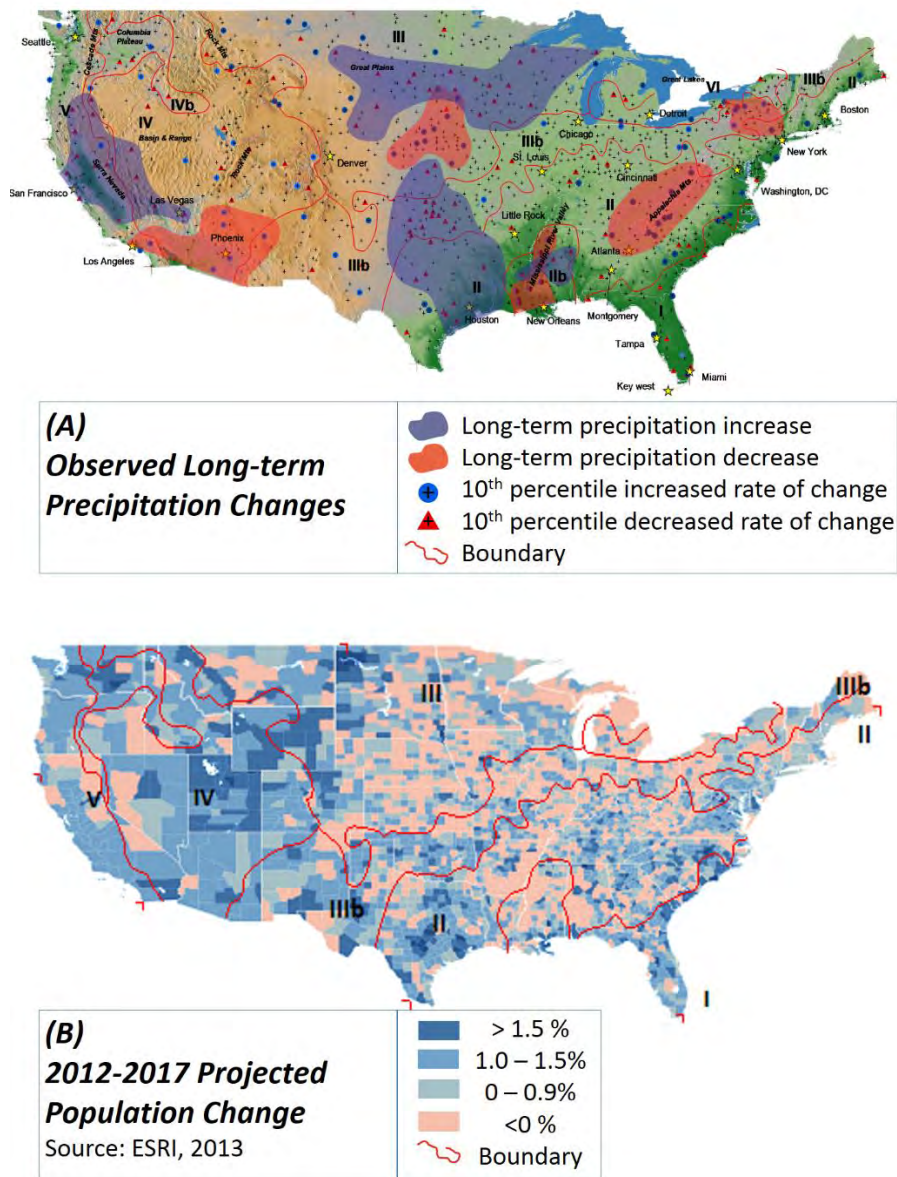
Figure 8   Spatial distributions of population change and long-term precipitation change in the contiguous U.S. (A). Areas of long-term precipitation decrease (red) and increase (blue) are delineated based on spatial aggregation of precipitation change rate over a ~98 year period. The six hydroclimatic provinces include: (I) Florida and Southeast coast, (II) Lower Mississippi — Ohio River valley — New England region, (III) Great Plains and Midwest, (IV) Ranges and Basins, (V) Western Coast, and (IV) Great Lakes. Detailed information on hydroclimatic provinces is available in U.S. EPA (2015a); (B). ESRI population data is presented for 2012-2017 on a county scale. Red lines mark the boundaries of hydroclimatic provinces.

increases or decreases in the 90th or 10th percentile. Several conclusions can be made in relation to the future water availability:

- Analysis of long-term precipitation variability has led to the identification of six hydroclimatic provinces, each possessing a unique set of precipitation variability and trend of change. These regional distributions reflect combined effects of a synoptic climate state and regional/local climatic factors.

- Among the regions expected to suffer worsening water availability conditions, portions of the Appalachian Mountains (P-II) and the Northeast (P-IIIb) have experienced a long-term precipitation decrease and increased precipitation variances with time (Figure 8A). Such changes will likely continue under intensified Atlantic atmospheric circulation.

- A region roughly centered about Phoenix, AZ in the Southwest U.S. (southern portions of P-IV and P-V in Figure 8A) has experienced an overall decrease in precipitation in response to the dynamics of El Nino Southern Oscillation (ENSO) and other climatic systems. The areal size of this region is expected to increase in the future, with the boundaries expanding eastward and northward into the Basin and Range physiographic province.

- Precipitation variance and the frequency of extreme precipitation events (high-intensity and droughts) have increased markedly since the mid-1900s (Bates et al., 2008). Regions that have experienced increased variance include the Northeast and the Atlantic coast, Ohio River basin, Lower Mississippi River basin, and the Southwest U.S. Intense storm events, preferential rain as opposed to snow, and prolonged drought are major types of climatic change that studies have projected for different parts of the U.S. (e.g., USCCSP, 2001; Barsugli, 2009; and references therein).

The second approach to precipitation projection involves using the Global Circulation Model (GCM) and/or Regional Climate Model (RCM). Several down-scaled nation-wide RCM databases are available including those of the U.S. Bureau of Reclamation (USBR)[4] and the NCAR[5]. Results from these climate model simulations indicate a small change in precipitation average, but a large variance over North America for the next 90 years (2010-2100) (IPCC, 2001, 2013). The EPA Office of Water has produced a national web portal that provides projected precipitation data.[6] These models are often validated against long-term precipitation observation data sets. Additional data from an adaptive, remote-sensing monitoring scheme can be used to produce projections for water resources planning and engineering design when the model accuracy is questionable (U.S. EPA, 2015b).

Figure 10 shows a generalized process in a down-scale modeling approach to generate precipitation projections at a local watershed. The details and technical basis of the process are given in U.S. EPA (2015a). The basic steps are:

- First, it is necessary to evaluate whether the RCM projection is based on bias-corrected GCM in pre-processing.

- Second, RCM downscaling requires a full consideration of the regional and local climate factors (Figure 10). Convective and orographic precipitation, and local effects of large water bodies can significantly affect local precipitation variability, especially during high-intensity precipitation events

---

[4] http://gdo-dcp.ucllnl.org/downscaled_cmip_projections
[5] http://www.narccap.ucar.edu/about/index.html
[6] http://water.epa.gov/infrastructure/watersecurity/climate/scenario.cfm
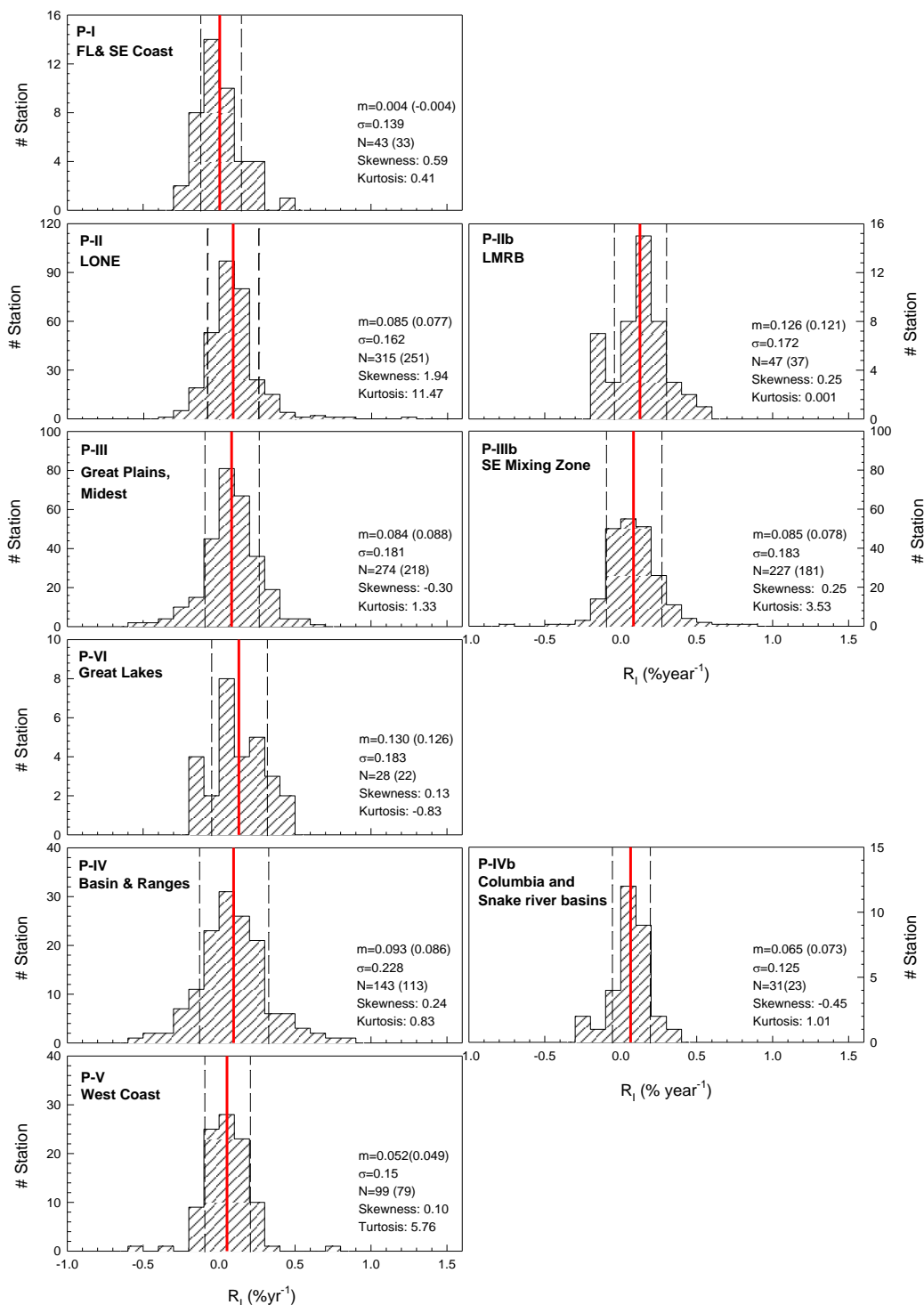
Figure 9   Statistics of the rates of precipitation change (R_I, %yr^{-1}) were calculated from long-range (~98 years) historical monthly precipitations measured at USHCN climate stations. The red line indicates the mean percent change and the dotted lines indicate the standard deviation range. (U.S. EPA, 2015a)

(U.S. EPA, 2015a). In some cases, the post-processing in bias correction is conducted to account for some, if not all, of these location-specific climatic consequences (Figure 10).

- Third, and most importantly, the RCM datasets are validated using independent data sets to improve their reliability. The process of model calibration and validation involves simulated reproduction of long-duration historical data (e.g., >60 years). This is done to ensure that the RCM simulations have properly captured the climate variability and local climate factors. Climate variability and local factors are shown in Table 2-4, and examined in detail in Section 4.0.

Watershed hydrological modeling of climate change impact

In regions such as the southwestern U.S., impacts from climate change can lead to less precipitation, Q_P, and more evapotranspiration, Q_{ET}. This may result in decreased surface water, Q_{SW}, and groundwater, Q_{GW}, flow (Figure 7), thus reducing water availability at watershed-scales. Climate change impacts on stream flow and water quality have been observed in watersheds across the U.S. for many communities relying on surface water (IPCC, 2007, 2013; Johnson et al., 2012; Tong et al., 2012; Ranatunga et al., 2014).

The effect that precipitation changes has on stream flow is not straightforward, but is critical to determine for quantification of water availability gaps. Changes in precipitation and land use can affect both stream flow and surface water quality for most watersheds. Tong et al (2012) quantitatively analyzed the contribution of these two factors to stream flows in the Little Miami River watershed in southwestern Ohio. U.S. EPA (2015a) published a generalized procedure for projecting stream flow changes as a result of land use change and climate change impacts. The procedure is shown in Figure 11.

Figure 10   A typical procedure in climate downscaling yielding the RCM dataset. Also shown is the validation process of precipitation projections for water resource planning.

Future precipitation and temperature at a location are used as the input values in a watershed hydrologic model using the Hydrological Simulation Program in Fortran (HSPF). A land use model is separately established in response to projected populations. Several land use projection models can be used (U.S. EPA, 2015a). One is the CA – Markov model (Figure 11). The CA-MC outputs are incorporated into the watershed HSPF model to generate stream flow projections. This integrated land use and climate change modeling has been applied successfully in urban and rural watersheds of diverse size (Tong et al., 2012; Ranatunga et al., 2014; Chen et al., 2015).

Figure 11   Schematic of a typical integrated modeling approach in projecting surface water quality and quantity changes in a watershed.

Water reclamation and ARS practices for the mitigation of water shortages represents a viable means of adapting to potential future climate change. Initial investigation results have indicated that water imbalances will be region-specific. In some regions, water availability stress will be driven by precipitation changes, while in other regions the predominant drivers will be by population change and socioeconomic activities.

3.2.3   *The socioeconomic factor*

Socioeconomic developments affect water demand with time. Larger population size and greater economic activity can generate greater water demand and lead to greater stress on sustainable water resource development. As a result, socioeconomic factors are pertinent considerations in ASR planning and engineering. Population growth thus far has been independent of water availability in the contiguous U.S. As shown in Figure 8, population growth in the U.S. is concentrated in the Southwest, West, Great Plains, Texas, and the Atlantic coastal states south of Virginia. In regions where there is increased population growth in the immediate future (Figure 8B) without a corresponding increase in the historical precipitation rate (Figure 8A), it may be difficult to meet increased water demands. These regions include:

- Most of the Basin-and-Range Hydroclimatic Province IV, particularly in Arizona, New Mexico, and southern Nevada, as well as Nebraska (Region III) and western Texas (Regions IIIb);

- The southern California area in the Western Coast Hydroclimatic Province V;

- Florida and southeast Georgia in the Florida and Southeast Coast Province I. The water shortage is largely due to rapid population growth in the past decades.

- Coastal Georgia, coastal and central North Carolina, and regions of Virginia in the Blue Ridge and Appalachian Mountains.

These regional assessments provide an overview of current water availability statuses and trends in the future climate. The results can lend support to regional planning and identification of focus areas for sustainable water resources management. Detailed water resource investigations performed by water managers typically focus on the watershed or local municipality-scale.

3.3 ASR-Need Analysis in Las Vegas – A Case Study

Total water management including the use of ASR applications was investigated to analyze potential options in water planning for Las Vegas, Nevada. This case study provides an example of the type of analysis which can be used in Level 1 of the DSS to determine whether water conservation is needed (e.g., what are the current and future water gaps) and whether ASR is a feasible means of closing these gaps. The investigation methodology, results and conclusions are described in Ranatunga et al (2014), forming the technical basis for this section.

3.3.1 *Geophysical settings*

The Las Vegas Valley in southern Nevada lies within the Great Basin and Mojave Desert sections of the Basin and Range physiographic province, bordering the West Spring Mountains to the west and Ground Gunnery Range to the north (Figure 12). The arid watershed has an area of approximately 4850 km^2 and an elevation at the valley floor of ~610 m. Most of the storm drains and stream channels within the valley are dry or low flow due to the arid Mediterranean climate, but some intermittent streams have become perennial streams due to increased wastewater discharge from urban areas (Piechota and Bastista, 2003).

Las Vegas was a small city during the early 20th Century. Most surface water in the basin was from summer flash floods, winter rains, and flow from artesian springs (Morris et al., 1997). The runoff drained to the Las Vegas Wash, a generally barren, gently-sloping, sandy channel that conveyed storm runoff and wastewater from the Las Vegas Valley to the Las Vegas Bay, an arm of Lake Mead. The Las Vegas Wash was dry for most of the year, and contained discharge only during brief periods of major storm runoff. As communities in the Las Vegas Valley grew, the amount of effluent discharges and surface flow that drained to the Las Vegas Wash and Lake Mead increased. The growing urban area discharged enough wastewater into the Las Vegas Wash to create a small, but perennial, stream flow by the 1950s. The ephemeral stream flowing into Lake Mead had been transformed into an active, 40-m-wide river channel by the end of the 20th Century (Buckingham and Whitney, 2007; USBR, 2009). Today, the flow of the Las Vegas Wash is composed of treated domestic wastewater effluent, treated industrial wastewater effluents, dry and wet weather runoff, and groundwater seepage. Industrial and domestic wastewater effluent discharges account for about 90% of the flow (Cooley et al., 2007). There are three major municipal wastewater treatment plants located along the Las Vegas Wash, which collect and treat the municipal wastewater generated in the Las Vegas Valley. There are nine additional permitted discharges along the Wash that contribute significantly to the flow (Piechota and Bastista, 2003).

The Las Vegas Valley climate is hot and arid. The average annual precipitation is 106 mm, occurring mostly as high-intensity, short-duration storms in July and August and low intensity rainfall in the winter months. The average monthly temperatures range from 9°C to 34°C, with an average annual temperature of 21°C. Average daily relative humidity ranges from 32 to 56 percent in mid-winter and from 11 to 28 percent in mid-summer. Evapotranspiration is high because of the high summer temperatures, high solar radiation in cloudless skies, low humidity, and frequently windy summer
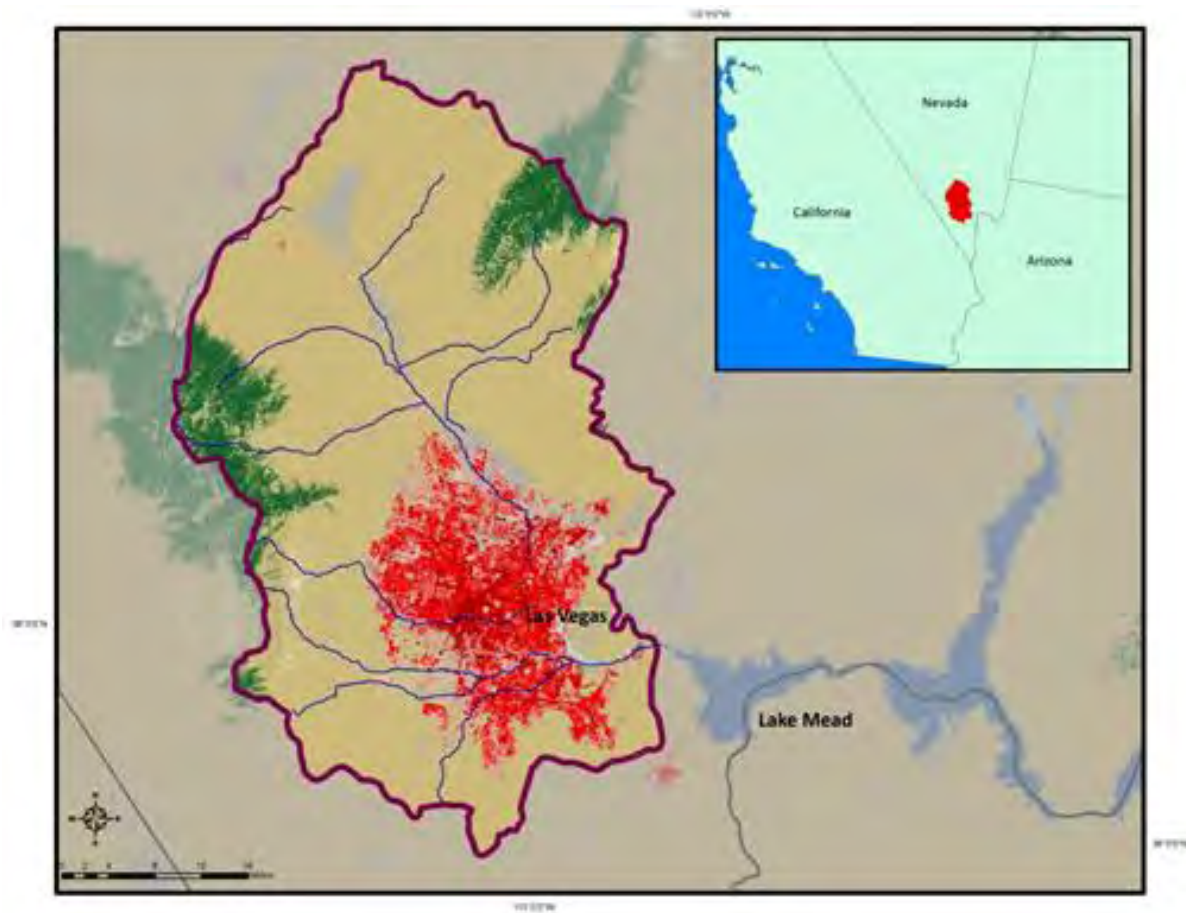
Figure 12   Location of the Las Vegas Wash watershed, Nevada. The color-shaded areas are green for shrub and forest, red for the built area of the Las Vegas metropolitan area, and blue for water bodies of Lake Mead.

conditions (Stave, 2001, Morris et al., 1997). Soils in the Las Vegas Valley are generally composed of gravel, windblown sands, and fine grained silts and clays. Valley floor soils typically have a low field capacity and high permeability. On steep slopes, especially along the Wash, the disturbed soils are particularly susceptible to erosion (Bureau of Land Management, 2004).

Over the last century, social and economic developments, including legalized gaming, the construction of Hoover Dam, industrial production for the Second World War, atomic testing, tourism, and the advent of the modern mega-resort, have steadily increased local populations and associated demands for water in Las Vegas (SNWA, 2009). Rising population has increased the volume of wastewater discharged into the Las Vegas Wash. The rapid urbanization and increase in impervious surfaces cause more storm water runoff to flow directly into the Wash rather than be absorbed by the soil. The increased water flow in the Wash not only accelerated soil erosion and destabilized the stream channel, but also significantly degraded wetland areas and contributed excessive sediment to the Las Vegas Bay (U.S. EPA, 2012b). Climatic change in the form of an overall drying of the region and increased frequency of extremely high precipitation events has also had a considerable impact on the region (USGS, 2000; Christensen et al., 2004).

Because Las Vegas is a major financial center and one of the fastest growing cities of the region, it is important to understand the conditions that affect future water resources. With increasing water demand and decreasing natural water supply, the need to investigate the watershed hydrology and accurately forecast the future water balance is becoming ever more essential. This confluence of factors makes the Las Vegas Wash a unique setting for examining the hydrologic impacts of urban growth and climatic changes.

3.3.2   Future conditions for planning

Future climate change scenarios

The future climate impacts of concern for planning in the Las Vegas Wash watershed include extreme weather events and a shift in winter precipitation patterns, which influence the winter and spring discharge (e.g., Barnet and Pierce, 2008; Karl et al., 2009; IPCC, 2007). Alterations in precipitation and evapotranspiration (ET) rates can affect the amount of annual runoff, groundwater, and soil moisture. The shifting weather patterns have caused certain areas, such as Las Vegas and other regions in the U.S. Southwest, to experience less precipitation and changes in precipitation seasonality. Most published reports (e.g.,, Barnet and Pierce, 2008; Karl et al., 2009; IPCC, 2007) predict that the watershed and region as a whole will very likely experience a decreasing availability of water resources. There is a large uncertainty and variations in these future precipitation projections. As a result, this investigation was based on the ranges of climate change obtained from the 2000 and 2009 annual reports published by the United States Global Change Research Program (USGCRP). Climate models from the Hadley Centre in the United Kingdom and the Canadian Centre for Climate Modeling and Analysis were utilized for analysis. To generate future likely precipitation and temperature scenarios, these modeling results were further combined with the climate change information from IPCC (2007) and the historical observations of USGCRP (2000) and Karl et al. (2009).

Based on the scenario with no explicit climate policies put into place to reduce greenhouse gas emissions, the global average air temperature is projected to rise by 2.4°C to 6.4°C by the end of this century, and the temperature of the study area will increase by 4°C by the horizon year of 2050 (IPCC, 2007; Karl et al., 2009). In terms of precipitation in 2050, the projection results differ among the global climate models. The Hadley model projects that there will be a substantial increase in precipitation, with a percentage increase of 80-100% over California and Nevada and ~20% elsewhere in the U.S. The Canadian model also predicted a large increase of 80-100% over southern California and an increase of ~20% in the Great Lakes and Northern Plains, however the Canadian model also found regions with precipitation decreases exceeding 20% in the Oklahoma panhandle and the eastern U.S. The IPCC projection found a dryer condition occurring in the Southwest U.S. and little change or increasing precipitation in the northern U.S. Because of the incongruent results, both the wet and dry scenarios for future precipitation were considering during the investigation. The wet scenario (Wet) considered a 20% increase in precipitation and 4°C increase in temperature, whereas the dry scenario (Dry) considered a 20% decrease in precipitation and 4°C increase in temperature (Table 3). The percentages were chosen to be within the range for precipitation increases and decreases observed for the Hadley and Canadian models. According to these climate scenarios, historical temperature and precipitation time series data were adjusted and inserted to the HSPF hydrological model for simulating the watershed.

Population growth projections

The close relationship between population growth of an area and its watershed hydrology is well known (e.g., Buckingham and Whitney, 2007). Prior to the rapid population increase and urban development of the area, the Las Vegas Wash was an intermittent stream that carried storm water to the Colorado River. Due to the recent urban developments and population growth, the Wash is now carrying not only storm water runoff, but also urban wastewater treatment effluent. The average daily flow has

increased from 0.736 m^3/s in 1970 to 6.23 m^3/s in 2000 (Piechota and Bastista, 2003). Therefore, in order to better postulate the future hydrologic conditions in the Wash, it is essential to estimate the population growth of the study area. This estimate can be used as a surrogate to estimate the amounts of urban discharge to the Wash and can be used to facilitate a more accurate projection of land use changes.

Table 3   Climate change scenarios for the Southwest U.S.*

Climate Scenario	Changes in Temperature/Precipitation
Wet	+ 4 ^{0}C, + 20% Precipitation
Dry	+ 4 ^{0}C, - 20% Precipitation

Note: * - Sources; USGCRP (2000) and Karl et al. (2009).

Previous publications (Gabriel and Accinelli, 2007; Harris, 2005; Miranda and Lima, 2010) show that the growth of a population can often be accurately portrayed by the logistic function. The logistic population growth model uses an 'S' shaped curve, implying that when the environment has adequate resources, the population will grow exponentially, and when the population is in proportion to the natural resources and in alignment with the environmental carrying capacity, it will grow at a much slower rate or even at a constant rate. However, when resources become limited and the population is larger than the environmental carrying capacity, the growth rate will decrease, and will ultimately become zero (Gabriel and Accinelli, 2007). In the Las Vegas Valley, the population growth pattern resembles that of a logistic curve (Figure 13). Before the mid-20th century, the population growth was slow. From 1970 through 2000, the average annual population growth in Southern Nevada was 7 percent per year. This is the time period with an exponential growth of population. By 2000, Southern Nevada's population had increased to nearly 1.5 million people (SNWA, 2009). By the end of the 20th century, the population growth had become constant, growing at a rate of 3.4 percent in 2009. According to the model predictions from the Center for Business and Economic Research at the University of Nevada, by 2015, the growth rate will be at 2.6 percent, and by 2030, it will level off at around 1 percent. The forecast predicts a growth rate of 0.8 percent in the year 2050.

In this investigation, the logistic function available in the SPSS Statistics software package, release version 16.0.2, was employed for population analysis. A curve fitting equation was generated and statistics were estimated based on the urban area population data. The SPSS output for the population logistic function provided a curve fitting R-squared value of 0.995, indicating a high level of significance. Using the logistic equation generated, the future population was estimated up to the horizon year of 2050 (Figure 13). According to the model outputs, the population of the valley will be about 3.77 million by the 2050, which is more or less similar to the predictions by the Center for Business and Economic Research at the University of Nevada, which estimated a population of 3.85 million.

Future land use change scenario

With the city expansion and population increase, the Las Vegas region has undergone significant changes in land use. Specifically, for the last fifty years, there has been an increase in urban areas and a decrease in agriculture and pasture lands (Adhikari et al., 2011).

Changes in land use/land cover will affect the hydrologic conditions. Generally, an increase in impervious surfaces will cause local decreases in natural interception, infiltration, percolation, and soil moisture storage. Hence, the amount of runoff will increase. Less infiltration during storms and increasing overflow of effluents will create higher peak flows (SNWA, 2009). It is common that watersheds with large amounts of impervious cover have significantly reduced groundwater recharge and increased storm
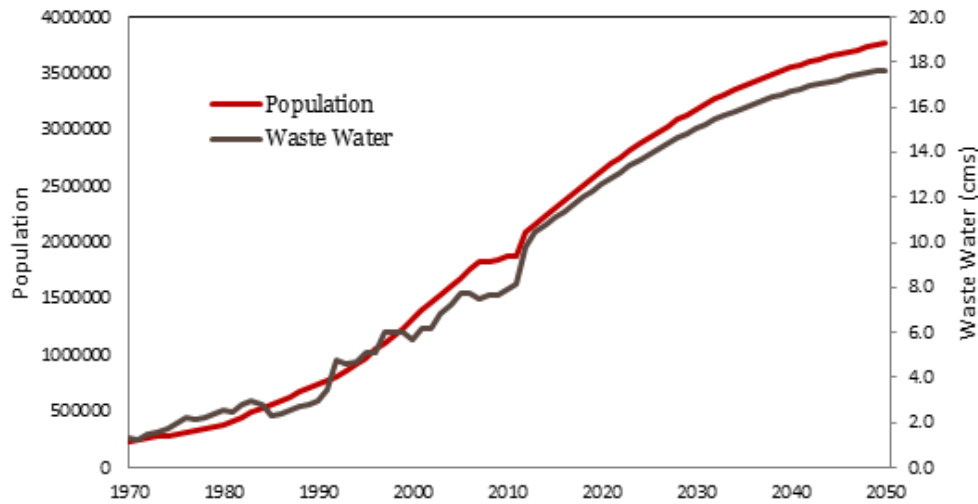
Figure 13   Future population and wastewater projection for the Las Vegas Wash watershed.

flow and flood frequency. With an increase in impervious cover, surface runoff has greater velocities, larger volumes, and shorter lag-times between peak rainfall and highest flow concentrations (Brun and Band, 2000). As the main drainage in a highly urbanized watershed, the Las Vegas Wash also shows similar characteristics in its hydrograph with sudden peak discharges that last for a short time period. To better understand the likely hydrologic impacts of urbanization, it is therefore essential to be able to predict future land use change.

A common approach to derive future land use scenarios is to use a land use model to simulate the future land use conditions. In this study, the CA land use model in IDRISI, developed for the Las Vegas Wash watershed by Sun et al. (2013), was used to simulate the land use conditions in the Las Vegas watershed for the year 2050. This model is an enhanced land use model coupling the CA–Markov model with a population variant to depict the effects of population growth on land use (Tong et al., 2012). Two sets of historical land use records were used to determine the pattern and the trend of land use and land cover changes, and an additional map was used for validation. The 1992 and 2001 land use/land cover maps from the USGS National Land Cover Dataset (NLCD) were adopted to develop the model, whereas the 2006 NLCD was used to validate the model. Additionally, the 2050 population estimate from the logistic equation was incorporated to the CA–Markov land use model to postulate the land use pattern in 2050. The projection results suggest that there would be a great increase in urban area and city expansion throughout the valley (Table 4). Figure 14 shows the postulated 2050 land use map of the Las Vegas watershed.

Estimating future wastewater discharge

More than 90% of the total water use of the Las Vegas Valley is population-dependent (SNWA, 2009). With the increase in urban population, more water is needed, and as Morris et al. (1997) and Buckingham and Whitney (2007) have suggested, more wastewater will be discharged into the Las Vegas Wash. The effects of the increase in population and tourism on stream discharge can be related to the increase in the discharge of treated sewage effluents and the volume of urban runoff from the increased amount of impervious surfaces. The wastewater generation and discharge are closely related to population in the watershed area (Figure 13). A linear regression between population and wastewater yielded a

35

highly significant Pearson correlation coefficient of 0.97 and a standard error of 0.002 (Ranatunga et al., 2014). Assuming the correlation remains constant in the future, if the water policy is unchanged, future wastewater generation can be estimated from the population alone.

Table 4. Land use projection for 2050

Land Cover/Use Type	1992 (Km^2)	2050 (Km^2)	% change from 1992
Urban	411.47	1875.77	355.87
Agriculture	29.48	2.78	-90.57
Forest	287.13	367.31	27.93
Water	2.54	43.41	1610.20
Range/Grass land	3730.44	2258.34	-39.46

3.3.3   Water budget analysis

Ranatunga et al (2014) described the modeling results of water budget analysis for the 2050 hydrologic conditions in the Las Vegas Wash watershed. Using a validated Hydrological Simulation Program in Fortran (HSPF), the quantitative analysis considers the effects of future climate, wastewater discharges generated from a growing population (WW), and the projected 2050 land use patterns (LU). The model was then used to simulate the impacts of wastewater discharge, climate change, and land use change under the following scenarios:

- Wastewater discharge with no change in climate and land use (Base + WW)
- Wastewater discharge with a wet climate and no land use change (Wet + WW)
- Wastewater discharge with a dry climate and no land use change (Dry + WW)
- Wastewater discharge with a wet climate and land use change (Wet + WW + LU)
- Wastewater discharge with a dry climate and land use change (Dry +WW + LU)
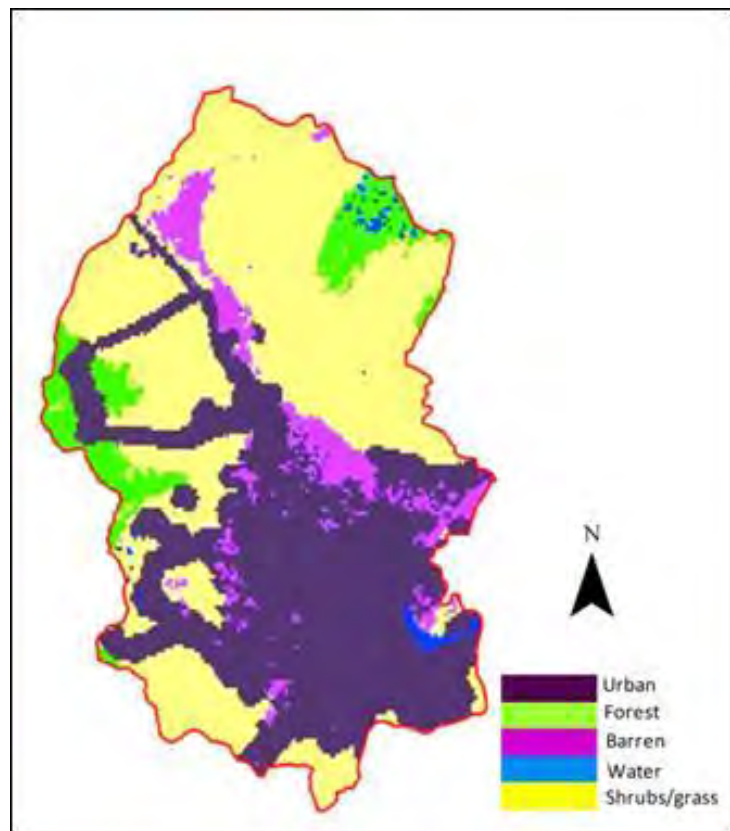
Figure 14   Projected 2050 land use/land cover map of Las Vegas Wash watershed.

Currently, water in the Colorado River is apportioned among the seven Colorado River Basin states for their total consumption or "net" use. Nevada receives $3.7*10^8$ m^3 of water per year from the

Colorado River for consumptive use (SNWA, 2009). Since Las Vegas is the main population center of the state, almost all of the apportioned water to Nevada is drawn by the city. A water credit for use in the same year is claimed when treated reclaimed water is returned to Lake Mead through the Las Vegas Wash. Each year, through this return flow credit, southern Nevada is able to divert more water than its consumptive use (SNWA, 2009; Cooley et al., 2007). As about 90% of the total stream discharge of the Wash is composed of treated wastewater (Piechota and Bastista, 2003; Cooley et al., 2007), the amount of urban wastewater generated from the population in the watershed is one of the most important factors determining future flow estimates.
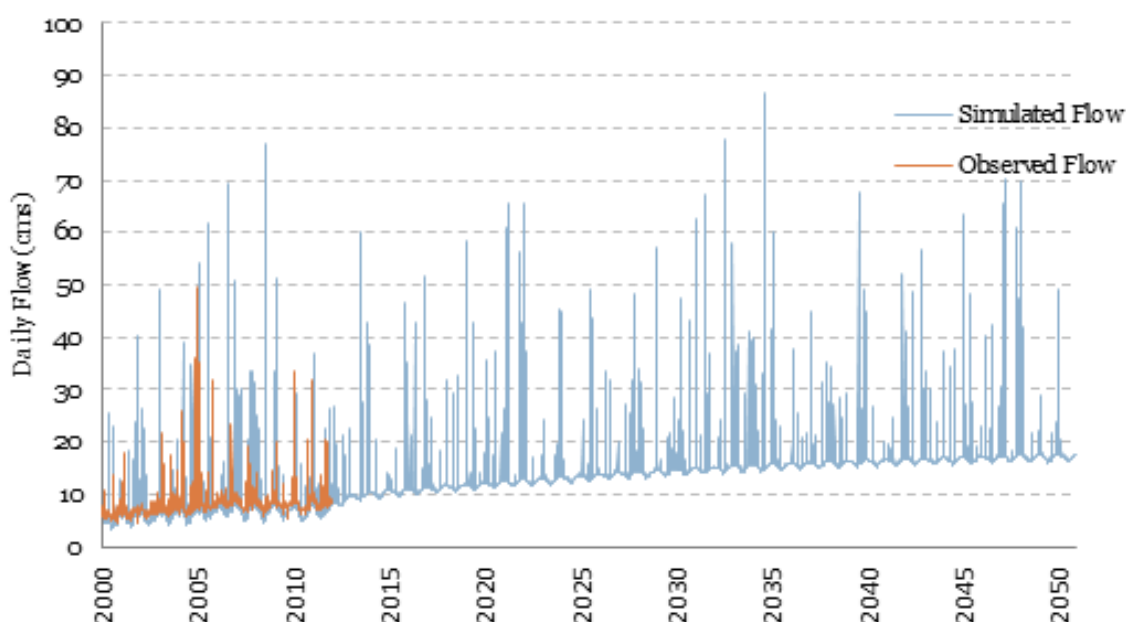
Figure 15   HSPF Simulated continuous stream discharge with wastewater projections for the Base + WW condition

The model simulations indicated that future land use and climate conditions will have a considerable effect on return water flows. Although climate and land use changes affect only 10% of the total stream discharge, changes in the peak flow can be observed under different climate and land use scenarios. As shown in Figure 15, the HSPF simulation reproduced the baseline flow fairly well during the calibration period, while it did miss several flow peaks. Even if no climate or land use changes occur in the future, the wastewater discharge to the Wash would still increase in response to the population increase. This increase is shown in both base flow and peak flows. The projected daily discharge of the Wash is a 2.5 fold greater in 2050 when compared to the observed flow in 1992. The average annual flow rate is projected to increase from 6.23 m^3/s in 1992 to 17.69 m^3/s by 2050.

The modeling results that include both climate and land use change show that land use changes have a significant impact on stream discharge. From Sun et al. (2013), the urban area of the Las Vegas Valley is projected to increase by 355% from 1992 to 2050 (Table 4). The increase in impervious surfaces has a significant impact on stream discharge, especially for the peak flow during storm events. This effect is amplified by climate change effects. Under the Wet climate change scenario (Wet + WW + LU), larger flow events occur at a higher frequency of 33 times a year (Table 5). Most importantly, the peak flow can

reach 373.78 m³/s. This scenario also gives the highest percentage increase of total discharge, 16.59%, with an average flow rate of 20.6 m³/s (Table 5).

Table 5. Projected high stream flows and average annual flow of the Las Vegas Wash in 2050 with returned wastewater under a set of climate and land use scenarios*

Scenario	Highest Flow Occurrences		Average Annual Flow	
	Frequency over 70 m³/s	Highest value (m³/s)	Flow rate (m³/s)	% change from Base + WW
Base + WW	1	70.51	17.66	
Wet + WW	4	83.25	18.01	1.95
Dry + WW	0	57.77	17.35	-1.78
Wet + WW + LU	33	373.78	20.60	16.59
Dry + WW + LU	16	106.19	18.42	4.28

Note: * - Modified from Ranatunga et al. (2014). Significant digits are from reference; m³/s –cubic meter per second. Scenarios modeled include: Wastewater (WW) discharge with no change in climate or land use (LU) = Base + WW; WW discharge with a wet climate and no LU change = Wet + WW; WW discharge with a dry climate and no LU change = Dry + WW; Wet + WW with land use change = Wet + WW + LU; Dry + WW with LU change = Dry +WW + LU.

For the scenario of a Dry climate with incorporated land use changes (Dry + WW + LU), the peak flow also increases, but to a lesser extent than for the Wet climate scenario (Table 5). On the other hand, the frequency of peak flow events is higher than for the base scenario (Base + WW) for the Dry scenario with no land use changes (Dry + WW). Among all the scenarios studied, the projections of this scenario are critical. Most of the other recent modeling efforts predict hot and dry climate trends and increased urbanization in this region in the future. According to the model projections, there would be 16 flow events with an average flow larger than 70 m³/s, and the largest flow event would be 106.19 m³/s (Table 5). Overall, for the Dry + WW + LU scenario, the total average flow would increase by 4.28% compared to the base scenario. This could be due to larger runoff volumes during storm events as a result of increasing impervious surfaces.

Generally, the results show a 2.5 fold increase in the average daily discharge into the Wash by the mid-21st century if the projected population growth continues. Apart from the increase in the average flows, there will be more extreme flood events caused by climate and land use changes. These kinds of destructive events can be controlled by applying best management practices (BMPs), such as constructing detention basins or ponds (Welty, 2009). It is also important to note that these projections are not able to account for technological advances which can occur in the future, leading to the increased efficiency of these BMPs. In this watershed, excessive use of detention basins is not encouraged as it may reduce the amount of runoff that will channel to Lake Mead, and the Las Vegas Valley may not get as many return flow credits. However, in order to control floods, it is necessary to have some detention basins. Currently, there are 39 detention basins throughout the watershed and another 30 basins have been planned (LVWCC, 1999). These detention basins are designed to reduce peak storm water flows by detaining water and releasing it over a period of less than seven days.

3.3.4   The role of water conservation and storage in meeting future water demands

Currently, the Southern Nevada Water Authority has operated a large ASR facility for consistent water supplies since 1985. Operation of this ASR system relies on water from Lake Mead. Water

withdrawn from the Lake is stored in the aquifer for use in other seasons. However, due to a decade of chronic drought in the area, water level in Lake Mead has dropped over 130 feet from 2000 to 2014 (SWNA, 2015). The inflow from Colorado River and other tributaries, including the Muddy River and Lower Virgin River, has shown consistent decline. In addition, these areas heavily depend upon the snowmelt from snow caps on high altitude mountains. As the climate warms, the peak flow at the snowmelt-fed streams has shifted to be earlier to the spring season.

Based on the quantitative investigation results, the total water balance between water supply and demand was further investigated for a period up to the year 2050. Figure 16 shows the time-evolution of major fixed fresh water supplies and the total demand estimated using population projections. Outcomes indicate that the Las Vegas Valley system should have an adequate water supply from the existing sources until the early 2020s. The plot analysis shows the cutoff year as 2024. After this time, the demand will exceed the total amount of water available, and the valley will need to find other alternative sources of fresh water. The estimated demand of water by 2024 is 9.55×10^8 m^3 per year, and this estimated demand increases up to 1.33×10^9 m^3 per year by 2050. Based on the 2010 SNWA annual report, the main sources of water supply for the area are the Colorado River, Las Vegas Valley groundwater supplemented by existing ASR operations, Virgin/Muddy Rivers Tributary and Coyote Spring Valley Groundwater Intentionally Created Surplus conservations, and Drop 2 Reservoir System Efficiency Intentionally Created Surplus. These supplies can provide adequate water until 2024. After that time, the model predicts that there may not be enough water to meet the demand.

The potential deficit after 2024 can be a challenge to water authorities in the Las Vegas Valley. The total water deficit is projected to increase up to nearly 2.46×10^8 m^3 per year by 2050 (Figure 16). According to the 2009 SNWA water resources plan, there are multiple potential sources that the authorities have targeted to bring more water to the valley. There are plans to draw water from other groundwater resources in Clark, Lincoln, and White Pine Counties. SNWA is also planning to build a massive pipeline system that would take underground water from the Great Basin aquifer system, located about 482.8 km north of Las Vegas, and pump it to Las Vegas. The plan calls for transferring up to 2.22×10^8 m^3 of water per year from rural Nevada to the Las Vegas Valley (Progressive Leadership Alliance of Nevada, 2006). However, these long-distance water transfer options can have detrimental environmental impacts; for example, water transfer from the Great Basin area could result in declining groundwater levels and could impact the area's biodiversity. Other potential water supplies include sea water desalinization, brackish water desalinization, and withdrawal from water banks, such as the Arizona, California, and Southern Nevada water banks.

Water conservation is the other option to reduce the future gap between water supply and demand. Through conservation practices, such as education, water pricing, regulations and incentives, and water-less landscaping, SNWA is planning to reduce the per capita water use by 0.753 m^3 per capita per day by 2035. With conservation practices, SNWA has already reduced consumptive use by roughly 7.9×10^7 m^3 annually between 2002 and 2008 (SNWA, 2009). It is anticipated that this conservation plan could save 3.4×10^8 m^3 of water annually by 2035.

The projected discharge analysis of Las Vegas Wash in this investigation indicates that the return flow credit from the Wash is a significant source of water. With an increase in population, the total indoor and outdoor water use will increase. Studies suggest that a higher outdoor water use may lead to a higher loss of water from the hydrologic system through evaporation (Qaiser et al., 2011; Stave, 2003). Therefore wastewater reuse for outdoor applications is less attractive than return flow and discharge back to Lake Mead for the return flow credit.
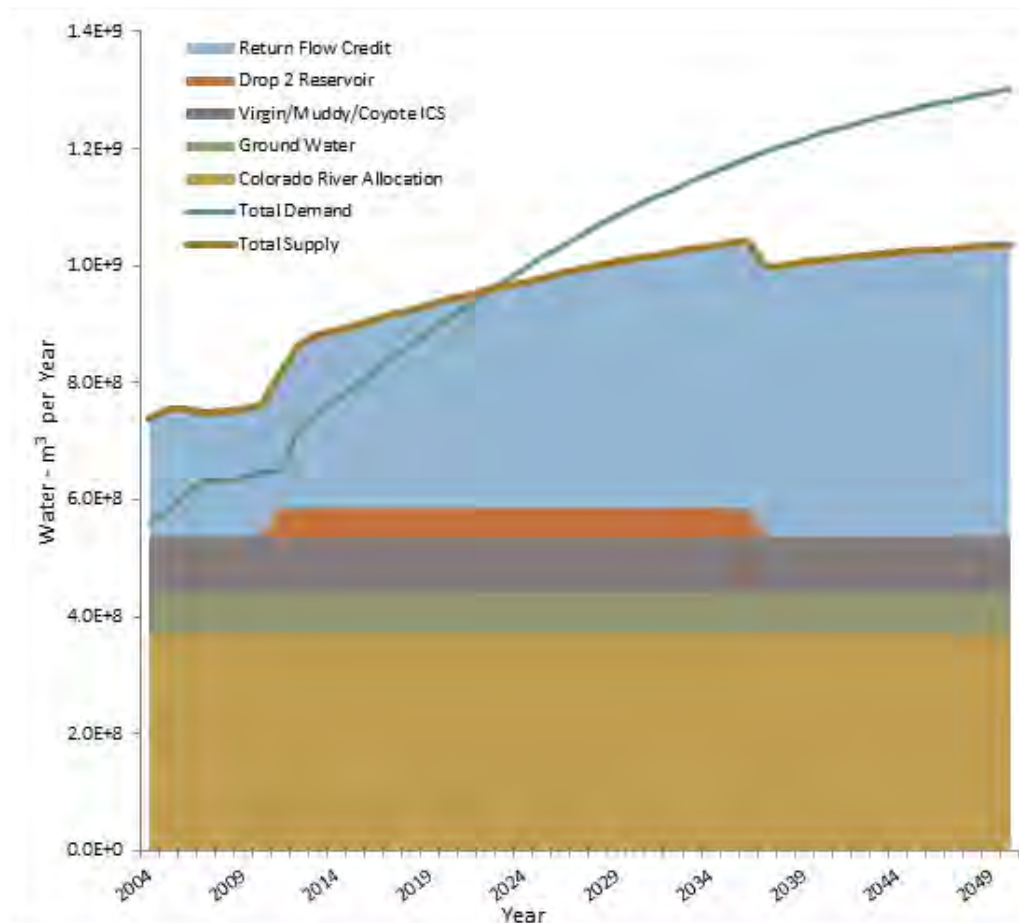
Figure 16   The projections of total water demand and supply, showing the importance of return flow credit from the Las Vegas Wash stream flow in the sustainable water supply for the region. Adopted from Ranatunga et al. (2014).

It is necessary to note the magnitude and composition of the Las Vegas Wash return flow. Reclaimed wastewater effluent is a large portion of the base flow, while overland runoff and flash flood water predominate the stream during peak flow events. The peak flow rate is many times greater than the base flow (See Figure 15 and Table 5). Lake Mead is one primary storage facility for surface runoff and return flows. Additional storage capacity could help capture the maximum amount of return flows during the peak flow periods, and can be later used to supplement water during the dry season. ASR expansion from the current "water bank" operation is therefore a viable option for planning, with the capture and storage of such large flows at the center of adaptation.

The Las Vegas case study shows how to conduct the climate change and water availability, as well as water demand in the ASR-Need analysis (See Figure 5). The results demonstrate the potential for ASR application to prevent future water gaps, which are predicted to occur by the year 2024. This analysis allows organizations such as the Southern Nevada Water Authority to be proactive when planning how to meet growing water demands, as well as incorporating the impacts of population growth and global climate change. This analysis method can be applied to other locations considering whether the implementation of ASR is a viable means of meeting future water demands. The Level 1 tool is designed

to support this analysis by including projections for current water demands, projected population increases, and projections for temperature and precipitation changes under different representative concentration pathways for GHG emissions.

4.0   ASR Facility Planning and Assessment

4.1   Assessment for ASR Planning

The initial stage of ASR site planning is often focused on hydrological and environmental assessment. Major objectives are: 1) Evaluate the hydrological viability of candidate ASR site, including injection rate, storage capacity, and injection-related geotechnical factors; 2) Assess likely geochemical compatibility of the storing groundwater aquifer and approximate the likelihood of negative groundwater impacts; and 3) When recovery is involved, determine the degree of hydraulic control over injected water and calculate the rate of recovery.

4.1.1   *Infiltration rate and storage capacity*

The overall water infiltration rate depends on the vertical water infiltration rate in vadose zone and, when directly injected into an aquifer, is a function of the injection well or infiltration trench design and aquifer hydraulic conductivity. Related groundwater principles for these determinations have long been established by Darcy's law for incompressible groundwater. For groundwater head (h) distribution in an aquifer with a flow sink/source term, G, the generalized Darcy's law is:

$$\frac{\partial h}{\partial t} = \alpha \nabla^2 h - G \qquad\qquad (5)$$

Hydraulic diffusivity (α) is a ratio of hydraulic conductivity (k) and specific storage (S_s) for confined aquifer (k/S_s), or a ratio of transmissivity and specific storage (T/S_s) for an unconfined aquifer, where the transmissivity $T(= k \cdot b)$ is a product of the hydraulic conductivity and aquifer thickness (b) (See Section 4.1.3 below).

The general Darcy's law has been applied to describe various groundwater systems and hydraulic devices such as wells, trenches and fractures. The familiar Theis (1935) equation, Jacob equation for wells in a confined aquifer, and the Boussinesq equation for homogeneous and isotropic aquifers are also commonly used. For practical engineers, the fundamentals of groundwater hydraulics, their complexity and their relevance to groundwater system design can be found in the book "Groundwater and Wells" by Driscoll (1986).

Furthermore, groundwater systems for ASR operation vary between locations. Commonly encountered types include groundwater flow in homogeneous isotropic, homogeneous anisotropic, inhomogeneous anisotropic, and leaky confined aquifers, and those counterparts in unconfined aquifers. In addition, natural groundwater aquifers may vary in lateral extent, contain impermeable layers or lenses, or contain geological discontinuities such as faults for conduit flows. This degree of complexity in hydrogeological groundwater systems will require numerical solutions to Eq.5 to determine the groundwater flow fields in ASR design and evaluation. This can be accomplished using 3-D flow packages such as MODFLOW from the U.S. Geological Survey. Such numerical modeling tools will be described in Section 5.0.

ASR planning and assessment commonly relies on fast and less accurate hydrogeological characterization of the flow systems. The planning focus is often limited to the assessment of hydraulic properties (e.g., infiltration rate and storage capacity), assessment of chemical fate and transport, and

groundwater geochemical compatibility. For simplicity, the governing Eq.5 is solved to yield an analytical equation for simple calculations. For hydraulics of an ASR well or trench, the following equations are widely utilized, which assume an infinite homogenous and isotropic aquifer.

Theiss solution for groundwater pumping or an injection well:

The most widely used Theiss equation specifies that the drawdown from a pumping well or mounding from injection is positively related to pumping or injection rate (Q), and inversely related to aquifer transmissivity $T (= k \cdot b)$,

$$ s = \frac{Q}{4\pi T} W \left(\frac{r^2 S}{4Tt} \right). \tag{6} $$

In this equation, the well function, $W(u)$, consists of $u = \frac{r^2 S}{4Tt}$ where r is the well radius and t is the time lapsed after the start of pumping or injection. The well function is often provided in graphic form in groundwater handbooks or engineering guidelines (e.g., Driscoll, 1986).

The SuperQ Excel spreadsheet model included in this DDS is based on the simple Theiss equation, and is suitable for rapid assessment in the planning phase. It is noted that the Theiss equation assumes a negligible regional groundwater flow field compared to the pumping or injection rate. There are many ASR applications which have multiple wells and are under a significant regional flow field. In these cases, the groundwater hydraulics of the ASR system is 2-D in nature. Thus, programs using 2-D flows are necessary in planning assessment. Such programs include the Hantush (1967) model and the more sophisticated WhAEM2000 (U.S. EPA, 2007) model in the DSS tool box.

Groundwater flow velocity or infiltration rate

Derived from Eq.5, the groundwater flow velocity or infiltration rate (v) is simply given by:

$$ v = nk \frac{h_2 - h_1}{x_2 - x_1} = nki \;, \tag{7} $$

where n is the effective aquifer/soil porosity, h_2 and h_1 are the groundwater heads at locations x_2 and x_1 along a flow path, respectively, and i is the hydraulic gradient. For vertical infiltration in the vadose zone, $i = 1$.

The modified Darcy equation in Eq.7 can be used to approximate the groundwater infiltration rate in the vadose zone. The groundwater flux or infiltration rate from a spreading basin or green infrastructure (e.g., rain garden) of area A is equal to $(nki)A$. Eq.7 can also be applied to estimate injection rate from an infiltration gallery penetrating into the top of an aquifer. In this analysis, the side wall area of the trench (A) is used and the hydraulic gradient i is averaged from the trench to the edge of groundwater mounding.

Groundwater storage capacity

Storing aquifers can have a limited storage capacity, particularly if they are shallow, unconfined aquifers. Many permeable geological formations, such as unconsolidated sands, can have a large variation of thickness and poor lateral extension, affecting their storage capacity. For example, sand lenses interbedded with impermeable clay layers can have a limited capacity.

In practice, the overall storage capacity for the target injection formation is estimated during the planning process, particularly for large ASR operations. The total storage volume is approximately equal to the total effective porosity in the storage aquifer formation.

4.1.2   Simplified fate and transport analysis

One important planning consideration is the hydraulic control of injected water, which can impact both the injected water recovery rate and the potential for groundwater contamination from residual and mobilized contaminants. In ASR planning, these considerations can be assessed in three areas.

Hydraulic controls

Hydraulic control over the migration of injected water in an ASR system has several management implications in ASR planning and assessment. The degree of hydraulic control determines the rate of recovery and thus ASR efficiency. The hydraulic control will also affect the fate and transport of residual contaminants in the injected water and the mobilization of contaminants from aquifer materials. Because of this significance, ASR design and evaluation may demand high confidence when assessing the hydraulic control and numerical methods, such as MODFLOW, are commonly used. In the planning phase, limited technical assessment may focus on achieving hydraulic control through a set of investigative options:

- *Hydrogeological assessment*. The ASR local and regional hydrogeology data may be collected and analyzed to assess the suitability of groundwater aquifers for potential ASR operations. For example, a shallow and self-contained aquifer is often more preferable than a deep potable aquifer under strong regional flow gradients. The aquifer depth increases ASR capital and operational costs, and a strong regional flow makes hydraulic control more difficult to achieve.

- *Groundwater flow modeling*. Groundwater modeling is conducted to quantitatively evaluate hydraulic control in ASR planning. For this objective, the groundwater system is simplified by applying a 2-D model instead of a 3-D numerical model. Modeling results are the basis for estimating the rate of recovery and groundwater flow fields. WhAEM2000 or its visual version are capable groundwater modeling during the ASR planning phase.

Fate and transport analysis

Contaminant transport during ASR operations is shown in Figure 3 and discussed in Section 2.1.3. The geochemical processes involved in transport include adsorption, ventilation, reaction and transformation. A generalized governing equation for solute transport in a porous media is given by:

$$\theta \frac{\partial C}{\partial t} = \theta \nabla^2 (D \cdot C) - \nabla(v_{x,y,z} C) - Q_s, \tag{8}$$

where C is the solute concentration in groundwater, θ is volumetric water content or degrees of soil saturation, and D is solute dispersion coefficient. On the right side of Eq.8, the first and the second term describe solute diffusion and advection, respectively, while the third term, Q_s, is a lump sum of the solute reaction, formation, and transformation terms.

Eq.8 is adopted to simulate solute transport in soil and groundwater even for complex hydrogeological conditions. MT3DMS, a multi-species 3-D transport model included in this DSS, can be used to simulate the advection, dispersion, and chemical reactions of contaminants in groundwater systems. These analysis results are suitable for the ASR system's design and evaluation phase.

For planning purposes, less accurate yet computationally-efficient models using analytical or semi-analytical solutions have been developed and used. Examples include AT123D (Yeh, 1981) and its updated version, AT123-AT (Burnell et al., 2012). These 1-D or 2-D models were developed by simplifying Eq.8 under a given set of assumptions. More details on analytical solute transport models are available in reviews, guides and books (e.g., Dagan, 1987; Anderson and Woessner, 2002). For the ASR DSS, the AT123D-AT and a related 2-D multi-species reaction model are described in Section 4.2.

Geochemical compatibility analysis

Injected water in an ASR operation is geochemically different from the native groundwater, which can potentially trigger reactions between the injected water and minerals in the hosting aquifer. Examples include arsenic mobilization and the dissolution of other heavy metals into the aqueous phase. Mineral precipitation and dissolution may also occur, leading to changes in aquifer hydrological properties. All of these potential scenarios are assessed during geochemical compatibility analysis.

The geochemical compatibility assessment can take several steps. The EPA UIC program has guidelines on the ASR geochemical compatibility analysis. The steps in this technical analysis include 1) Chemical characterization of injected water, native groundwater, and geological formations, 2) Modeling and analysis of geochemical conditions in ASR operation scenarios, 3) Qualitative and quantitative assessment of potential geochemical reactions, 4) Development of potential technical solutions through pre-injection treatment (See Figures 3 and 5) and monitoring program development.

ASR planning may take the first two steps and conduct a qualitative assessment of the geochemical compatibility. This analysis may hinge on hydrological and geochemical data collected during ASR DSS Level 1 activities (See Figure 5). Commonly used analysis methods include:

- *Geochemical change monitoring and analysis*. Groundwater chemistry changes at a given location during water injection and recovery phases. The changes in major ionic species concentrations are shown in Piper diagrams, which serve as geochemical evidence to support an operation permit application at an aquifer recharge site. These types of geochemical analyses are often integrated with the investigation of potential mineral reactions, providing direct evidence for likely geochemical changes.

- *ASR reference site information*. Additionally, geochemical information about other relevant sites can help the compatibility analysis during the planning phase. Geochemical data from nearby or regional ASR operations occurring in the same or similar geological formations can help when evaluating the injected water compatibility and identifying major controlling environmental factors

4.1.3 *Arsenic mobilization assessment*

The mobilization of arsenic and other heavy metals at ASR facilities is a major concern to the EPA UIC program due to their detrimental environmental and human health impacts. Natural and secondary arsenic contamination in groundwater has been reported worldwide and at many ASR sites in the U.S. (Welch et al., 2000; Neil et al., 2012). This ASR DSS has singled out arsenic as an indicative contaminant for planning assessment and design/evaluation analysis.

Multivalent arsenic species (As^{3+}, As^{5+}) have different geochemical mobility in groundwater. Changes in water chemistry (e.g., pH, Eh, TSS) inside and near the injection bubble can lead to the breakdown of arsenic-bearing minerals and the dissolution of soluble arsenic complexes into the groundwater. In Appendix A, an extensive technical investigation is described on the specific geochemical processes and mechanisms of arsenic mobilization from arsenopyrite in reclaimed water and model wastewaters. These EPA investigation results have been published in Neil et al. (2014; 2012).

In summary, there are several nano- to micro-scale processes controlling arsenic fate and transport during ASR, and hence their environmental impact. The outcome of these processes will affect ASR planning, design and operation. Currently there are no established arsenic control guidelines for the implementation of ASR, in part due to inadequate knowledge of the soil-water interactions and factors controlling arsenic mobilization (Asano and Cotruvo, 2004). Nonetheless, these new observations on the geochemical pathways in the As-Fe-S-Cl-N system have implications for the longer term fate and transport of arsenic in groundwater aquifers. Major geochemical inferences from the EPA investigations include:

- Arsenic mobilization in groundwater is balanced between the oxidative breakdown of host minerals, such as arsenopyrite, and the precipitation of iron oxides and iron-oxyhydroxides. The latter promotes the co-precipitation or sorption of soluble arsenic in groundwater.

- Arsenic associated with the stable iron oxide minerals will be trapped as long as the aqueous environment is favorable for Fe^{3+} (e.g., oxidative environments). High TOC content in the injected water can enhance biological activities, creating locally reductive conditions. These reductive conditions could prevent arsenopyrite oxidative dissolution, but could also potentially lead to the destabilization of arsenic trapped in iron oxides where present.

- Activation energies for arsenic mobilization in aerobic and anaerobic systems containing sodium nitrate, sodium chloride, and wastewater samples were experimentally determined. Differences in activation energies between the systems indicate that the mechanisms controlling arsenopyrite dissolution and the propensity for arsenic mobilization can vary with dissolved oxygen presence.

These considerations form a basis for developing ASR monitoring programs, modeling arsenic fate and transport, and determining pretreatment requirements for the injected water. Pretreatment is often a necessary part of ASR systems (See Figure 1). There is currently a knowledge gap on how water pretreatment and water withdrawal will affect arsenic mobilization. The EPA investigation on arsenopyrite−water interactions has revealed the following observations:

1) The difference in water chemistry (pH, Eh, ORP, etc.) between the injected water and native groundwater can cause arsenic mobilization in groundwater. Pretreatment of the injected water to reduce this difference can thus minimize adverse reactions.

2) Several geochemical pathways are involved in dissolution and precipitation of arsenic-bearing iron oxyhydroxides, and thus control arsenic mobility. The processes are facilitated by the presence of DOM, chloride ions, nitrate, sulphur and oxidants (or ORP) under a given set of pH-Eh conditions. On the other side, excessive Fe^{3+} concentrations in groundwater can lead to iron oxyhydroxide precipitation and enhanced arsenic encapsulation.

3) Biological activities enhanced by DOM can lead to local reductive environmental conditions, which can prevent arsenopyrite oxidation but may also promote iron oxide and iron oxyhydroxide dissolution.

4) Injection-withdrawal operation and groundwater cycling can change the environmental conditions in the ASR formation, thus affecting the arsenic mobility. Predictive modeling of groundwater hydrology can help with ASR monitoring and with developing injected water pretreatment requirements.

Therefore, during ASR planning and assessment, geochemical analysis of the injected water and native groundwater is necessary to estimate the likelihood of arsenic mobilization. Such analysis may help to assess whether the aquifer is suitable for ASR operation and whether there is a need for above-ground pretreatment of the injected water. As described in Appendix A, multiple factors, including aquifer site hydrology, can impact arsenic mobility. Thus, detailed geochemical modeling and engineering analysis is necessary during the ASR design and evaluation phase. This consideration is described in Section 5.0.

4.1.4   *Data sources and assessment limitations*

ASR planning and assessment, as described above, is based on the quantitative analysis of site hydrology and contaminant fate and transport. For this analysis, the pertinent site-specific data include:

- *Site hydrology*. Published geological and hydrological investigations are available for many parts of the U.S. Investigations of ASR sites that are in close geographic proximity or have similar hydrogeologic settings can be a valuable reference for ASR planning and assessment. The ASR DSS Level 1 provides pertinent weblinks to USGS, EPA, and other data sources. Because of large variations in ASR site hydrology, site-specific hydrologic data and analyses are preferable. Technical information and data sources are available from the EPA UIC program[7]. One of the most important hydrologic parameters is the soil permeability and aquifer conductivity. Their variations are used to quantify the hydrological heterogeneity, and are important to ASR planning and assessment.

- Hydrological investigation methods include soil grain size analysis for the vadose zone, and slug tests and pumping tests for aquifers. Unconfined aquifers are most commonly used for in ASR operations. Methods the hydrological characterization of unconfined aquifers are well examined and documented in the literature (e.g., Fetter, 1994; Yang and Gates, 1997; Batu, 1998; and references therein).

- *Geochemical characterization of native groundwater and injected water*. Chemical compositions of the native groundwater and injected water are necessary to assess their interactions at an ASR site. For the areas of analysis described in the preceding section, a set of the geochemical data is necessary including ORP, pH, Eh, DOM, cation species (particularly Fe^{3+} and Fe^{2+}), as well as S, P, Cl, and N. These geochemical data can be obtained during conventional sampling of groundwater and reclaimed water.

- *Modeling and quantitative analysis*. In the ASR planning phase, quantitative modeling of injected water infiltration, flow and geochemical reactions in groundwater only has the objective of assessing the overall groundwater flow, hydraulic control, and adverse geochemical reactions. The results are limited to determining the feasibility of ASR operations for a given site. Detailed ASR operational design and evaluation often require more detailed technical and modeling analysis, particularly on site heterogeneity and geochemical reactions including arsenic mobilization. The technical approach supporting this analysis is presented in Section 5.0.

4.2   Assessment tools in the ASR DSS

Analytical models (partial differential equations with initial and boundary conditions that mathematically describe solute transport) can be used to estimate the flux and concentration of dissolved pollutants in groundwater. These models typically simulate advection, hydrodynamic dispersion, linear sorption, and first order reactions that affect pollutant fate and transport. A number of solutions have been presented over the past 50 years for various source terms, initial conditions, and boundary conditions. When equations have a closed form solution, they are called analytical models. When numerical methods (e.g. integration) are necessary to calculate the concentrations in the closed form solution, they are called semi-analytical models.

4.2.1   *Hantush (1967) 2-D Transient Mounding Excel Spreadsheet Model[8]*

Analytical equations (partial differential equations with initial and boundary conditions that mathematically describe groundwater flow) can be used to estimate the magnitude and radius of groundwater mounding beneath an infiltration basin or dry well, but the accuracy of these results is limited by simplifying assumptions that are inherent to solving non-linear differential equations. Hantush (1967) proposed an equation describing the "growth and decay of groundwater mounds in response to

---

[7] http://water.epa.gov/type/groundwater/uic/aquiferrecharge.cfm#links
[8] Modified from Carleton (2010), pp. 22-24

uniform percolation." The Hantush equation and similar equations are widely implemented to estimate water-table mounding beneath septic systems and other similar infiltration structures that can reasonably be considered steady-state (i.e., infiltration is constant over time) (Finnemore, 1995). However, few studies have implemented this equation to the more challenging scenario of transient conditions (infiltration occurs over a limited duration, then ceases). This scenario is addressed by the numerical solution, which utilizes Microsoft Excel. The numerical solution is distributed by the USGS and linked to herein.

Hantush (1967) assumes a water-table aquifer of infinite extent and finite thickness with a horizontal, impermeable base. The solution also includes the Dupuit assumptions of horizontal flow and a negligible change of transmissivity with a change in the head. Hantush (1967) solves the general 2-D groundwater flow equation by assuming boundary conditions that allows the use of a Laplace transform with respect to time and the Fourier cosine transform with respect to x and then y to derive an integral that can be solved. The solution that Hantush derived by making these assumptions provides results that correspond well with similar analytical solutions and with some field measurements.

Finite-difference numerical simulations of groundwater mounding show that vertical anisotropy can lead to simulated groundwater-mound heights on the order of 15 percent higher than those simulated using an analytical solution with the assumption that flow is strictly horizontal. In addition, simulations that include storage in, and delayed yield from, the unsaturated zone result in less groundwater mounding than that obtained by neglecting the unsaturated zone. Therefore, the height of groundwater mounding is underestimated by the Hantush equation where vertical anisotropy is present and overestimated where an unsaturated zone is present.

The Excel spreadsheet developed by the USGS using the Hantush equation calculates the magnitude of groundwater mounding. The required input values (aquifer thickness, horizontal hydraulic conductivity, specific yield, basin size, and recharge rate and duration) are straightforward and can be measured or estimated from published values. This spreadsheet allows users to specify input variables and generate reasonable, quantified, reproducible estimates of groundwater mounding beneath water infiltration structures.

4.2.2   *SuperQ: 2-D Transient Well Hydraulics Superposition Excel Spreadsheet Model*

Based on simplifying assumptions (e.g., uniform aquifer transmissivity and storage coefficient) and superposition theory, analytical solutions for well hydraulics equations, such as the Theis (1935) equation, that are implemented in aquifer test analysis software programs (e.g., Aqtesolv, AquiferWin32, and AquiferTestPro) can be used to forward calculate the time-dependent drawdown (and mounding) caused by extraction and injection from multiple wells with time-varying pumping rates, considering barrier and recharge boundary effects. These commercial software programs can thus be used to model aquifer storage and recovery operations and evaluate related design and system performance issues.

Free software developed to calculate hydraulic head changes caused by multiple wells with variable pumping rates and aquifer boundaries based on the Theis (1935) or other well hydraulics equations were not found during recent searches. Thus, Tetra Tech developed an Excel spreadsheet program named SuperQ that can be used to model the 2-D transient effects of aquifer storage and recovery pumping involving multiple wells, time-varying pumping rates, and boundary conditions represented using image well theory (Ferris et al., 1962). Two analytical solutions are currently included in SuperQ: the Theis (1935) solution for transient flow to a fully-penetrating well in a uniform confined aquifer with no leakage and the Hantush and Jacob (1955) solution for transient flow to a fully

47

penetrating well in a uniform leaky confined aquifer. Drawdown calculations are made using functions programmed by Hunt (2005).

The SuperQ program utilizes an Excel spreadsheet to document user inputs. The user specifies the aquifer transmissivity and storage coefficient, aquitard properties (thickness and vertical hydraulic conductivity), pumping well information (well locations, pumping periods, pumping rates), initial hydraulic head information, head change calculations, times and locations, and boundary conditions. Calculated drawdown and head values are reported in table format, which can be exported to contouring programs such as Surfer, in Excel hydrographs, and as areal drawdown and head plots using Excel's 'clunky' surface graphing utility. An output report is also written. Compiled values of storage coefficients and transmissivities for different types of geologic media are provided for reference. Different spreadsheet tabs are used to input program data, report output data, and provide reference hydraulic property data.

SuperQ has been tested by comparing results for various simulation scenarios with the Aqtesolv program. Simulation results match between the two programs. Note, however, that SuperQ is undergoing further development and testing. Not all boundary condition options have been incorporated into SuperQ, Additional error checking will also be added into the program (for example, to prevent input of pumping wells on the wrong side of boundaries, which could add erroneous pumping in the pertinent model domain). An updated version of SuperQ will be provided within the next few months.

4.2.3   2-D model: WhAEM2000 version 3.2.1[9]

WhAEM2000 (U.S.EPA, 2007) is a public domain AEM code that simulates 2-D steady flow caused by pumping wells, hydrologic boundaries (river, recharge, and no-flow conditions), and inhomogeneous zones. It incorporates an easy-to-use graphical user interface (GUI). Base maps for a project can be selected from a graphical index map for the State on an EPA webserver or input from others sources and file types (including shp, dwg, dxf, jpg, bmp, sid, tiff and other formats). Program operation and modeling practice is documented in the EPA report "Working with WhAEM2000" using Vincennes, Indiana as a case study (U.S.EPA, 2007). Frequently asked questions are addressed by Kraemer (2005).

The AEM method, which is described in detail by Strack (1989) and Haitjema (1995), avoids the discretization of a groundwater flow domain by grids or element networks. Instead, only the surface water features in the domain are discretized, broken up in sections (usually a few hundred), and entered into the model as input data. Each of these stream sections or lake sections is represented by a closed form analytic solution: the analytic element. The comprehensive solution to a complex, regional groundwater flow problem is then obtained by the superposition of all analytic elements in the model. Traditionally, the superposition of analytic functions was considered to be limited to homogeneous aquifers with a constant transmissivity. However, by formulating the groundwater flow problem in terms of appropriately chosen discharge potentials, rather than piezometric heads, the analytic element method becomes applicable to both confined and unconfined flow conditions, as well as to heterogeneous aquifers. The analytic elements are chosen to best represent certain hydrologic features. For instance, stream sections and lake boundaries are represented by line sinks, while small lakes or wetlands may be represented by areal sink distributions. Areal recharge is modeled by areal source distributions (areal sinks with a negative strength). Streams and lakes that are not fully connected to the aquifer are modeled by line sinks

---

[9] Modified from U.S. EPA WhAEM 2000 website https://www.epa.gov/exposure-assessment-models/whaem2000.

or area sinks with a bottom resistance. Discontinuities in aquifer thickness or hydraulic conductivity are modeled by using line doublets (double layers). Specialized analytic elements may be used for special features, such as drains, cracks, slurry walls, etc.

WhAEM2000 can be used to simulate steady-state 2-D hydraulic head contours, streamlines, and particle tracks associated with aquifer storage and recovery operations. Visual AEM is another free AEM program, while commercial AEM groundwater modeling software are also available.

4.2.4   2-D model: Visual AEM released in February 2009[10]

Visual AEM is freeware authored by James R. Craig and Shawn Matott of the University of Waterloo. It provides a graphical user interface (GUI) for single and multi-layer analytic element modeling of (mostly) steady-state groundwater flow and numerical/analytical modeling of vertically-averaged contaminant transport with the object-oriented codes Bluebird and Cardinal, the multilayer code TimML, and the public domain AEM code Split.

Visual AEM is designed for simplicity of use, but includes many robust tools and methods for developing regional scale groundwater flow and transport models or local scale models nested in larger hydrogeologic domains. Version 1.04 (released in 2009) supports: regional and local scale flow and transport modeling; simulation of flow in confined and unconfined single-layer or multi-layer aquifers; capture zone delineation; particle tracking; analytical, finite element, and finite difference simulation of multi-species solute transport; plume animation and visualization; automated calibration; advanced output options (ArcView®, ArcMap®, Surfer®); multiple basemaps and DEMs in various formats (.jpg, .gif, .bmp, .ddf, .grd, .bna, .dxf); pre- and post-processing in Surfer®; grid and mesh generation and editing tools; and an editable geologic media database.

Visual AEM features include: 2-D single-layer or vertical groundwater flow modeling (steady-state or with Theis wells); quasi-3-D multi-layer groundwater flow modeling (steady-state); 2-D finite element and finite difference multispecies contaminant transport modeling; 2-D analytical contaminant transport modeling; particle tracking; parameter estimation; and transect/cross-sectional analysis. The program facilitates modeling of 2-D single and multi-layer steady state groundwater flow using a wide range of hydrogeologic features, including rivers, drains, and lakes, which can be specified based on: head, resistance, or extraction rate; recharge/leakage zones (circular or polygonal); vertical and horizontal wells; inhomogeneities (polygonal, circular, or elliptical) in aquifer base, thickness, porosity, hydraulic conductivity; slurry walls; fractures; and flux-specified and no-flow boundaries. The transport features of Visual AEM include advection, dispersion, diffusion, sorption, first-order decay of multiple solutes, and source zones (with specified dissolved and sorbed initial conditions).

4.2.5   Fate and transport of residual contaminants in injected water

4.2.5.1   2-D model: AT123D-AT

Analytical models (partial differential equations with initial and boundary conditions that mathematically describe solute transport) can be used to estimate the flux and concentration of dissolved pollutants in groundwater. These models typically simulate advection, hydrodynamic dispersion, linear sorption, and first order reactions that affect pollutant fate and transport. A number of solutions have been

---

[10] Modified from Visual AEM Homepage

presented over the past 50 years for various source terms, initial conditions, and boundary conditions. When equations have a closed form solution, they are called analytical models. When numerical methods (e.g. integration) are necessary to calculate concentrations in the closed form solution, they are called semi-analytical models.

Developed in 1981, the AT123D program consists of semi-analytical solutions for 1-, 2-, or 3-D dissolved pollutant transport in a homogeneous aquifer subject to a uniform, stationary regional flow field (Yeh, 1981). AT123D-AT (Burnell et al., 2012) updates this model to include modern programming methods, correct errors in the pulse source, improve numerical integration solvers, include the new Green's functions for a finite-depth aquifer, dynamically allocate arrays for large numbers of nodes, and improve computational efficiency. In recent years, the model has been widely utilized to estimate dissolved chemical concentrations at receptor wells for use in risk assessments. AT123D-AT is a flexible semi-analytical model capable of simulating the advective-dispersive transport of pollutants from a wide variety of source configurations in aquifers bounded by various boundary conditions. The analytical solutions to the governing equations are based on the use of Green's functions. This approach combines the product of point and/or integrated line source solutions in each of the three principle directions to solve advective-dispersive transport from point, line, planar, or rectangular sources. The modeled aquifer is infinite in the horizontal direction of flow but can be approximated as finite or infinite in the transverse-horizontal and vertical directions. The source considered may be instantaneous, steady (finite or infinite in length), or variable over time. The strength of the model lies in the user's ability to choose various source and aquifer configurations and the time-variant source option. This flexibility makes the model ideally suited for coupling with unsaturated zone transport models.

A 1-D finite difference model is included in the ASR DSS to simulate unsaturated advection-dominated transport. The unsaturated zone software simulates 1-D transport to the water table from infiltration basins in the unsaturated zone. The unsaturated zone model is a 1-D finite difference code that represents the source as a Dirichlet boundary (specified concentration). The model simulates advection-dominated transport and sorption in the unsaturated zone. The model is flexible in that it allows the user to specify initial concentrations in the unsaturated zone based on available field data. The calculated mass flux at the water table from this unsaturated zone model is the input for the source zone in the AT123D-AT model.

4.2.5.2 2-D model: Analytical multi-species sequential first-order reaction model

This 1-D, 2-D, or 3-D multi-species model is a useful risk-based screening model to examine not only the parent compounds but also their potentially more toxic degradation products at downgradient groundwater receptor locations. This analytical solute transport model assumes a continuous point, line, or vertical planar source and simulates advection, linear sorption, and first-order sequential reaction. The model simulates the steady-state plume extent of up to 5 sequentially degrading dissolved chemicals (e.g. pesticides or chlorinated solvents) in groundwater. The 1-D model uses a point source and includes longitudinal hydrodynamic dispersion. The 2-D and 3-D models use a line or vertical planar source with advection-dominated transport and transverse horizontal and/or vertical dispersion.

Given particular assumptions, the exact analytical solutions in the multi-species model are not subject to significant errors (Burnell et al., 2012, West et al., 2007). This modeling tool includes an estimate of the time for the plume to reach steady-state and estimates the spatial moments (center of mass, and plume spread around the center of mass) of the steady-state plume.

A MS Windows-based GUI has been developed for the DSS for easy input of model parameters and post-processing. The required input values (source concentration, source width and depth,

groundwater velocity, longitudinal and transverse dispersion coefficients, retardation factor, and rate constants) are straightforward and can be measured or estimated from published values. Once the user enters these input parameters, the model run button rapidly calculates the steady-state plume concentrations. The 1-D model results of each chemical are presented as concentration vs. distance along the plume centerline. For 2-D visualization of the model results, the model post-processing allows the user to overlays plume contours of each chemical over a user-specified base map.

5.0   ASR Evaluation and Engineering Design

ASR design and performance evaluation are essential for managers and engineers to achieve water resource management objectives. Following the ASR planning phase, engineering design and evaluation are the next step to determine the hydraulic control and water quality changes in an ASR system (See Figure 5). Important design and evaluation variables include hydraulic control, residence time, and water quality constraints.

5.1   ASR Hydraulic Properties and Hydrologic Control

As noted in previous sections, ASR system types vary from place to place. Some are only limited to aquifer recharge or soil infiltration in the vadose zone. For this application, groundwater vertical infiltration rate is the most important design variable. On the other hand, injection-withdrawal ASR operations have the function of making up water shortages or storing excess water. Thus, the objective of these operations will depend on several engineering factors including the rate of recovery, the steady state capture zone size, and the minimum groundwater residence time.

5.1.1   Particle tracking, capture zone and rate of ASR recovery

Capture Zone

Capture zone of an ASR system is defined as the region which is hydraulically influenced by the groundwater withdrawal wells. For complete hydraulic control of the injected water volume, the capture zone size must be large enough to encompass the injected water and its flow path over time during ASR operation. Technically, the hydraulic control is evaluated under steady state conditions.

The capture zone size is a function of ASR site hydrology and the hydraulic design of the water injection-recovery system. Factors affecting the efficiency include aquifer properties (leakiness, transmissivity, groundwater flow velocity), well design and operation (e.g., capture zone, injection and withdrawal rates, well conditions), and the duration of water storage. A detailed hydrological investigation, the basis for proper design and evaluation, often involves modeling the groundwater flow fields under various ASR operation conditions.

The capture zone theory was first developed in the 1990s for hydrological application to groundwater pump-and-treat remediation. Mathematical modeling of capture zone size has been outlined in the literature and several numerical and analytical methods are available. Analytical capture zone models (Yang et al., 1997; Matott et al., 2008; U.S. EPA, 2007, 2008) can be used to determine the location and capture size in relatively simple groundwater systems. These 2-D analytical solutions can be used to approximate the composite capture zone of multiple groundwater pumping wells using the hydraulic superposition principles of groundwater flow. One of these methods is WhAEM2000 (U. S. EPA, 2007), a public domain AEM code that simulates 2-D steady flow caused by pumping wells, hydrologic boundaries (river, recharge, and no-flow conditions), and inhomogeneous zones. The applicability of this model has been verified in practice.

For more complex groundwater flow systems or injection-recovery system configurations, robust and computationally intensive numerical modeling packages are more appropriate than analytical solutions. The MODFLOW numerical model developed by USGS is a widely used modeling tool and has several extensions available. It is briefly described in subsequent sections, while more detailed technical documentation is available from the USGS.[11]

Rate of Recovery

The rate of recovery depends on ASR site hydrology and the hydraulic design of the water injection-recovery system. Factors affecting the efficiency include aquifer properties (leakiness, transmissivity, groundwater flow velocity), well design and operation (e.g., capture zone, injection and withdrawal rates, well conditions), and the duration of water storage. In all cases, a detailed hydrological investigation is needed for proper design and evaluation. This investigation often involves computer modeling of the groundwater flow fields under various ASR operation conditions.

One utility of the hydrological module of the ASR DSS is to calculate the groundwater capture zone and track particles in the groundwater (Figure 6). For ASR operation, the injection-withdrawal induced local groundwater flow is superimposed upon a regional flow field. The composite flow field is then the basis to determine the rate of recovery and residence time of injected water in the aquifer undergoing ASR.

Transient Particle Tracking

Transient particle tracking is the other important quantitative method for ASR design and evaluation. Based on the solution to the governing Eq.1, the particle position $\{x, y, z\}$ in the aquifer is computed at each time step. Post-processing of the simulation data produces flow pathways at each time interval for injected water in the injection-recovery well pairs. An example is shown in Figure 17.

Figure 17   Example of particle tracking from an injection well (top well in the figure) to a recovery well (bottom well in figure). Head contours of groundwater elevations are marked. The simulation was carried out using MODFLOW.

One important objective of transient particle tracking is to calculate the volume-weighted average residence time and range of injected water in the storage. The residence time of injected water in an aquifer is one important criterion in ASR design to ensure biological integrity in recovered water. Many states have adopted a minimum residence time, including Texas, California, and Florida. Particle tracking results, such as those in Figure 17, help when developing ASR configuration and operation standards. When necessary, testing well and groundwater tracer tests are often prescribed. An example is given in Section 5.1.1.2.

The second objective of groundwater particle tracking is to investigate the capture zone under ASR operational scenarios for sites with complex hydrogeological conditions. Capture zone can be
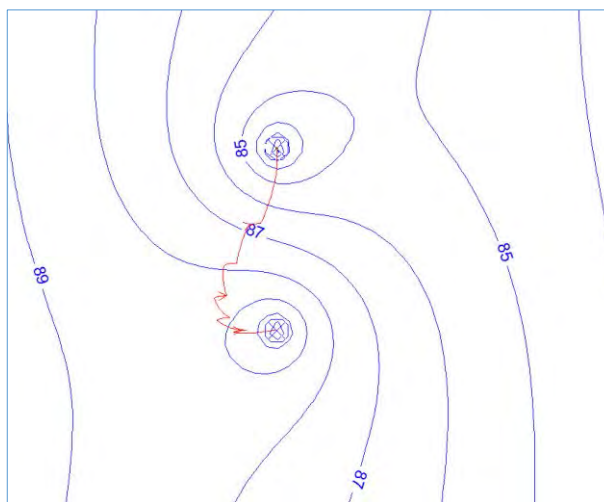
---

[11] http://water.usgs.gov/ogw/modflow/MODFLOW.html

estimated by using the analytical solutions, as discussed earlier in this section. Transient particle tracking enables more accurate of the groundwater capture by the ASR pumping wells

5.1.2   USGS MODFLOW Transient Numerical Groundwater Flow Model Code and MODPATH Transient Particle Tracking Code

MODFLOW is the USGS's 3-D finite-difference groundwater model. MODFLOW is considered an international standard for simulating and predicting groundwater conditions and groundwater−surface water interactions.

Originally developed and released in 1984 solely as a groundwater-flow simulator, MODFLOW's modular structure has provided a robust framework for the integration of additional simulation capabilities, which build on and enhance its original scope. The family of MODFLOW-related programs now includes programs which can simulate coupled ground- and surface water systems, solute transport, variable-density flow (including saltwater), aquifer system compaction and land subsidence, parameter estimation, and groundwater management. Many new capabilities have been added to the original model. MODFLOW-2005 (v.1.11.00), the most current release of MODFLOW, is the most stable and well-tested version of the code.

MODFLOW-2005 simulates steady and transient (non-steady) groundwater flow in aquifer layers, which can be confined, unconfined, or a combination of confined and unconfined, while aquitards restrict groundwater flow. This model can be applied to simulate flow to wells, areal recharge, evapotranspiration, flow to drains, and flow through river beds. The hydraulic conductivity may differ spatially and anisotropically, and the storage coefficient may be heterogeneous. Specified head and specified flux boundaries can be simulated as a head dependent flux across the model's outer boundary. This allows water to be supplied to a boundary block in the modeled area at a rate proportional to the current head difference between a "source" of water outside the modeled area and the boundary block.

MODPATH is a particle-tracking post-processing model that computes 3-D flow paths using output from groundwater flow simulations based on MODFLOW, the USGS finite-difference groundwater flow model. The program uses a semi-analytical particle-tracking scheme that allows an analytical expression of a particle's flow path to be obtained within each finite-difference grid cell. A particle's path is computed by tracking the particle from one cell to the next until it reaches a boundary, an internal sink/source, or satisfies another termination criterion.

Data input to MODPATH consists of a combination of MODFLOW input data files, MODFLOW head and flow output files, and other input files specific to MODPATH. Output from MODPATH consists of several output files, including a number of particle coordinate output files intended to serve as input data for other programs that process, analyze, and display the results in various ways.

5.1.3   Particle Tracking Example

Model Construction

A hypothetical example of flow field prediction and particle tracking analysis is illustrated for ASR design. In this exercise, the ASR DSS was applied to examine the effects of an injection and extraction well design configuration assuming no net change in groundwater storage in a hypothetical aquifer undergoing ASR with typical hydraulic properties. The USGS groundwater flow model, MODFLOW, was applied to examine transient changes in groundwater levels over time and the effect of the spacing between an injection well (200 gpm) and extraction well (200 gpm) that operate over time. Based on the simulated groundwater flow field from MODFLOW, the USGS groundwater particle tracking model, MODPATH, was then applied to examine changes in 3-D groundwater particle pathways over time.

The model area was one square miles. The sandy aquifer was assumed to have a saturated thickness of 100 feet and was divided into 3 layers of equal thickness (33.3 ft) consisting of fine- or coarse-grained sand (Figure 18). All three layers were assumed to be anisotropic with a horizontal and vertical conductivity ratio (k_v/k_H) of 0.1, and a uniform storage coefficient of 0.0001. The k_H values were 100, 30, and 50 feet/day for layers 1, 2, and 3, respectively, allowing for differential groundwater flow velocities in the well field.

3-D groundwater flow from the injection well toward the extraction well was simulated. Model grid spacing varied from 12.5 feet near the injection well to 50 feet at the outer regions of the model domain. The injection well and extraction well were assumed to operate during alternate months, with initial recharge of treated water and then extraction of groundwater every other month. The following ASR well arrangement scenarios were investigated:

Figure 18 Hypothetical example of a three-layer sandy aquifer in 3-D groundwater flow modeling for ASR system design using the ASR DSS models.

Base Scenario: One injection well; no recovery well;

Paired injection-recovery well scenarios: Well spacing at 400, 800 and 1400 feet.

Model Results

The effects of well spacing on the recovery of treated recharge water were evaluated for different well designs. The groundwater flow model results were presented using both spatial maps and time series plots of groundwater elevations over time in both the injection and extraction wells.

The injection of water into the stratified aquifer causes groundwater mounding near the well and differential groundwater flow in the three layers of the groundwater aquifer, which have different hydraulic conductivities. The particle trajectory is shown in Figure 19. Regional groundwater flows from the left to the right of the cross section. Groundwater mounding at the injection well dissipates away from this point. The differential response of the layers to water injection is apparent in the spacing of flow vectors at each time step. The unit-time flow vector is the most spaced in the first layer, which has the highest conductivity of $k_H = 100$ft/day, in contrast to the closely spaced flow vectors for the middle layer, which has the lowest conductivity of $k_H = 30$ft/day. This difference indicates that the least permeable layer to the water injection can cause hydraulic resistance. For the same reason, the injection well loses its efficiency when boreholes are plugged by biological growth or precipitation.

Figure 20 shows the spatial map of the hydraulic head distribution for the paired well configurations at three well distances. Also shown is the particle tracking among the design scenarios. For the comparison, all aquifer properties, well designs, and operations remained the same among the three scenarios except for spacing of the recovery wells. In these scenarios, there are limited changes in the groundwater elevation near the ASR injection and extraction wells because the cone of depression from pumping is limited by recharge from the injection well.

k_H=100 ft/day

k_H=30 ft/day

k_H=50 ft/day
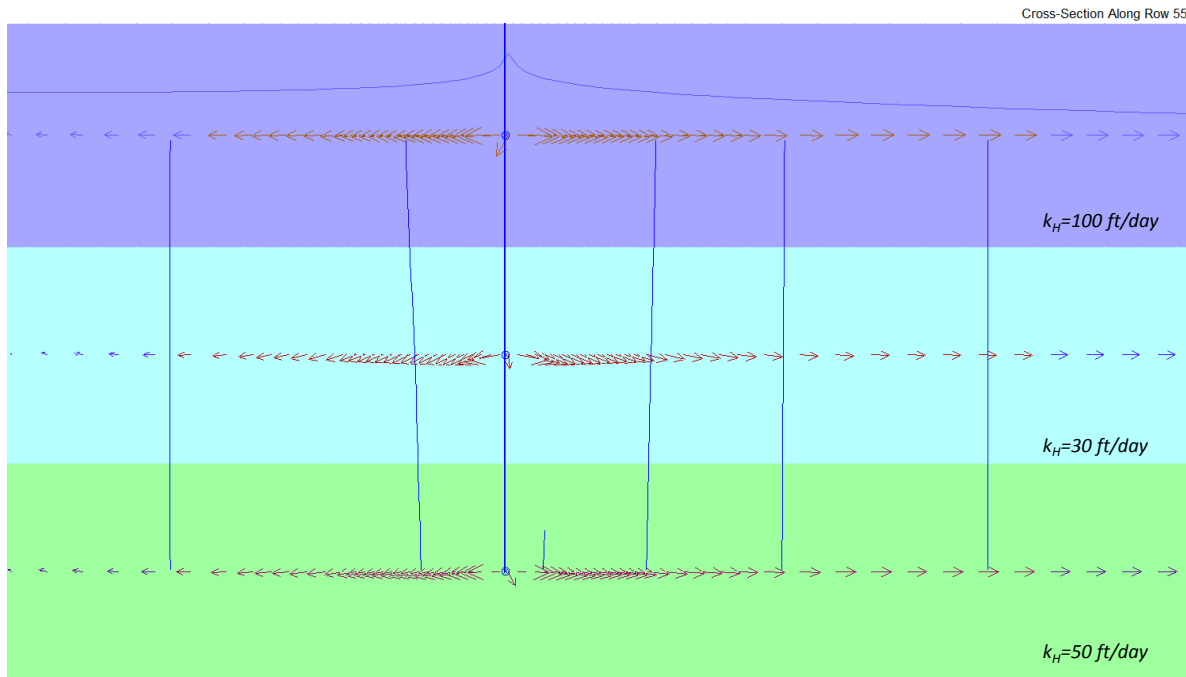
Figure 19   Particle tracking in profile across the injection well, with injection occurring across the entire well depth. Flow vector at each time step is shown at the middle in each of the three layers.

When the injection well and extraction well are closely spaced (<800 feet apart), the results of particle tracking indicate that there will be full recovery of recharge water particles by the recovery well. On the other hand, when the injection and extraction wells are far apart (1400 ft), recharge water may not be recovered by the extraction well. This poor recovery is clearly shown in Figure 20.

During the ASR cycling operations, the aquifer dewatering effects are worth noting for unconfined aquifers. Groundwater injection can raise the groundwater table, while pumping by recovery wells dewaters the aquifer. Frequently, an ASR system is operated in sequential injection-storage-withdrawal modes. This operation leads to fluctuation of the groundwater level in the aquifer.

For the pair of ASR wells at 800 feet spacing (Figure 20), for example, the groundwater level was calculated using MODFLOW simulation. Figure 21 shows the time series plot of the water level at the recovery well. For monthly cycling of the injection-recovery operation, the level will fluctuate by approximately 4 feet with no net change in groundwater storage. The groundwater fluctuation in other location varies. However, these simulations indicate that the aquifer zone will experience cyclic changes in redox potential and other environmental conditions. These changes have implications for the mobilization of arsenic and other redox-sensitive contaminants.

Implications

This simple example is only intended for DSS illustration. Aquifer hydrology and ASR configurations will be more complicated in the field. Nonetheless, this example illustrates how the DSS can assist in ASR design and evaluation to determine important parameters, such as the hydraulic control, rate of recovery, and water table fluctuations.
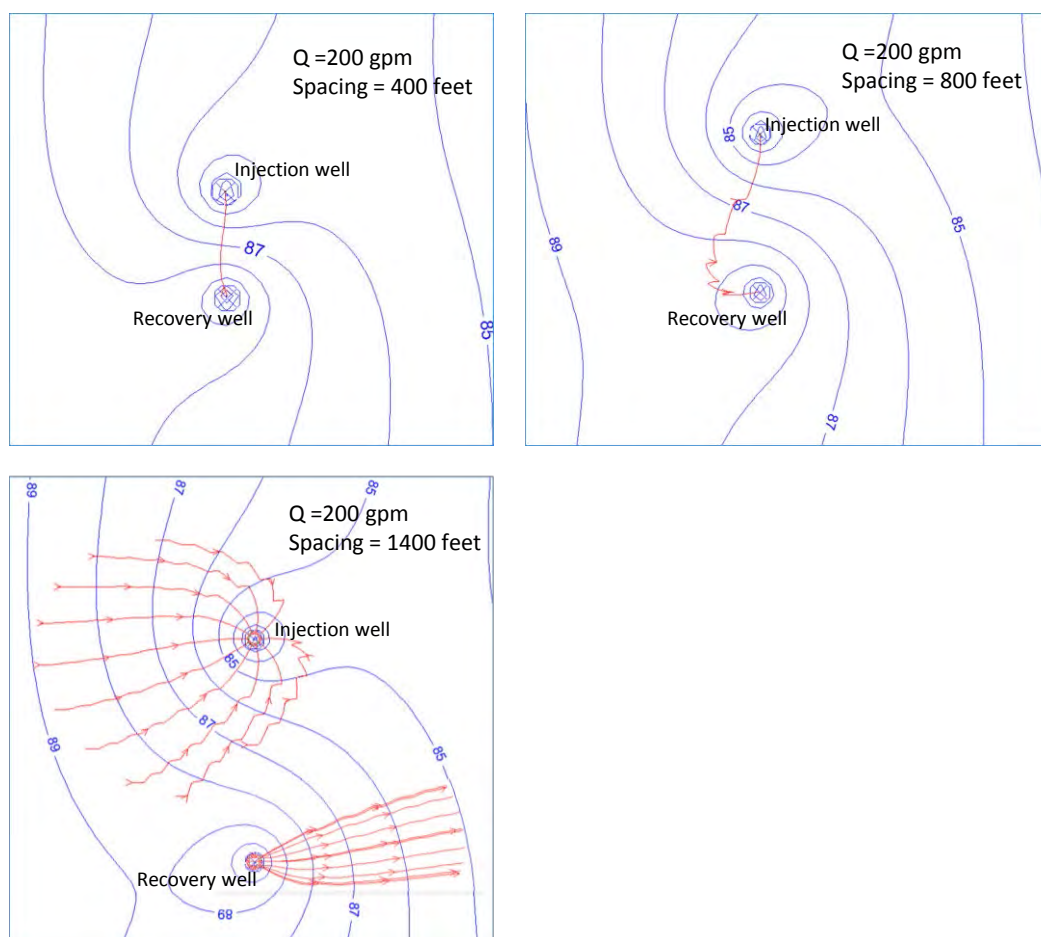
Figure 20   Particle tracking for three design scenarios of two paired injection-recovery wells, with the injection well remaining stationary and the recovery well moving farther away. Physical model is shown in Figure 18.

5.2   Fate and Transport of Residual Contaminants in Injected Water

In an ASR operation, the residual contaminants in injected water are transported and transformed as the water flows in the vadose zone and in the saturated groundwater aquifer. These processes are schematically shown in Figure 3. For ASR design and evaluation, detailed quantitative model simulation can help evaluate contaminant concentrations and determine pre-treatment requirements.

Water quality impact analysis can be conducted using analytical fate and transport models for simple hydrologic settings. The models included in the ASR DSS include AT123D, the 2-D multi-species fate and transport model, WhAEM2000, and Visual AEM. The latter two analytical models also incorporate finite element and finite difference numerical schemes for 2-D multispecies contaminant transport and particle tracking. These analytical models are described in Section 4.2.

Two numerical models, MT3DMS and SEAWAT, are described here for complex hydrogeological settings and ASR configurations. Both models were developed by USGS and are based
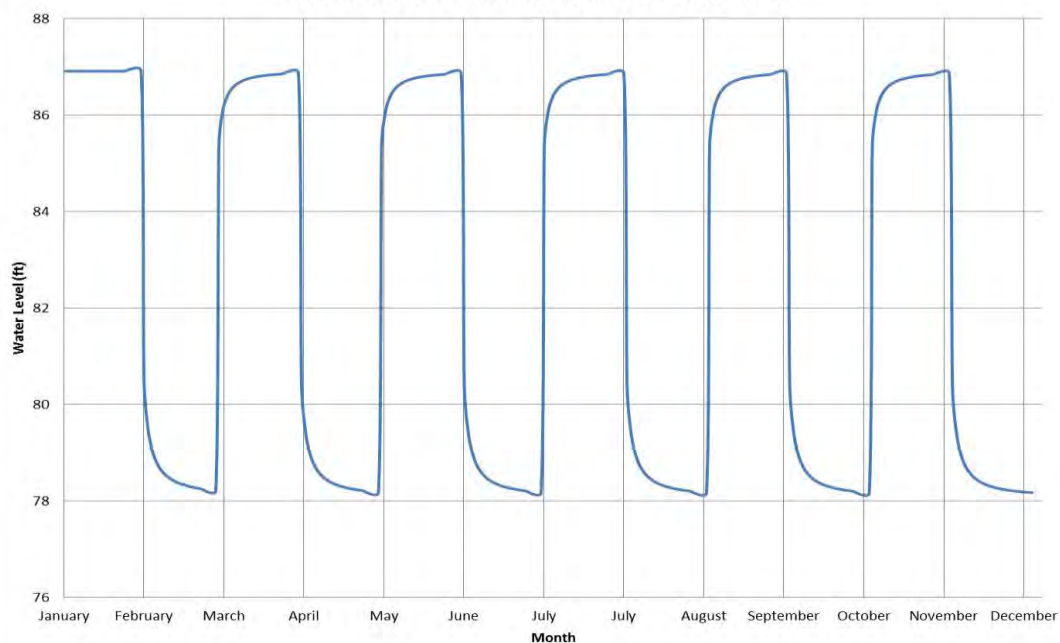
Figure 21   Computer-simulated well head at the recovery well in the well distance of 800 feet in the pair well design scenario. Nearly 10 feet of groundwater fluctuation is predicted for the monthly injection-recovery ASR operation.

on the fundamental groundwater flow and mass transport equations in Eq.5 and 8, respectively. Recently, these models have been incorporated into the groundwater modeling platform PHAST.

5.2.1   *MT3DMS for multi-species transport in groundwater systems*

MT3DMS is a new version of the Modular 3-D Transport model, where MS denotes the multi-species structure for accommodating add-on reaction packages. MT3DMS has a comprehensive set of options and capabilities for simulating advection, dispersion/diffusion, and chemical reactions of contaminants in groundwater flow systems under general hydrogeological conditions.

MT3DMS is unique in that it includes three major classes of transport solution techniques in a single code: 1) The standard finite difference method; 2) The particle-tracking-based Eulerian-Lagrangian methods; and 3) The higher-order finite-volume TVD method. Since no single numerical technique has been shown to be effective for all transport conditions, the combination of these solution techniques, each having its own strengths and limitations, is believed to offer the best approach for solving the most wide-ranging transport problems with desired efficiency and accuracy.

MT3DMS can be used to simulate changes in concentrations of miscible contaminants in groundwater considering advection, dispersion, diffusion and some basic chemical reactions, with various types of boundary conditions and external sources or sinks. The chemical reactions included in the model are equilibrium-controlled or rate-limited linear or non-linear sorption, and first-order irreversible or reversible kinetic reactions. It should be noted that the basic chemical reaction package included in MT3DMS is intended for single-species systems. An add-on reaction package such as RT3D or SEAM3D must be used to model more sophisticated, multi-species reactions.

57

MT3DMS can accommodate very general spatial discretization schemes and transport boundary conditions, including: 1) Confined, unconfined or variably confined/unconfined aquifer layers; 2) Inclined model layers and variable cell thickness within the same layer; 3) Specified concentration or mass flux boundaries; and 4) The solute transport effects of external hydraulic sources and sinks such as wells, drains, rivers, areal recharge and evapotranspiration.

5.2.2   *SEAWAT for three-dimensional variable-density groundwater flow and transport*

The SEAWAT program is a coupled version of MODFLOW and MT3DMS designed to simulate three dimensional, variable-density, saturated groundwater flow. Flexible equations were added to the program to allow fluid density to be calculated as a function of one or more MT3DMS species. Fluid density may also be calculated as a function of fluid pressure. The effect of fluid viscosity variations on groundwater flow was included as an option. Fluid viscosity can be calculated as a function of one or more MT3DMS species, and the program includes additional functions for representing the dependence on temperature. Although MT3DMS and SEAWAT are not explicitly designed to simulate heat transport, temperature can be simulated as one of the species by entering appropriate transport coefficients. For example, the process of heat conduction is mathematically analogous to Fickian diffusion. Heat conduction can be represented in SEAWAT by assigning a thermal diffusivity for the temperature species (instead of a molecular diffusion coefficient for a solute species). Heat exchange with the solid matrix can be treated in a similar manner by using the mathematically equivalent process of solute sorption. By combining flexible equations for fluid density and viscosity with multi-species transport, SEAWAT Version 4 represents variable-density groundwater flow coupled with multi-species solute and heat transport. SEAWAT Version 4 is based on MODFLOW-2000 and MT3DMS and retains all of the functionality of SEAWAT-2000.

SEAWAT Version 4 also supports new simulation options for coupling flow and transport, and for representing constant-head boundaries. In previous versions of SEAWAT, the flow equation was solved for every transport time step, regardless of whether or not there was a large change in fluid density. A new option was implemented in SEAWAT Version 4 that allows users to control how often the flow field is updated. New options were also implemented for representing constant-head boundaries with the Time-Variant Constant-Head Package. These options allow for increased flexibility when using constant-head flow boundaries with the zero-dispersive flux solute boundaries implemented by MT3DMS at constant-head cells.

The report contains revised input instructions for the MT3DMS Dispersion Package, Variable-Density Flow Package, Viscosity Package, and Constant-Head Package. The report concludes with seven cases of an example problem designed to highlight many of the new features.

5.3   Geochemical Compatibility and Water Quality Changes

5.3.1   *Arsenic mobilization from aquifer materials*

One aspect of geochemical compatibility which must be incorporated into ASR models is arsenic mobilization from aquifer materials. Section 4.1.3 outlined the preliminary considerations for arsenic mobilization assessment. Appendix A provides a more detailed summary of arsenic mobilization mechanisms and ASR processes. These assessments together indicate several geochemical conditions which control arsenic mobilization into groundwater. The redox environment is one of the primary factors. Redox cycling of iron regulates the fate and transport of many elements of concern due to the formation of iron oxyhydroxides, which can act as a powerful sorbent for aqueous contaminants. During

ASR, the redox potential of groundwater environments can change, leading to the oxidative dissolution of reduced iron minerals such as arsenopyrite. In reaching a geochemical steady-state condition, arsenic released into groundwater is counter-balanced by attenuation processes. Attenuation processes include co-precipitation with or sorption by iron oxyhydroxides and the precipitation of arsenic-containing minerals. Based on these results, the geochemical pathways leading to arsenic mobilization and attenuation will depend on the following major geochemical conditions at the ASR site.

- The difference in water chemistry (pH, Eh, ORP, etc.) between injected water and native groundwater can cause of arsenic mobilization in groundwater. Pretreatment of injected water to reduce the water chemistry differences can thus minimize adverse reactions.

- Several geochemical pathways are involved of the dissolution and precipitation of arsenic-bearing iron oxyhydroxides, influencing arsenic mobility. These processes are facilitated by the presence of DOM, chloride ions, nitrate, sulphur and oxidants (or ORP) under a given pH-Eh condition.

- Biological activities enhanced by DOM can lead to local reductive environmental conditions, preventing arsenopyrite oxidative dissolution and inhibiting iron oxyhydroxide formation. Although this effect is not currently quantified for ASR sites, DOM presence and concentration variation in space can be used as an indicator.

Controlling arsenic mobilization will thus involve the following major steps: 1) Geochemical and mineralogical analysis of arsenic-bearing minerals in the native groundwater aquifer; 2) Model projection of groundwater conditions in the injection bubble and mixing zones; and 3) Pre-treatment specification for injected water. The purpose of these investigations is to reduce arsenic mobilization and promote arsenic co-precipitation with iron oxides and oxyhydroxides. Alternatively, arsenic mobilization can be minimized by chemically conditioning injected water to resemble the composition of native groundwater. The applicability of this treatment is case specific, and largely depends on the engineering and operational economics.

5.3.2   *Geochemical simulation using PHREEQC and PHREEQCI*

In the ASR DSS, the geochemical package PHREEQC Version 3 (Parkhurst and Appelo, 2013) and PHREEQCI, a GUI to PHREEQC, are available from the USGS. PHREEQC implements several types of aqueous models to perform a wide variety of aqueous geochemical calculations: 1) Speciation and saturation-index calculations; 2) Batch-reaction and 1-D transport calculations with reversible and irreversible reactions, which include aqueous, mineral, gas, solid-solution, surface-complexation, and ion-exchange equilibria, and specified mole transfers of reactants, kinetically-controlled reactions, mixing of solutions, and pressure and temperature changes; and 3) Inverse modeling, which finds sets of mineral and gas mole transfers that account for differences in composition between waters within specified compositional uncertainty limits

A 1-D transport algorithm in PHREEQC can be used to simulate dispersion and diffusion, solute movement in dual porosity media, and multicomponent diffusion, where species have individual, temperature-dependent diffusion coefficients, but ion fluxes are modified to maintain charge balance during transport. The inverse modeling capability of PHREEQC allows identification of reactions that account for observed water composition along a flowline or with time during an experiment. Sorption and desorption can be modeled as surface complexation reactions or as (charge neutral) ion exchange reactions. It has two models for surface complexation: 1) A model based on the Dzombak and Morel (1990) database for the complexation of heavy metal ions on hydrous ferric oxide (Hfo, referred to as ferrihydrite), and 2) The CD-MUSIC model, which also allows for multiple binding sites on each surface. The CD-MUSIC model has more options to fit experiment data and was developed for sorption on

goethite. Ion exchange can be modeled using several conventions. Kinetically-controlled reactions can also be modeled.

PHREEQC is used to evaluate geochemical processes associated with mine drainage, radioactive-waste isolation, contaminant migration, natural and engineered aquifer remediation, aquifer storage and recovery, water treatment, natural systems, and laboratory experiments. More technical information and application examples can be found on the USGS website.

5.3.3   3-D Modeling Tool –PHAST[12]

The ASR DSS contains a more integrated program PHAST (PHREEQC and HST3D) for simulation of multicomponent, reactive solute transport in three-dimensional saturated groundwater flow systems. PHAST can model a wide range of equilibrium and kinetic geochemical reactions. The flow and transport calculations are based on a modified version of HST3D and geochemical reactions are simulated using PHREEQC, which is embedded in PHAST. PHAST and Phast4Windows are available at the USGS.

PHAST is applicable to the study of natural and contaminated groundwater systems at a variety of scales ranging from laboratory experiments to local and regional field scales. PHAST can be used in studies of migration of nutrients, inorganic and organic contaminants, and radionuclides; in projects such as aquifer storage and recovery or engineered remediation; and in investigations of the natural rock/water interactions in aquifers. PHAST is not appropriate for unsaturated-zone flow, multiphase flow, or density-dependent flow.

A variety of boundary conditions can be accommodated in PHAST to simulate flow and transport, including specified- head, flux (specified-flux), and leaky (head-dependent) conditions, as well as the special cases of rivers, drains, and wells. Chemical reactions in PHAST include: 1) Homogeneous equilibria using an ion-association or Pitzer specific interaction thermodynamic model; 2) Heterogeneous equilibria between the aqueous solution and minerals, ion exchange sites, surface complexation sites, solid solutions, and gases; and 3) Kinetic reactions with rates that are a function of solution composition. The aqueous model (elements, chemical reactions, and equilibrium constants), minerals, exchangers, surfaces, gases, kinetic reactants, and rate expressions may be defined or modified by the user.

The PHAST simulator may require large amounts of memory and long Central Processing Unit (CPU) times. To reduce the long CPU times, a parallel version of PHAST has been developed that runs on a multiprocessor computer or on a collection of computers that are networked. Only the flow and transport file is described in detail in the PHAST documentation report. The other two files, the chemistry data file and the database file, are identical to PHREEQC files, and a detailed description of these files is in the PHREEQC documentation. ModelMuse and Phast4Windows are Windows GUIs for PHAST.

5.4   Simulation example: arsenic transport in long-term aquifer storage

5.4.1   Model Background in PHAST/MODELMuse simulation

This example reproduces the PHAST example 4 (Parkhurst et al., 2010) for a reactive-transport model to simulate the water composition evolution over a geologic time frame in the Central Oklahoma aquifer. It is assumed that the aquifer initially contained brines similar to those found at a similar depth in the area. Aquifer recharge with a constant influx of freshwater from precipitation is considered to be the

---

[12] Modified from Parkhurst et al. (2010).

mechanism for chemical evolution in the aquifer over a geologic time frame. This hypothesis is examined in the case study. A similar approach can be used for the simulation of arsenic fate and transport during ASR injection and recovery over the operational time frame.

In the Oklahoma aquifer example, the PHAST/ModelMuse package in the DSS was used to simulate flow, transport, and reactions at a regional scale (90 km [kilometers] by 48 km) for an aquifer with both confined and unconfined regions and a complex 3-D flow pattern. The conceptual model for the calculation assumes that brines initially filled the aquifer. The aquifer contains calcite, dolomite, and clays with cation exchange capacity, and hydrous ferric oxide surfaces. The initial compositions of the cation exchangers and surfaces are in equilibrium with the brine, which contains arsenic. Arsenic is initially sorbed on the hydrous ferric oxide surfaces. The aquifer is assumed to be recharged with rainwater that is concentrated by evaporation and equilibrated with calcite and dolomite in the unsaturated zone. This water then enters the saturated zone and reacts with calcite and dolomite in the presence of the cation exchanger and hydrous ferric oxide surfaces. A period of 1,000,000 years of flushing the brine-filled aquifer with freshwater is simulated.

Model Construction

The model domain is approximately 31 nodes in the X direction (3,000-m node spacing), 17 nodes in the Y direction (3,000-m node spacing), and 9 nodes in the Z direction (50-m node spacing). The northern and southern boundaries of the model are near rivers that provide satisfactory boundary conditions. The eastern boundary of the model coincides with the eastern extent of the geologic units of the aquifer. The extent of freshwater in the aquifer is used to set the western boundary of the model.

The hydraulic conductivity was taken from Parkhurst et al. (1996), but the horizontal hydraulic conductivity was decreased to attain a maximum head in the aquifer that was consistent with the measured water table (Parkhurst et al., 1996). The longitudinal dispersivity (2,000 m) and horizontal and vertical transverse dispersivities (50 m) were set arbitrarily to be less than or equal to the node spacing.

Simulation Results

Figure 22 shows the simulation results for concentration of chloride after 240,000 years, 500,000 years, 740,000 years, and 1,000,000 years. The three-dimensional view of the active grid region is from
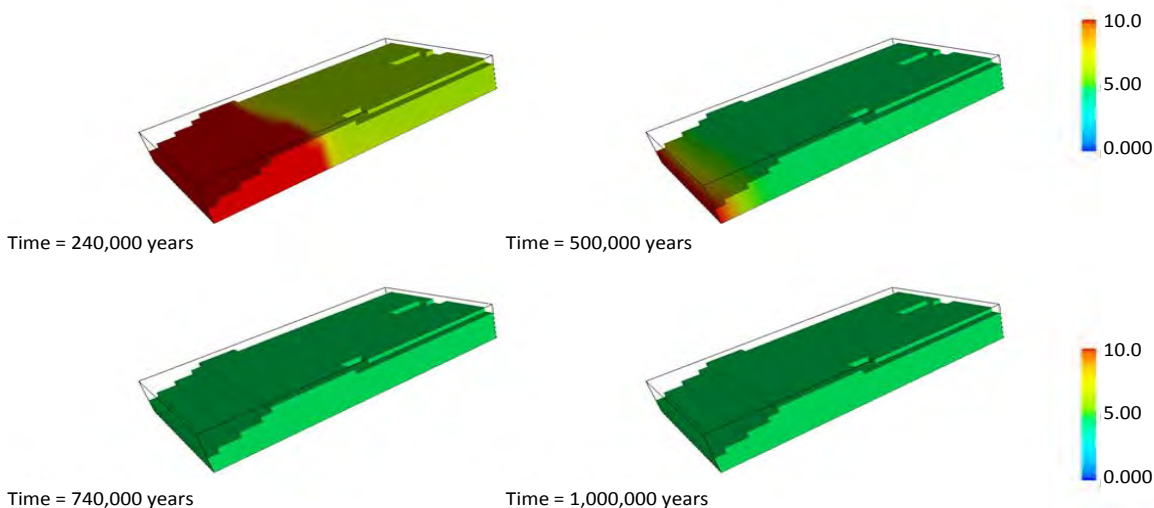
Figure 22. Model-predicted distribution of chloride concentrations (mg/L).

61
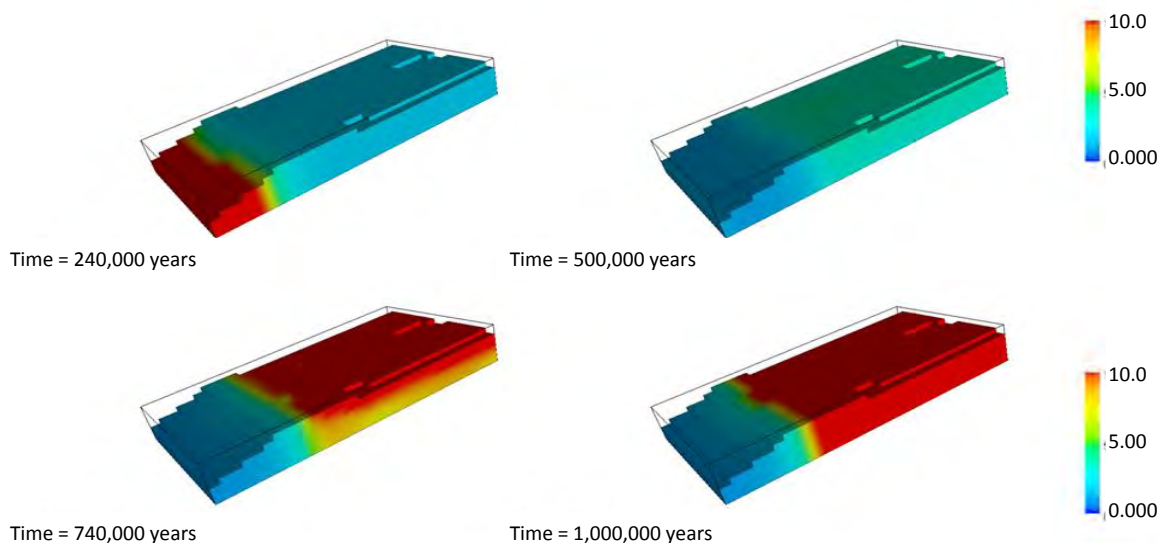
Figure 23. Model-predicted distribution of calcium concentrations (mg/L).

the southwest, which shows a part of the grid region is missing—the inactive grid region—at the western end of the grid region. Also, the top layer of cells is not shown because the cells are dry. Parts of the second layer of cells near the rivers are also not shown because they are dry. Figure 22 clearly shows that the concentration of chloride will significantly decrease over time.

Figure 23 shows the simulation results for concentration of calcium after 240,000 years, 500,000 years, 740,000 years, and 1,000,000 years. The concentration of calcium also significantly decreases over time. The yellow areas in the eastern two-thirds of the active grid region in Figure 23 represent areas where sodium has been removed from the exchanger, and calcium and magnesium are the dominant cations in solution and on the exchanger. In the western one-third of the active grid region, brines have been mostly removed, but sodium persists as the dominant cation in solution and on the exchanger.

The low concentration zones of Figure 23 correspond to high pH zones in Figure 24. Figure 24 shows the simulation results for pH after 240,000 years, 500,000 years, 740,000 years, and 1,000,000 years. The pH is high in these zones because of the dissolution of calcite and dolomite, which is enhanced due to the exchange of calcium and magnesium for sodium on the exchanger. Figure 25 shows the simulation results for concentration of arsenic after 240,000 years, 500,000 years, 740,000 years, and 1,000,000 years. The zones of high pH correspond closely with large arsenic concentrations in Figure 25.

The level of detail in these models makes the Level 3 analysis particularly important for developing safe and sustainable ASR, since results can be used to predict both what geochemical reactions can occur and the extent of these reactions. Groundwater sources are a vital resource which must be protected. While ASR can protect these sources from the detrimental impacts of groundwater overdrafting, it is equally important to ensure that ASR itself does not deteriorate groundwater quality. Level 3 analysis will be the strongest tool in developing ASR operations that protect and enhance groundwater resources.
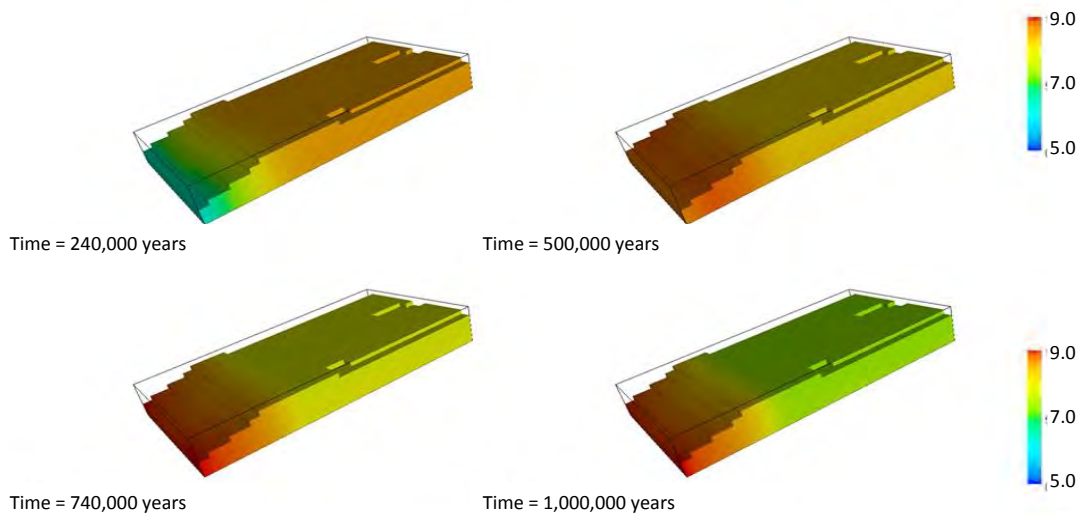
Figure 24. Model-projected spatial distribution of pH values in groundwater.
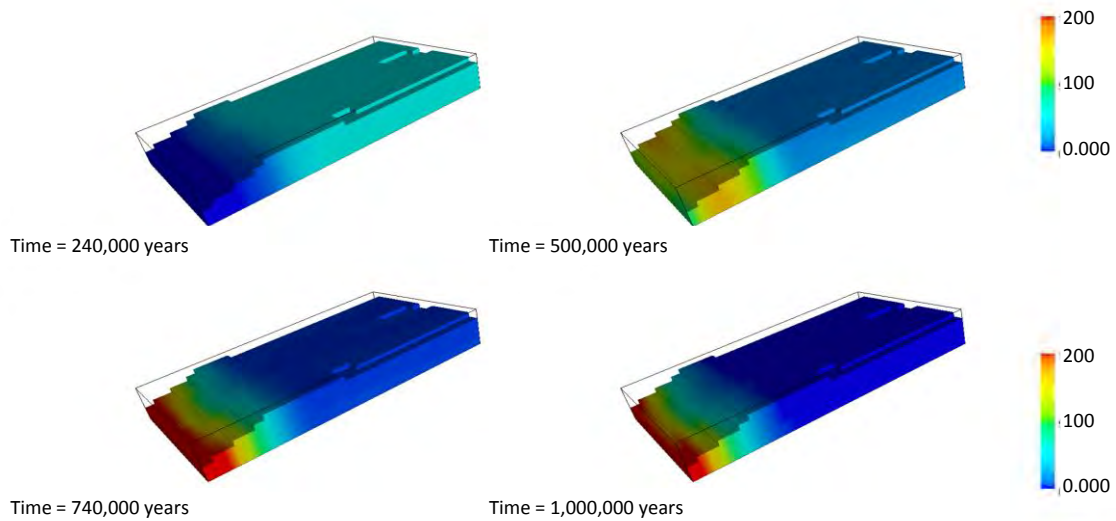
Figure 25. Model projected distribution of arsenic concentrations (μg/L) in groundwater.

6.0 Conclusion

One of the greatest challenges in the coming years will be meeting increased water demands. Population growth and dynamic climate change have led to widespread gaps in water availability, and the challenge to our groundwater resources is projected to continue. The development of AR and ASR technologies is a vital component in addressing these water gaps by closing our cycle of water use and

capturing water from extreme precipitation events, as well as protecting natural ecosystems by mitigating the impacts of groundwater overdrafting, such as the drying of wetlands and land subsidence. AR and ASR operations must be run in a manner that protects groundwater resources while giving us the maximum benefit through informed site selection and operational parameters. The Level 1-3 tools presented in this DSS form a technical basis for AR and ASR best practices.

The three levels of tools cover AR and ASR system development from the earliest stages of ASR-Need analysis, to planning and assessment, design, and evaluation. A case study for Las Vegas shows how ASR-Need analysis can be used to determine the potential for ASR to meet future water gaps. This analysis will be supported by the Level 1 tool, which focuses on ASR feasibility. The Level 1 tool includes resources to examine water demand, population growth projections, and climate change scenarios, which can inform projections for future water demand and availability. This tool is also a valuable resource for information on state-specific ASR regulations and permitting needs, as well as current information on ASR site locations and technical information, such as records of arsenic-contamination of groundwater and site mineralogy, which can be used to inform site selection.

The Level 2 tool has additional capabilities to support ASR planning and assessment. This level of analysis includes simple models for hydrological and environmental assessment. Outcomes from the Level 2 analysis can be used to further assess potential ASR sites in order to evaluate operational parameters including injection rate, storage capacity, and injection-related geotechnical factors. This tool can also be used to determine the geochemical compatibility of the groundwater aquifer formation minerals with injected water to determine the likelihood of negative groundwater impacts.

Finally, Level 3 tools will be used to evaluate ASR design and performance to achieve water resource management objectives. Following Level 2 analysis, engineering design and evaluation assessment incorporated into Level 3 tools must be applied to determine the hydraulic control and provide a more detailed analysis of water quality changes in during ASR operation, including particle transport analysis and long term evaluation of the changes in groundwater quality that result both from geochemical reactions between injected water and aquifer bedrock, and mixing between injected water and resident groundwater. Important design and evaluation variables which are assessed at this level include hydraulic control, residence time, and water quality constraints.

Together, the three tools presented in this DSS can be used to develop and support the safe and sustainable implementation of AR and ASR, ensuring that these technologies can be widely applied to meet growing water demands and prevent water availability gaps, while protecting our most abundant source of freshwater for residential, industrial, and agricultural needs.

7.0   References

Adhikari, A. R., K. Acharya, S.A. Shanahan, and X. Zhou, (2011). Removal of nutrients and metals by constructed and naturally created wetlands in the Las Vegas Valley, Nevada. *Environmental Monitoring and Assessment,* 180, 97-113.

Al-Zubari, W.K., (1998). Towards the establishment of a total water cycle management and re-use program in the GCC countries. *Desalination*, 120, 3-14.

Anderson, M.P., and W.W. Woessner, (2002). *Applied groundwater modeling: Simulation of flow and advective transport, Volume 4*. Academic Press, San Diego, 381p.

Angelakis, A.N., M.H.F. Marecos Do Monte, L. Bontoux, and T. Asano, (1999). The status of wastewater reuse practice in the Mediterranean Basin: Need for guidelines. *Wat. Res*., 33 (10): 2201-2217.

Appelo, C.A., M. J. J. Van Der Weiden, C. Tournassat, and L. Charlet, (2002). Surface Complexation of Ferrous Iron and Carbonate on Ferrihydrite and the Mobilization of Arsenic. *Environ. Sci. Technol.*, 36 (14), 3096–3103.

Arthur, J. D., A. A. Dabous, and J.B. Cowart, (2002). Mobilization of arsenic and other trace elements during aquifer storage and recovery, southwest Florida. In *U.S. Geological Survey Artificial Recharge Workshop Proceedings* (pp. 47-50).

Asano, T., and J.A. Cotruvo, (2004). Groundwater recharge with reclaimed municipal wastewater: health and regulatory considerations. *Wat. Res.*, 38, 1941-1951.

Asano, T., and A. D. Levine, (1996). Wastewater reclamation, recycling and reuse: past, present, and future. *Water science and technology*, 33(10-11), 1-14.

Barnett, T.P., and D.W. Pierce, (2008). When will Lake Mead go dry? *Water Resources Research*, 44, 1-10.

Barsugli, J., C. Anderson, J. B. Smith, and J. M. Vogel, (2009). *Options for improving climate modeling to assist water utility planning for climate change.* Water Utility Climate Alliance, San Francisco, CA. 144p.

Bates, B.C., Z.W. Kundzewicz, S. Wu and J.P. Palutikof, Eds., (2008). Climate Change and Water. *Technical Paper of the Intergovernmental Panel on Climate Change*, IPCC Secretariat, Geneva, 210 pp.

Batu, V., (1998). *Aquifer Hydraulics: A Comprehensive Guide to Hydrogeologic Data Analy*sis. John Wiley & Sons, Inc. New York, NY.

Bloetscher, F., C.H. Sham, J.J. Danko III, and S. Ratick, (2014). Lessons Learned from Aquifer Storage and Recovery (ASR) Systems in the United States. *Journal of Water Resource and Protection*, *6*(17), 1603.

Bloetscher, F. (2015). *M63 Aquifer Storage and Recovery* (Vol. 63). American Water Works Association.

Board of County Commissioner, (2008). *Manatee County Water Supply Facilities Work Plan*, Manatee County Administrative Center Commission Office Commission, Bradenton, Florida

Bouwer, E.J., P.L. McCarty, and J.C. Lance, (1981). Trace organic behavior in soil columns during rapid infiltration of secondary wastewater. *Wat. Res.,* 15, 151-159.

Brun, S.E., and L.E. Band, (2000). Simulating runoff behavior in an urbanizing watershed. *Computers, Environment and Urban Systems*, 24, 5-22.

Buckingham, S. E., and J.W. Whitney, (2007). GIS methodology for quantifying channel change in Las Vegas, Nevada. *J AWWA*, 43, 888-898.

Bureau of Land Management (BLM), (2004). *Las Vegas valley disposal boundary: Environmental impact statement*. Retrieved from www.blm.gov/nv/st/en/fo/lvfo/blm_programs/planning/las_vegas_valley_disposal.html

Burnell, D.K., Lester, B.H. and J.W. Mercer, (2012). Improvements and corrections to AT1230 Code, *Ground Water*, 50(6), 943-953.

Carleton, G.B., (2010). Simulation of Groundwater Mounding Beneath Hypothetical Stormwater Infiltration Basins, *USGS Scientific Investigations Report 2010-5102*, 64 p.

Chang, N.-B., C. Qi, and Y.J. Yang, (2012). Optimal expansion of a drinking water infrastructure system with respect to carbon footprint, cost-effectiveness and water demand. *J. Environmental Management*, 110, 194-206.

Chen, J.C., N.B. Chang, and W.K. Shieh, (2003). Assessing wastewater reclamation potential by neural network model. *Eng. App. Artificial Intel.,* 16, 149-157.

Chen, H., Tong, S.T.Y., Yang, H., and Yang, Y.J., (2015). Simulating the hydrologic impacts of land-cover and climate changes in a semi-arid watershed. *Hydrological Sciences Journal*, DOI: 10.1080/02626667.2014.948445.

Christensen, N. S., A. W. Wood, N. Voisin, D.P. Lettenmaier, and R. N. Palmer, (2004). The effects of climate change on the hydrology and water resources of the Colorado River basin. *Climatic Change*, 62, 337-363.

Chu, J., J. Chen, C. Wang, and P. Fu, (2004). Wastewater reuse potential analysis: Implications for China's water resources management. *Wat. Res*., 38, 2746-2756.

Cooley, H., T. Hutchins-Cabibi, M. Cohen, P. H. Gleick, and M. Herger, (2007). Hidden Oasis: water conservation and efficiency in Las Vegas. Retrieved from the Pacific Institute and Western Resources Advocates website at http://www.pacinst.org/reports/las_vegas/hidden_oasis.pdf

Craig, J.R., and S. Matott, (2009). Visual AEM User's Manual, downloaded from program Help, 115 p.

Dagan, G., (1987). Theory of solute transport by groundwater. *Ann. Rev. Fluid Mech*., 19, 183-215.

DeSimone, L.A., B.L. Howes, P.M. Barlow, (1997). Mass-balance analysis of reactive transport and cation exchange in a plume of wastewater-contaminated groundwater. *J. Hydrol*., 203, 228-249.

Driscoll, F.G., (1986). *Groundwater and wells*. Johnson Screens, 1089p.

Dzombak, D.A., and F.M. Morel, (1990). *Surface complexation modeling: Hydrous ferric oxide*. Wiley ISBN 978-471-63731-8. 416p.

Ellsworth, W. L. (2013). Injection-induced earthquakes. *Science*, 341(6142), 1225942.

Ferris, J.G., D.B. Knowles, R.H. Brown, and R.W. Stallman, (1962). Theory of Aquifer Tests. *USGS Water-Supply Paper 1536 E*, 174p.

Fetter, C.W., (1994). *Applied Hydrogeology*; Third Edition. Prentice-Hall, Inc., Englewood Cliffs, NJ.

Finnemore, E. J., (1995). A program to calculate ground-water mound heights. *Ground Water,* 33(6), 139-143.

Friedler, E., (2001). Water reuse – an integral part of water resources management: Israel as a case study. *Wat. Policy*, 3, 29-39.

Gabriel, B. J., and E. Accinelli, (2007). The Ramsey model with logistic population growth. *Economics Bulletin*, 3, 1-8.

Georgopoulou, E., A. Kotronarou, A. Koussis, P.J. Restrepo, A. Gomez-Gotor, and J.J. Rodriguez Kimenez, (2001). A methodology to investigate brackish groundwater desalination coupled with aquifer recharge by treated wastewater as an alternative strategy for water supply in Mediterranean areas. *Desalination*, 136, 307-315.

Greskowiak, J., H. Prommer, G. Massmann, C.D. Johnston, G. Nützmann, and A. Pekdeger, (2005). The impact of variably saturated conditions on hydrogeochemical changes during artificial recharge of groundwater. *App. Geoch*., 20, 1409-1426.

Haitjema, H.M., (1995). *Analytic Element Modeling of Groundwater Flow*, Academic Press, New York, 394.

Hantush, M.S., (1967). Growth and decay of groundwater-mounds in response to uniform percolation, *Water Resources Research*, 3(1), 227-234.

Hantush, M.S. and C.E. Jacob, (1955). Non-steady radial flow in an infinite leaky aquifer. *American Geophysical Union Trans.*, 36, 95-100.

Harbaugh, A.W., (2005). MODFLOW-2005, The U.S. Geological Survey Modular Ground-Water Model - the Ground-Water Flow Process. *USGS Techniques and Methods 6-A16*, 253 p.

Harris, S., (2005). Diffusive logistic population growth with immigration. *Applied Mathematics Letters*, 18, 261-265.

Haruvy, N., (1998). Wastewater reuse: Regional and economic considerations. *Res., Cons. Recyc.*, 23: 57-66.

Hunt, B., (2005). Visual basic programs for spreadsheet analysis. *Ground Water*, 43(1), 138-141.

Intergovernmental Panel on Climate Change (IPCC), (2001). Climate Change: Synthesis Report. *In*. Watson, R.T. and the Core Writing Team, eds., *A Contribution of Working Groups I, II, and III to the Third Assessment Report of the Intergovernmental Panel on Climate Change*. Cambridge University Press, Cambridge, United Kingdom, and New York, NY, USA, 398 pp.

IPCC, (2007). Contribution of Working Group II to the fourth assessment report of the Intergovernmental Panel on Climate Change. Cambridge University Press. Cambridge, UK.

IPCC, (2013). Climate Change 2013: The Physical Science Basis. Contribution of Working Group I to the Fifth Assessment Report of the Intergovernmental Panel on Climate Change [Stocker, T.F., D. Qin, G.-K. Plattner, M. Tignor, S.K. Allen, J. Boschung, A. Nauels, Y. Xia, V. Bex and P.M. Midgley (eds.)]. Cambridge University Press, New York, 1535 pp.

Karl, T.R., J.M. Melillo, and T.C. Peterson, (2009). *Global Climate Change Impacts in the United States*. New York, NY: Cambridge University Press.

Katz, Brian G., Sandra M. Eberts, and Leon J. Kauffman, (2011). Using Cl/Br ratios and other indicators to assess potential impacts on groundwater quality from septic systems: a review and examples from principal aquifers in the United States. *Journal of Hydrology,* 397(3), 151-166.

Keeting, E. H., J. Fessenden, N. Kanjorski, (2010). The impact of CO_2 on shallow groundwater chemistry: observations at a natural analog site and implications for carbon sequestration. *Environmental Earth Sciences*, 60(3), 521-536

Khan, S., R. Tariq, C. Yuanlai, and J. Blackwell, (2006). Can irrigation be sustainable? *Ag. Wat. Management*, 81, 87-99

Kraemer, S. R., (2005). *Frequently Asked Questions about WhAEM2000*, USEPA website, Athens, GA.

Johnson, T., J. Butcher, A. Parker, and C. Weaver, (2012). Investigating the sensitivity of U.S. streamflow and water quality to climate change: U.S. EPA Global Change Research Program's 20 Watersheds Project. *J. Water Resour. Plann. Manage.*, 138(5), 453–464.

Jones, G. W., and T. Pichler, (2007). Relationship between pyrite stability and arsenic mobility during aquifer storage and recovery in Southwest Central Florida. *Environmental Science & Technology*, 41(3), 723-730.

Langevin, C.D., D.T. Thorne Jr., A.M. Dausman, M.C. Sukop, and W. Guo, (2007), *SEAWAT Version 4: A Computer Program for Simulation of Multi-Species Solute and Heat Transport*. USGS Techniques and Methods. Book 6, Chapter A22, 39 p.

Las Vegas Wash Coordination Committee (LVWCC), (1999). Las Vegas Wash comprehensive adaptive management plan. Retrieved from Las Vegas Wash Project Coordination Team website at http://www.lvwash.org/html/resources_library_lvwcamp.html

Lo, K.W., Y-C. Jin, and T. Viraraghvan, (2002). Transport of bacteria in heterogeneous media under leaching conditions. *J. Env. Eng. Sci*., 1, 383-395.

Lucho-Constantino, C.A., M. Alvarez-Suarez, R.I. Beltran-Hernandex, F. Prieto-Garcia, H.M. Poggi-Varaldo, (2005). A multivariate analysis of the accumulation and fractionation of major and trace elements in agricultural soils in Hidalgo state, Mexico irrigated with raw wastewater. *Env. Int'l*, 31, 313-323.

Manka, J., and M. Rebhun, (1982). Organic groups and molecular weight distribution in tertiary effluents and renovated waters. *Wat. Res.,* 16: 399-403.

Matott, L.S., A. J. Rabideau, and J. R. Craig, (2008). Pump-and-treat optimization using analytic element method flow models. *Advances in Water Resources*, 29, 760–775

Mearns, L. O., W. J. Gutowski, R. Jones, L.-Y. Leung, S. McGinnis, A. M. B. Nunes, and Y. Qian, (2009). A regional climate change assessment program for North America. *EOS,* 90(36), 311-312

Mearns, L.O., D.P. Lettenmaier, and S. McGinnis, (2015). Uses of results of regional climate model experiments for impacts and adaptation studies: the example of NARCCAP. *Curr. Clim. Change Rep.*, 1:1-9.

Milhous, R. (1998) Restoring River Substrate Using Instream Flows: The Gunnison and Trinity Rivers. *Engineering Approaches to Ecosystem Restoration*: pp. 925-930.

Miller, G.W., (2006). Integrated concepts in water reuse: managing global water needs. *Desalination*, 187: 65-75

Miranda, L. C. M., and C. A. S. Lima, (2010). On the logistic modeling and forecasting of evolutionary processes: Application to human population dynamics. *Technological Forecasting and Social Change*, 77, 699-711.

Morris, R. L., D. A. Devitt, A.M. Crites, G. Borden, and L. N. Allen, (1997). Urbanization and water conservation in Las Vegas valley, Nevada. *J. Water Resources Planning and Management*, 123, 189-195.

Neil, C. W., Y. J. Yang, and Y.-S. Jun, (2012). Arsenic mobilization and attenuation by mineral-water interactions: implications for managed aquifer recharge. *Journal of Environmental Monitoring 14*, (7), 1772-1788.

Neil C., Y.J. Yang, D. Schupp, and Y-S. Jun, (2014). Water chemistry impacts on arsenic mobilization from arsenopyrite dissolution and secondary mineral precipitation: Implication for managed aquifer recharge. *Environmental Science and Technology*, 48(8), 4395-4405.

Parkhurst, D.L., S. Christenson, and G.N. Breit, (1996). Chapter C, Ground-Water-Quality Assessment of the Central Oklahoma Aquifer, Oklahoma: Results of Investigations. USGS Water-Supply Paper 2357.

Parkhurst, D.L., K.L. Kipp, and S.R. Charlton, (2010), PHAST Version 2—A Program for Simulating Groundwater Flow, Solute Transport, and Multicomponent Geochemical Reactions. *USGS Techniques and Methods 6–A35*, 235 p.

Parkhurst, D.L., and C.A.J. Appelo, (2013). Description of input and examples for PHREEQC version 3—A computer program for speciation, batch-reaction, one-dimensional transport, and inverse geochemical calculations. *U.S. Geological Survey Techniques and Methods, book 6, chap. A43*, 497 p., available only at http://pubs.usgs.gov/tm/06/a43.

Pasch, J., and P. Macy, (2005). Building sustainable wastewater reuse in Jordan. *Wat. Supply*, 5: 17-25.

Pereira, L.S., T. Oweis, A. Zairi, (2002). Irrigation management under water scarcity. *Ag. Wat. Management*, 57, 175-206.

Piechota, T., and J. Bastista, (2003). Source water assessment for the Las Vegas valley surface waters. Carson City, NV. *State of Nevada, Bureau of Health Protection Services*.

Pitt, R., Clark, S., and Field, R. (1999). Groundwater contamination potential from stormwater infiltration practices. *Urban water*, *1*(3), 217-236.

Pollock, D.W., (2012). User Guide for MODPATH Version 6—A Particle-tracking Model for MODFLOW. *USGS Techniques and Methods, book 6, chap. A41*, 58 p.

Progressive Leadership Alliance of Nevada (PLAN). (2006). *Las Vegas valley groundwater development project: Where does it start? Where will it end?* Retrieved from Progressive Leadership Alliance of Nevada Web site at www.planevada.org

Qadir, M., B.R. Sharma, A. Bruggeman, R. Choukr-Allah, and F. Karajeh, (2007). Non-conventional water resources and opportunities for water augmentation to achieve food security in water scare countries. *Ag. Wat. Management*, 87, 2-22.

Qaiser, K., S. Ahmad, W. Johnson, and J. Batista, (2011). Evaluating the impact of water conservation on fate of outdoor water use: a study in an arid region. *Journal of Environmental Management*, 92, 2061-2068

Ranatunga T., S. T.Y. Tong, Y. Sun, and J.Y. Yang, (2014). A total water management analysis of the Las Vegas wash watershed, Nevada. *Physical Geography*, 35(3), 220-244

Scheytt, T.J., P. Mersmann, and T. Heberer, (2006). Mobility of pharmaceuticals carbamazepine, diclofenac, ibuprofen, and propyphenazone in miscible-displacement experiments. *Cont. Hydrol.,* 83:53-69.

Sen, T.K., D. Das, K.C. Khilar, and G.K. Suraishkumar, (2005). Bacterial transport in porous media: New aspects of the mathematical model. *Colloids and Surface A: Physicochemical and Engineering Aspect*, 260, 53-62.

Shelef, G., and Y. Azov, (1996). The coming era of intensive wastewater reuse in the Mediterranean region. *Wat. Sci. Tech.*, 33(10-11), 115-125.

Sheng, Z., (2005). An aquifer storage and recovery system with reclaimed wastewater to preserve native groundwater resources in El Paso, Texas. *J. Env. Management*, 75, 367-377.

Schroeder, R.A., (2002). Transport and fate of water-quality indicators after 40 years of artificial recharge with treated municipal wastewater to the Central Ground-water basin in Los Angeles County. *In* G.R. Aiken and E.L. Kuniansky, eds., *U.S. Geological Survey Artificial Recharge Workshop Proceedings*, April 2-4, 2002, Sacramento, California. U.S. Geological Survey, Open-file Report 02-89, pp.42-46

Stave, K. A., (2001). Dynamics of wetland development and resource management in Las Vegas Wash, Nevada. *J AWWA*, 37, 1369–1379.

Stave, K.A., (2003). A system dynamics model to facilitate public understanding of water management options in Las Vegas, Nevada. *Journal of Environmental Management*, 67, 303-313.

Southern Nevada Water Authority (SNWA), (2009). *Water Resources Plan 09*. Southern Nevada Water Authority, Las Vegas, Nevada. Retrieved from Southern Nevada Water Authority Website at http://www.snwa.com/ws/resource_plan.html

Southern Nevada Water Authority (SNWA), (2015). *Water Resource Plan 2015*. Southern Nevada Water Authority, Las Vegas, Nevada. Retrieved from Southern Nevada Water Authority Website at https://www.snwa.com/assets/pdf/wr_plan.pdf

Strack, O.D.L., (1989). *Groundwater Mechanics*, Prentice Hall.

Sun, Y., S.T.Y. Tong, M. Fang, and Y.J. Yang, (2013). Exploring the effects of population growth on future land use change in the Las Vegas Wash watershed: An integrated approach of geospatial modeling and analytics. *Environment, Development, and Sustainability*, 15, 1495-1515

Tabelin, C.B., T. Igarashi, and R. Takahashi, (2012). Mobilization and speciation of arsenic from hydrothermally altered rock in laboratory column experiments under ambient conditions. *Applied Geochemistry*, 27(1), 326–342

Theis, C.V., (1935). The relation between the lowering of the piezometric surface and the rate and duration of discharge of a well using groundwater storage. *American Geophysical Union Trans.*, 16, 519-524.

Thomas, J.-S., and B. Durham, (2003). Integrated water resource management: looking at the whole picture. *Desalination*, 156, 21-28.

Tong, S.T.Y., Y. Sun, T. Ranatunga, J. He, Y. J. Yang, (2012). Predicting plausible impacts of sets of climate and land use change scenarios on water resources. *Applied Geography*, 32, 477-489

Toze, S., (2004). Reuse of effluent water – benefits and risks. *Proc. 4th International Crop Science Congress*, Brisbane, Australia.

U.S. Bureau of Reclamation (USBR), (2009). *Colorado River Basin Salinity Control Project-Las Vegas Wash Unit-Title II*. Retrieved from U.S. Department of Interior Web site at http://www.usbr.gov/projects/Project.jsp?proj_Name=CRBSCP+-+Las+Vegas+Wash+Unit+-+Title+II#Group608790

U.S. Climate Change Science Program (USCCSP), (2001). *Climate change impacts on the United States: The potential consequences of climate variability and change*. Cambridge University Press, New York.

U.S. EPA. (2001). Technical program overview: Underground injection control regulations. *EPA 816-R-02-025*. Washington DC

U.S. EPA. (2004). Guidelines for water reuse. *EPA/625/R-04/108*. Washington DC, 443p.

U.S. EPA, (2007). Working with WhAEM2000, Capture Zone Delineation for a City Wellfield in a Valley Fill Glacial Outwash Aquifer Supporting Wellhead Protection, *USEPA/600/R-05/151*.

U.S. EPA. (2008). A Systematic Approach for Evaluation of Capture Zones at Pump and Treat Systems. *EPA/600/R-08/003*, Washington, DC.

U.S. EPA, (2012a). Guidelines for water reuse. *Environmental Protection Agency, Municipal Support Division Office of Wastewater Management Office of Water Washington, DC. Agency for International Development Washington DC EPA/625/R-04/108*, Cincinnati, OH US EPA/625/R-04/108.

U.S. EPA, (2012b). *Nonpoint Source program success story: Best Management Practices Drastically Reduce Sediment and Restore Water Quality in Las Vegas Wash*. http://water.epa.gov/polwaste/nps/success319/state_nv.cfm

U.S. EPA, (2015a). *National Water Infrastructure Adaptation Assessment, Part II: Characterize Climatic Change Impacts for Water Adaptation Planning and Engineering*. Under Review.

U.S. EPA, (2015b). *National Water Infrastructure Adaptation Assessment, Part VI: Climate Change Adaptation Methods and Case Studies*. Under Review.

U.S. EPA, (undated). Class V UIC study Sheet – Aquifer recharge wells and aquifer storage and recovery wells. http://www.epa.gov/UIC

U.S. Geological Survey (USGS), (2000). Flood of July 8, 1999, in Las Vegas Valley, Southern Nevada. *USGS Factsheet 80*, U.S. Department of the Interior.

U.S. Global Change Research Program (USGCRP), (2000). *Climate Change Impacts on the United States: The Potential Consequences of Climate Variability and Change*. Retrieved from the National Assessment Synthesis Team Website at http://downloads.globalchange.gov/nca/nca-2000-report-overview.pdf

Wallis, I., H. Prommer, C. T. Simmons, V. Post, and P. J., Stuyfzand, (2010). Evaluation of conceptual and numerical models for arsenic mobilization and attenuation during managed aquifer recharge. *Environmental science & technology 44*, (13), 5035-5041.

Wang, X., A. Burguess, and Y.J. Yang, (2013). A scenario-based water conservation planning support system (SB-WCPSS). *Stochastic Environmental Research and Risk Assessment*, 27(3), 629-641.

Weber, S., S. Khan, and J. Hollender, (2006). Human risk assessment of organic contaminants in reclaimed wastewater used for irrigation. *Desalination*, 187:53-64.

Weeks, E.P., (2002). A historical overview of hydrologic studies of artificial recharge in the U.S. Geological Survey. *In* G.R. Aiken and E.L. Kuniansky, eds., U.*S. Geological Survey Artificial Recharge Workshop Proceedings*, April 2-4, 2002, Sacramento, California. U.S. Geological Survey, Open-file Report 02-89, pp.5-12.

Welch, A.H., D.B. Westjohn, D.R. Helsel, and R.B. Wanty, (2000). Arsenic in ground water of the United States-- occurrence and geochemistry. *Ground Water*, 38(4), 589-604.

Welty, C. (2009). The Urban water budget. *In* L.A. Baker, ed, *The Water Environment of Cities*. New York, NY, Springer, pp. 17-28.

West, M. R., B. H. Kueper, and M. J. Ungs, (2007). On the use and error of approximation in the Domenico (1987) solution. *Ground Water*, 45(2), 126-135.

Westerhoff, P., and M. Pinney, (2000). Dissolved organic carbon transformations during laboratory-scale groundwater recharge using lagoon-treated wastewater. *Waste Management*, 20, 75-83.

World Health Organization (WHO), (2006). *Guidelines for the safe use of wastewater, excreta and greywater: volume 2, Wastewater use in agriculture*. World Health Organization, France.

Yang Y. J., and J.A. Goodrich, (2014). Toward quantitative analysis of water-energy-urban-climate nexus for urban adaptation planning. *Current Opinion in Chem Engrng*, 5, 22-28.

Yang, Y. J., J.A. Goodrich, S.Y. Li, and R.C. Haught, (2007). AST/R-based water reuse as a part of the total water solution for water-stressed regions: An overview of engineering practice and regulatory prospective. *Water Environmental and Water Resources Congress 2007*, Tampa, Florida.

Yang, Y. J., R. D. Spencer, and T. M. Gates, (1997). Analytical Solutions for Determination of Non-Steady- State and Steady-State Capture Zones. *Groundwater Monitoring & Remediation*, 15, 101–106.

Yang, Y. J., and T. M. Gates, (1997). Well-bore skin effect and slug test data analysis for aquifers of low permeability. *Ground Water*, 55(6), 931-937.

Yang, Y. J., D. J. Murray, and J. A. Goodrich, (2007). Water Resources Adaptation to Global Changes: Risk Management through Sustainable Infrastructure Planning and Management. *Water resource adaptation to GCC, 08 Water Down Under,* Adelaide, Australia

Yates, M.V., and Y. Ouyang, (1992). VIRTUS, a model of virus transport in unsaturated soils. *App. Env. Microbiol.*, 58(5), 1609-1616.

Yeh, G. T., (1981), AT123D: Analytical Transient One-, Two-, and Three-Dimensional Simulation of Waste Transport in the Aquifer System. *ORNL-5602*, Oak Ridge National Laboratory, Oak Ridge, TN.

Zheng, L., J. A. Apps, Y. Zhang, T. Xu, and J. T. Birkholzer, (2009). On mobilization of lead and arsenic in groundwater in response to CO_2 leakage from deep geological storage. *Chemical Geology*, 268, 281–297.

Zheng, C., (2010). *MT3DMS v5.3 Supplemental User's Guide*. Technical Report to the U.S. Army Engineer Research and Development Center, Department of Geological Sciences, University of Alabama, 51 p

Appendix A

Literature Review and Experimental Analysis of Arsenic Re-mobilization at ASR Sites*

*   Modified from Neil et al. (2012) (*Journal of Environmental Monitoring,* 14, 7, 1772-1788) and Neil et al. (2014) (*Environmental Science and Technology*, 48, 8, 4395-4405)

1. Arsenic Occurrence and Natural Sources

Arsenic remobilization is a principal challenge in groundwater and at ASR sites. After conventionally treated effluent undergoes tertiary treatment, the effluent, i.e., reclaimed wastewater, can be a common water source for ASR operation (Sheng, 2005; Pavelic et al., 2005; Vanderzalm et al., 2006). Not only is the use of reclaimed water cost effective, but natural attenuation processes in the vadose zone and underlying aquifer have been shown to remove residual pathogens from the injected secondary water (Wilson et al., 1995; Asano and Cotruvo, 2004).

However, recent studies at ASR field sites have shown that reclaimed water recharge can trigger unfavorable soil–water interactions releasing arsenic, a toxic metalloid, from aquifer materials. Unfavorable soil-water interactions can release arsenic from aquifer materials resulting in dangerously high levels of arsenic in groundwater in large areas of the U.S., Australia, Germany, and China (e.g., Pavelic et al, 2005; Greskowiak et al., 2006). Table A-1 shows locations around the globe where elevated arsenic has been measured as a result anthropogenic groundwater recharge. For example, Jones and Pichler (2007) reported that while injection waters to an ASR site in South Central Florida contained 3 μg/L of arsenic, recovered levels ranged from 10-130 μg/L. Despite the observations and intense studies in multiple aquifer systems, consensus has not been reached on the dominant cause of arsenic remobilization (Jones and Pichler, 2007; Wallis et al., 2010). This ambiguity in knowledge is further complicated by many potential sources for arsenic, and by the attenuation processes that occur concurrently within the aquifer (Wang and Mulligan, 2006; Wallis et al., 2011).

Arsenic exists naturally in aquifer formations in several forms (Figure A-1). Frequently, arsenic is incorporated into pyrite (FeS_2), in quantities as large as 10wt%. Substitution of arsenic into pyrite crystalline structure occurs under both oxidizing and reducing conditions, and the resulting structure contains AsS dianion groups (Blanchard et al., 2007). The product, called arsenian pyrite, is less stable than pyrite and will dissolve more rapidly in water. Arsenic can also be substituted into marcasite (FeS_2), which is arranged in an orthorhombic structure, as compared to the cubic structure of pyrite. This mineral is less geochemically stable than pyrite, and compared to arsenian pyrite, arsenic-substituted marcasite has a larger arsenic solubility in water (Reich and Becker, 2006). In addition, the substitution product can be either a stable solid solution, or metastable. The metastable solid will eventually form nano-domains of pyrite or marcasite and arsenopyrite (Reich and Becker, 2006).

Arsenopyrite (FeAsS), which contains a 1:1:1 ratio of iron, sulfur, and arsenic, has a monoclinic structure similar to that

a) Arsenopyrite   b) Scorodite
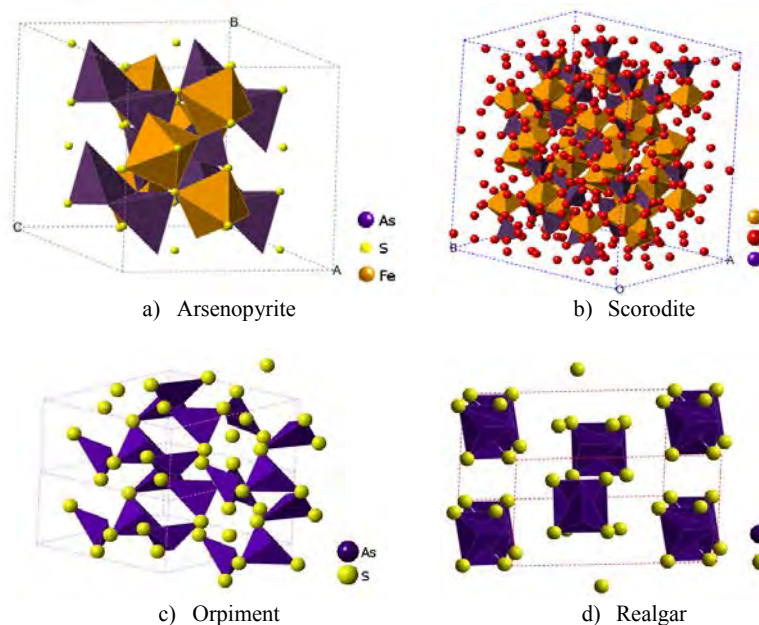
c) Orpiment   d) Realgar

Figure 1: Structures of arsenic-containing minerals created using Crystal Maker V.2.3.

Figure A-1   Structures of arsenic-containing minerals. After Neil et al. (2012).

74

_____

Table A-1.   Location and conditions for recharge-influenced arsenic mobilization.
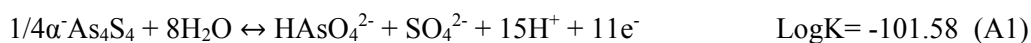
Site	Recharge Water	Aquifer Type	Site Characteristics	Arsenic Level	Reference
ASR Site					
Full-scale ASR trial at Bolivar, South Australia	Reclaimed water from the Bolivar Water Reclamation Plant	Carbonate Aquifer	Injection flow rate: 7.9-11.9 L/s Recovery flow rate: 8.7-15.9 L/s Depth: 100-160 m $K_{average}$: 3 m/day	Injected: 0.04 ± 0.03 μM Ambient: 0.04 ±0.03 μM Recov.: 0.30 ± 0.16 μM	Vanderzalm et al. (2011)
Southwest-Central Florida Groundwater Basin, USA	Surface water	Highly permeable carbonate rocks, Suwannee Limestone, Ocala Limestone	K: 0.98-30 m/day Pyrite: 276-32,406 mg/kg As wt% pyrite: 0.01-1.12	Injected and storage zone: 3 μg/L Recovered: 10-130 μg/L	Wallis et al. (2011) Jones and Pichler (2007)
San Joaquin Valley, California, USA	Surplus water from the Stockton East Water District Water Treatment Plant	Fluvial sediment of the Pleistocene Modesto and Riverbank Formations	Injected flux: 2.5×10^6 m^3/surface area Depth: 60 m	Injected: <5 μg/L Recovered: 7-10 μg/L	McNab et al. (2009)
Fox River Valley, Green Bay, Wisconsin, USA	Surface water and groundwater from another aquifer	Sandstone and limestone	Transmissivity: 102 m^2/day	Recovered: 3-60 μg/L	Bahr et al. (2002) Brown et al. (2006)
Manatee, Florida, USA	Reclaimed water	Carbonate aquifer	Aquifer τ: 0.5 months Salinity: 2000 mg/L T: 26ºC; flow rate: 5.26 m^3/min Storage: 19,000 m^3	Injected: ND Ambient: 8 μg/L Recovered: 24 μg/L	Overacre et al. (2006)
Ruhr Valley, Western Germany	Bank infiltration	Sandy sediment, anoxic Pleistocene aquifer	V: 0.21-0.82 m/day	Maximum of .185 μM for V = 0.21 m/day Maximum 0.340 μM for V = 0.82 m/day	Schlieker et al. (2001)
Pumping station Schuwacht (Hydron-ZH), Netherlands	Treated and aerated groundwater.	Coarse, sandy sediments of the Sterksel formation	Water periodically injected, flow rate: 30 m^3/h for 2 days Depth: 20-30 m	Injected: 0 μg/L Recovered: 9-14 μg/L	Appelo et al. (2002)

_____

Table A-1 continued.

Site	Recharge Water	Aquifer Type	Site Characteristics	Arsenic Level	Reference
Aquifer recharge site					
Western Snake River Plain, Idaho, USA	Crop irrigation with surface water	Alluvial gravels and sands	Recharge rate: > 50 cm/year Average O_2: 4.8 mg/L	Surface irrigation: 7 µg/L Seep water: 38 µg/L	Busbee et al. (2009)
Hetao basin, Northwest China	Alluvial fan overflow and irrigation channels	alluvial-pluvial sand, fluvial-lacustrine sandy silt, silty clay and organic matter rich clay	K=10-20 m/day	Moderate flow (recharge) zone: 30.6 µg/L Low flow: 131 µg/L Discharge zone: 34 µg/L	Guo et al. (2008)
Madison River Valley, Montana, USA	Arsenic-rich river water and irrigation	Quaternary alluvium and tertiary volcano-clastic sediment,	Groundwater flow rate: 0.34 m^3/s Transmissivity: 2490 m^2/day	Recharge: 41-74 µg/L Oxic zone: 25-50 µg/L Reduced zone: 60-160 µg/L	Nimick (1998)

Note: K is the hydraulic conductivity, V is the linear velocity of the fluid, and τ is residence time.

of marcasite (Brostigen and Kjekshus, 1970). Arsenopyrite is the most commonly occurring As-bearing mineral in Earth's crust, and is very stable under natural conditions (Mandal and Suzuki, 2002; Gonzalez et al., 2006). However, the exposure of these minerals to either oxidizing or acidic aqueous conditions may result in mineral decomposition which may release arsenic into the environment (Verplanck et al., 2008). Under oxidizing conditions, the solubility of arsenopyrite is limited by the solubility of scorodite ($FeAsO_4 \cdot 2H_2O$), an oxidation product of arsenopyrite. Acidic or reducing surficial conditions can result in the transformation of arsenopyrite into realgar (α-As_4S_4) or orpiment (As_2S_3). Both of these are monoclinic arsenic sulfides with very low solubilities, and may provide some mitigation of arsenic mobility in reducing environments. These three minerals would release arsenic through the following reactions (Sadiq et al., 2002):

$$1/4\alpha^- As_4S_4 + 8H_2O \leftrightarrow HAsO_4^{2-} + SO_4^{2-} + 15H^+ + 11e^- \qquad \text{LogK= -101.58 (A1)}$$

$$As_2S_3 + 20H_2O \leftrightarrow 2HAsO_4^{2-} + 3SO_4^{2-} + 38H_+ + 28e^- \qquad \text{LogK= -219.21 (A2)}$$

$$FeAsO_4 \cdot 2H_2O + H^+ \leftrightarrow Fe_3^+ + HAsO_4^{2-} + 2H_2O \qquad \text{LogK= -11.67   (A3)}$$

The most likely culprits of increased arsenic during ASR are arsenopyrite and arsenian pyrite due to aqueous chemistry changes (e.g. changes in reduction-oxidation potential, dissolved oxygen levels, and pH) induced by reclaimed water injection.

Physiochemical and biological process mechanisms at nano- to macro-scales are responsible for arsenic mobilization from arsenic-bearing minerals and for arsenic sinks present within groundwater aquifers. Table A-2 describes these reactions pathways. Mechanisms that can promote arsenic remobilization include the oxidation of arsenic-bearing minerals and reduction of arsenic-containing ferrihydrite, as well as the impact of groundwater aquifer hydrology and microbial activity on the kinetics of arsenic release. The mechanisms which can attenuate aqueous arsenic concentrations in natural and ASR systems include arsenic sorption onto iron-oxyhydroxides and co-occurring arsenic-sulfide precipitation. Some of the processes operate for both remobilization and attenuation.

2. Arsenic remobilization and dissolution mechanisms

Arsenopyrite and arsenian pyrite are redox sensitive minerals. Changes in the oxidation-reduction potential can trigger physico-chemical processes that affect total aqueous arsenic concentrations in groundwater. The composition of reclaimed water can differ from resident groundwater in terms of the concentrations of salts, metal ions, organic compounds, and dissolved oxygen. Injection of reclaimed water can, therefore, serve as a trigger which destabilizes arsenopyrite leading to an increase in arsenic mobility.

2.1. Oxidation of Arsenic-bearing minerals

Naturally, dissolved oxygen is not abundant in deep aquifers. However, it can be present in shallower aquifers or introduced by the injection of oxygenated reclaimed water through wells and other recharge facilities. Table A-3 provides empirically derived rate laws for arsenopyrite oxidation. In principle, molecular oxygen will interact with arsenopyrite through the following mechanism (Walker et al., 2006):

$$4FeAsS + 6H_2O + 11O_2(aq) \leftrightarrow 4Fe^{2+} + 4H_3AsO_3 + 4SO_4^{2-} \qquad (A4)$$

Both iron and arsenic could then be further oxidized through the following two reactions:

$$H_3AsO_3 + H_2O \leftrightarrow HAsO_4^{2-} + 4H^+ + 2e^- \qquad (A5)$$

$$Fe^{2+} + 3H_2O \leftrightarrow Fe^{III}(OH)_3 + 3H^+ + e^- \qquad (A6)$$
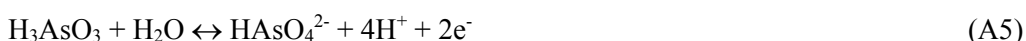
Table A-2: Processes impacting aqueous arsenic mobility*.

Description	Proposed Mechanism	References
Arsenic Mobilization Processes		
Arsenic-containing pyrite dissolution	Oxidation by O_2: $FeAsS + 1.5H_2O + 2.75O_{2(aq)} \leftrightarrow Fe^{2+} + H_3AsO_3 + SO_4^{2-}$ Oxidation by Fe^{3+}: $FeAsS(s) + 7H_2O + 11Fe^{3+} \leftrightarrow 12Fe^{2+} + H_3AsO_3(aq) + SO_4^{2-} + 11H^+$	Walker et al. (2006) Yu et al. (2007)
Reduction of arsenic-bearing ferrihydrite	Reduction by bio-organisms in the presence of acetate**: $8FeOOH + CH_3COO^- + 15H_2CO_3 \rightarrow 8Fe^{2+} + 17HCO_3^- + 12H_2O$	McArthur et al. (2001)
Labile arsenic release	Competitive desorption from iron oxides or clay minerals due to anionic ligand (silicate, phosphate, carbonate, etc.) concentration influx	Violante and Pigma (2002) Waychunas et al. (2008) Jain and Loeppert, (2000)
Arsenic Attenuation Processes		
Sorption onto ferrihydrite	$Fe^{2+} + 3H_2O \leftrightarrow Fe(OH)_3 + 3H^+ + e^-$	Salzsauler et al.(2005)
Precipitation of arsenic-containing minerals	Precipitation of scorodite: $Fe^{3+} + HAsO_4^{2-} + 2H_2O \leftrightarrow FeAsO_4 \cdot 2H_2O + H^+$ Precipitation of arsenic-sulfides	Salzsauler et al. (2005)

Note: 	* - Adopted from Neil et al. (2012).
	** - Used as a model organic compound.

Table A-3: Empirically derived rate laws for arsenopyrite oxidation by compounds of interest*.

Conditions	Rate Law	Reference
T = 25ºC	$R_{O_2(aq)} (\text{mol m}^{-2}\text{s}^{-1}) = 10^{-7.41\pm0.47} \times a_{O2}^{0.76\pm0.11} \times a_{H+}^{-0.12\pm0.01}$; a_i=activity i	Asta et al. (2010)
T= 25ºC, pH = 2, I= 0.01 M	$R_{Fe^{3+}}$ (mol mineral m^{-2} s^{-1})= $-10^{-5.00}(M_{Fe^{3+}})^{1.06\pm0.11}$	McKibben et al. (2008)
T = 25ºC, pH = 2-4, I = 0.01 M	$R_{O_2(aq)}$ (mol mineral m^{-2} s^{-1}) = $-10^{-6.11}(M_{O_2(aq)})^{0.33\pm0.18}(M_{H^+})^{0.27\pm0.09}$	McKibben et al. (2008)
T = 25ºC, pH = 2	$R_{Fe^{3+}}$ (mol s^{-1})= $-1.45\times10^{-3}(A)(m_{Fe^{3+}})^{0.98}$ A=Arsenopyrite surface area (m^2); m_i=mol i kg^{-1}	Rimstidt et al. (1993)
pH = 1.8-6.4	$R_{O_2(aq)} (\text{mol m}^{-2}\text{s}^{-1}) = 10^{\frac{-2211\pm57}{T}}(M_{O_2(aq)})^{0.45\pm0.05}$	Yu et al. (2007)
T = 25ºC, pH = 6.3-6.7, DO = 0.3-17 mg L^{-1}	$R_{O_2(aq)} (\text{mol m}^{-2}\text{s}^{-1}) = 10^{-10.14\pm0.03}$	Walker et al. (2006)
T= 40ºC, pH = 1.6 12% solids and microorganisms	$R_{bio}(\text{kg m}^{-3}\text{d}^{-1}) = 2.1$	Miller and Hansford (1992)
T = 25ºC pH = 1.1 $E_{initial}$ = 615 mV	$R \text{ (mol } L^{-2}\text{ s}^{-1}) = \dfrac{[Fe_{total}]\frac{zF}{RT}\frac{dE}{dt}}{(1+\frac{[Fe^{3+}]}{[Fe^{2+}]})(\frac{5}{\frac{[Fe^{3+}]}{[Fe^{2+}]}}+6)}$ z=moles of electrons transferred; F=Faraday constant; E=reduction-oxidation potential	Ruitenberg et al. (1999)
Alkaline solution 265.4 < pO₂ < 1053 kPa	$\dfrac{dn_{FeAsS}}{dt} = ke^{\frac{-15.1\,kJ}{RT}}[OH^-]^{0.23}$	Koslides and Ciminelli (1992)
T = 120-180ºC pO₂ = 2-20 atm 0.5 N H₂SO₄	$-\dfrac{dN}{Sdt} (mol \min^{-1} cm^{-1}) = 49.527e^{\frac{-8672}{T}}pO_2$ S=total surface area of FeAsS particles	Papangelakis and Demopoulos(1990)

Note: * - Adopted from Neil et al. (2012), T = temperature, I = Ionic strength, DO=Dissolved oxygen.

Salzsauler et al. (2005) studied a system containing these two reactions at the arsenopyrite residue stockpile in Snow Lake, Manitoba Canada, which formed as a result of mining arsenopyrite-associated gold. Arsenopyrite was found to be stable under high pH and low E_h conditions; however after oxidation, Fe^{2+} and As^{3+} was released and secondary mineral precipitation occurred

Figure A-2   Eh-pH diagrams from Salzsauler et al (2005). Activity of arsenate=10^{-3}, Fe(II)=10^{-4} and SO_4=10^{-2}. Adopted from Neil et al. (2012).

as predicted in the E_h-pH diagram shown in Figure A-2. Site measurements indicated that while the E_h was dictated by the Fe^{2+}/Fe^{3+} couple, the equilibrium would also be affected by pH, because lower pH values increased the ratio of As^{3+} to As As^{5+}. Groundwater pH values in the analysis here generally ranged between 7 and 9, and E_h values between 0 and 0.2 V. Under these conditions, the formation of goethite and amorphous $Fe(OH)_3$ were kinetically favorable. Both of these minerals have the capability of sorbing aqueous arsenic. A decreased E_h under the same pH conditions would result in the formation of AsS_2^-, while lowering the pH under the same Eh conditions would form H_3AsO_3. Neither of these conditions would mitigate arsenic mobility. As shown in Figure A-2, scorodite also forms in near-neutral pore solutions (pH $\approx$ 7, E_h $\approx$ 0.1 V) thorough the following reaction:

$$Fe^{3+} + HAsO_4^{2-} + 2H_2O \leftrightarrow FeAsO_4 \cdot 2H_2O + H^+ \qquad (A7)$$

The formation of scorodite can immobilize the arsenic in groundwater. However, this reaction would also lower the pH of the system, decreasing the supply of As^{5+} due to both consumption during reaction and less favorable reduction-oxidation conditions. Consequently, the saturation index with respect to scorodite would decrease, reaching a geochemical equilibrium, because As^{5+} is needed for continuous precipitation.

In addition to the influx of oxidants and reductants such as O_2, Fe^{3+}, and total organic carbon (TOC) during ASR, the oxidation states of metal may also be impacted by microbial activity. Nesbitt et al. (1995) studied the oxidation of arsenopyrite by air-saturated distilled water and found that microbial processes caused changes to the mineral surface and structure. The surface iron layer in arsenopyrite transformed into Fe^{3+}-oxyhydroxides, and this transformation provides a potential source of arsenic attenuation through arsenic sorption onto the mineral surfaces. They also reported diffusion of iron and arsenic atoms from within the bulk mineral to its surface, as opposed to electron transfer. At the surface, As(-I) was oxidized, forming As^{5+} and As^{3+} oxyhydroxides. These oxidized arsenic species dissolve readily into solution as aqueous arsenate (AsO_4^{3-}) or arsenite (AsO_3^{3-}). Although these surface altering processes also occurred on arsenopyrite oxidized in air, the rate of oxidation was significantly enhanced by the presence of water; In Nesbitt's study, following 25 hours of reaction in the air, only 22% of the surface iron had transformed to Fe^{3+}-oxyhydroxides, compared to 64% on the sample reacted in the presence of water.
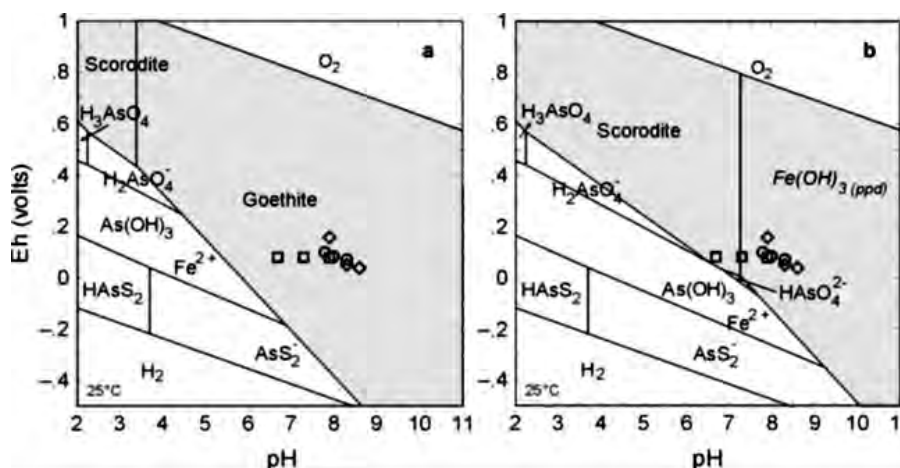
80

McKibben et al. (2008) investigated the differences between oxidation of arsenopyrite by dissolved oxygen, Fe^{3+}, and NO_3^-, and also examined temperature effects on the oxidation process. Temperature experiments revealed non-Arrhenius behavior, including the promotion of an inhibitory side reaction that prevented FeAsS dissolution. This side reaction was hypothesized to be the precipitation of arsenic-sulfide minerals at higher temperatures. According to Rimstidt et al. (1993), the activation energy for the oxidation of arsenopyrite becomes negative at temperatures greater than 25ºC, implying that oxidation occurs under ambient conditions. Comparison between the oxidation rates by Fe^{3+} and O_2 showed that Fe^{3+} oxidized arsenopyrite at a rate at least one order of magnitude faster than by dissolved oxygen. The molal specific rates were determined to be:

$$R_{Fe^{3+}} \text{ (moles mineral m}^{-2}\text{ s}^{-1}) = -10^{-5.00}(M_{Fe^{3+}})^{1.06\pm0.11} \tag{A8}$$

$$R_{O_{2(aq)}} \text{ (moles mineral m}^{-2}\text{ s}^{-1}) = -10^{-6.11}(M_{O_{2(aq)}})^{0.33\pm0.18}(M_{H^+})^{0.27\pm0.09} \tag{A9}$$

Results from the NO_3^- study did not show dissolution by either oxidative or proton-promoted dissolution when under anaerobic conditions.

These results are consistent with other studies examining the oxidation of arsenopyrite by Fe(III) (Yu et al. 2004, 2007). Not only is Fe(III) found often in reclaimed water, but it can be a product of arsenopyrite or arsenian pyrite dissolution from solids in the subsurface (e.g. Eq.3). Oxidation by Fe(III) occurs according to the following pathway (Yu et al., 2004):

$$FeAsS(s) + 7H_2O + 11Fe^{3+} \leftrightarrow 12Fe^{2+} + H_3AsO_3(aq) + SO_4^{2-} + 11H^+ \tag{A10}$$

Although this reaction will deplete aqueous Fe^{3+}, it can be recreated through the reoxidation of Fe^{2+} by dissolved oxygen or by iron-oxidizing bacteria in the environment. In particular, at lower pHs, the oxidation of FeAsS by aqueous Fe^{3+} would dominate over the oxidation by dissolved oxygen. For example, at pH 1.8, the activation energy of FeAsS oxidation by Fe^{3+} is 16 kJ/mol, as compared to 43 kJ/mol for dissolved oxygen, which would allow for fast oxidation by Fe^{3+} (Yu et al., 2004).

Despite the greater potential impact of Fe^{3+} on arsenopyrite oxidation, the effect of oxygen is expected to prevail at ASR sites because the occurrence of very acidic (i.e. pH 1.8) groundwater is rare and oxygen is ubiquitous in injected secondary water. It should be observed, however, that not all studies agreed on the influence of dissolved oxygen on arsenopyrite dissolution. Walker et al. (2006) found that changes in dissolved oxygen levels between 0.3 and 17 mg/L did not impact dissolution over a pH range of 6.3–6.7. As a result, they concluded that the rate-determining step was not the electron donation to the oxidant, dissolved oxygen, but rather the removal of electrons from As^{-1} or S^{-1} and electron transfer to the oxygen atom in water. Modeling this process is further complicated because the oxidation of arsenopyrite does not necessarily release arsenic and ferrous iron congruently. While iron will be released at a stoichiometric ratio during FeAsS dissolution, As and S display lower dissolution rates (McKibben et al., 2008). This occurs because the Fe can readily leave the lattice structure while As and S are retained on the surface due to differences in the oxidation rates of the individual elements. By contrast, both Buckley and Walker (1988) and McGuire et al. (2001) found elemental sulfur remaining on the mineral surface, while both Fe and As were oxidized and leached out; McGuire et al. hypothesized that this sulfur was the product of a complex oxidation pathway.

Another mechanism for arsenic mobilization is sulfide-arsenide exchange in the presence of an oxidant (Zhu et al., 2008). This mechanism likely proceeds through the binding of aqueous sulfide to iron on the surface of arsenopyrite or arsenian pyrite, destabilizing arsenic within the mineral lattice. As^{-1} is consequently more vulnerable to oxidation processes, ultimately forming pyrite and an aqueous arsenite or arsenate species. For aquifers that contain H_2S, this reaction may proceed through the following mechanism (Heinrich and Eadington, 1986):

$$4FeAsS + 4H_2S + 5O_2(g) + 2H_2O \leftrightarrow 4FeS_2 + 4H_3AsO_3 \tag{A11}$$
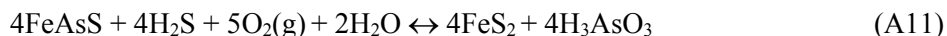
This reaction can continue until most of the reactive surface arsenic atoms are released, and proceed further through the oxidation of surface pyrite or fracturing of the surface, which would expose new arsenic-rich sites (Zhu et al., 2008). In the reaction, the source of aqueous sulfide is often a product of sulfate-reducing bacteria through the following mechanism (Jøgensen, 1983):

$$2CH_3CHOHCOO^- + SO_4^{2-} \leftrightarrow 2CH_3COO^- + 2HCO_3^- + H_2S(aq) \qquad (A12)$$

These bacteria are most likely to flourish under anaerobic conditions, which are not conducive to sulfide-arsenide exchange. Therefore, in order for this process to take place there must first be an environment that favors H_2S generation. The oxidant would then be introduced to the system, potentially through the injection of oxygenated secondary water during ASR. This could induce the oxic or hypoxic conditions prerequisite to Reaction (11) taking place. Under conditions where sulfide and an oxidant are present in groundwater, this reaction is more thermodynamically favorable than oxidation by molecular oxygen (Zhu et al., 2008). It can occur in the absence of oxygen, when another oxidant such as Fe^{3+}, Mn^{4+}, or nitrate (i.e. electron acceptors) is present.

2.2 Reduction of arsenic-containing ferrihydrite

While the aforementioned mechanisms point to the solubilization of arsenic as a result of oxidation, reducing conditions can also mobilize arsenic from aquifer materials. This process generally occurs through the reduction of arsenic-bearing ferrihydrite $[Fe(OH)_3]$ (Zhu et al., 2008; Zheng et al., 2004; McArthur et al., 2001). Ferrihydrite strongly sorbs arsenic, and desorption is less likely to occur until the mineral degrades through dissolution. There exist other processes that can affect the sorption of arsenic to ferrihydrite. Both ferrous iron and carbonate may form surface complexes on ferrihydrite resulting in arsenic displacement (Appelo et al., 2002). Furthermore, phosphate and silicate will compete with arsenate (As^{5+}) for sorption sites on the mineral surface (Violante and Pigna, 2002; Jain and Loeppert, 2000; Waychunas et al., 2007; Dixit and Hering, 2003).

Arsenic exists in many aquifer formations associated with ferrihydrite, either through sorption or co-precipitation. Reduction processes can result from interactions between As-bearing ferrihydrite and ammonium, sulfide, and organic matter. Frequently, these reductants are products of microbial processes. For example, ferrihydrite reduction by organic matter (e.g. acetate) occurs through the following reaction (McArthur et al., 2001):

$$8FeOOH + CH_3COO^- + 15H_2CO_3 \rightarrow 8Fe^{2+} + 17HCO_3^- + 12H_2O \qquad (A13)$$

where acetate is a product of microbial metabolism of organic matter. McArthur et al. (2001) speculated on the impact of peat beds within aquifers as a source for this organic matter. Their study showed that there was a correlation between areas with high groundwater arsenic levels and the location of these peat beds. Simeoni et al. (2003) studied the impact of fulvic acid on As^{5+} sorption to ferrihydrite. It was found that fulvic acid can both inhibit sorption and displace sorbed arsenic from the surface; the fulvic acid could reduce ferrihydrite at a rate of 30 nM/h. In addition, humic and fulvic acids can affect the rate of microbial ferrihydrite reduction. Wolf et al. (2009) found that both humic acid and fulvic acid accelerated the reduction of ferrihydrite through electron shuttling in the presence of microorganisms. The reducing capacity of humic acid was 1.8 eq/mol, compared to 0.6 eq/mol for fulvic acid. In addition, citric acid can prevent As^{5+} sorption onto ferrihydrite and both citric and fulvic acids can prevent As^{3+} sorption onto ferrihydrite (Grafe et al., 2002).

Reduction is not limited to ferric iron within the mineral matrix; reduction of arsenic on the mineral surfaces can also occur. The efficacy of ferrihydrite as an arsenic sorbent stems from its ability to form surface complexes with aqueous As^{3+} and As^{5+}. The impact of arsenic speciation on this binding has been studied extensively (Goldberg and Johnston, 2001; Cheng et al., 2009; Tufano et al., 2008; and Sverjensky and Fukushi, 2006). Goldberg and Johnston (2001) found that As^{5+} forms inner-sphere

complexes with amorphous Fe oxides, while As^{3+} forms both inner- and outer- sphere complexes. Inner-sphere complexation refers to the specific binding of the arsenic ion to the mineral surface, while outer-sphere complexation refers to the electrostatic interactions between the ion and surface (Cheng et al., 2009). As^{5+} forms a bidentate binuclear complex, meaning that each arsenic anion chemically forms two bonds with the surface metal ions. This type of surface complexation is stronger and less likely to dissociate than the monodentate binuclear complex which forms through the singular bond of As^{3+} anions to ferrihydrite. This inner-sphere As^{3+} complex will dominate under high surface coverage, whereas lower coverage will result in binuclear outer-sphere complexes (Cheng et al., 2009). As a result of the weaker binding of As^{3+} to ferrihydrite compared to As^{5+}, Peters and Burkert (2008) and Smedley and Kinnburgh (2002) showed the reduction of As^{5+} on the ferrihydrite surface will result in a certain degree of remobilization. Increases in pH can also lead to desorption of As^{5+}.

Tufano et al. (2008) compared the reduction of arsenic and iron in a system containing As^{5+} sorbed on ferrihydrite. This was accomplished by exposing arsenic-loaded ferrihydrite to mutant microbial strains which reduced either As or Fe, as well as *Shewanella* sp. ANA-3, which reduced both. They found that the largest proportion of arsenic was released due to the As reduction, and the smallest proportion was released due to Fe reduction. This was explained by an equilibration between dissolution and reprecipitation of ferrihydrite which can occur during iron reduction. Because ferrihydrite is less thermodynamically stable, some magnetite (Fe_3O_4) in addition to ferrihydrite will precipitate following reductive dissolution and can further remove arsenic from the system. In addition, intermediate phases such as green rust [$Fe_4^{+2}Fe_2^{+3}(OH)_{12}SO_4 \cdot 3H_2O$] can form during iron oxyhydroxide mineral precipitation and will preferentially sorb aqueous arsenic (Jonsson and Sherman, 2008; Randall et al., 2001). Interestingly, this process was not observed for arsenic sorbed to a more stable mineral, such as goethite, or under arsenic reducing conditions. The net result is the increased arsenic mobilities in these systems.

These findings are consistent with those of Fendorf et al. (2010) in a study of arsenic variation in groundwater in South and Southeast Asia. This study speculated that the primary source of arsenic mobilization in the case described was the weathering of coal and arsenic-containing sulfides. Initially, arsenic will be transferred to iron oxides; however, arsenic can be freed through microbial reduction of Fe^{3+} to Fe^{2+} or As^{5+} to As^{3+} by organisms described in the following section, and through competition for surface sites by other ligands such as phosphate and carbonate.

2.3 Impact of Microbial Activity

Often, the reduction-oxidation potential of the system is dictated by microbial activity within the aquifer. Table A-4 contains a summary of native bacteria which have been studied due to their ability to metabolize the minerals of concern. The impact of microbial activity on the kinetics of arsenic release is critical to consider because they can catalyze both the oxidative dissolution of arsenic-bearing pyrite and the reduction of ferrihydrite (O'Day et al., 2004; Islam et al, 2004; Corkhill and Vaughan, 2009). There must be a supply of organic carbon for microbial activity to be significant. Therefore, the rate of arsenic release will be faster in the presence of reactive organic carbon and for mineral-bound arsenic, as compared to the presence of recalcitrant organic carbon and for arsenic bound to Fe oxides. Under anaerobic conditions within the aquifer, there could be native iron-oxidizing or -reducing bacteria, as well as sulfur-oxidizing or -reducing bacteria.

McGuire et al. (2001) studied changes in mineral surface speciation during microbial-mediated dissolution in order to study sulfide mineral dissolution in natural systems. For this experiment, a sulfur-oxidizing (*Thiobacillus caldus*), iron-oxidizing (*Ferroplasma acidarmanus*), and a mix of sulfur and iron-oxidizing microorganisms (*T. caldus*, *F. acidarmanus*, and *Leptospirillum ferrooxidans*) were utilized. Bacteria were cultured with a mixture of crushed and polished samples of arsenopyrite, marcasite, and pyrite. Cell growth and structural changes on the single crystal surface were observed using scanning

Table A-4: Microbes Impacting Fe/As Oxidation and Reduction in Aquifers.

Bacteria Name	Description	Reference
Desulfotomaculum auripigmentum	Bacteria capable of reducing As(V) to As(III) and precipitating orpiment or amorphous As_2S_3	O'Day et al. (2004)
Thiobacillus caldus	Sulfur-oxidizing bacteria	McGuire et al. (2001)
Ferroplasma acidarmanus	Iron-oxidizing bacteria	McGuire et al. (2001)
Leptospirillum ferrooxidans	Iron-oxidizing bacteria	McGuire et al. (2001)
Pseudomonas species	Used in bioremediation, can be pathogenic	Islam et al. (2004)
Clostridium species	Anaerobic bacteria, grow best on carbohydrates	Islam et al. (2004)
Nitrosolobus species	Ammonia-oxidizing bacteria	Islam et al. (2004)
Thiobacillus ferrooxidans	Iron-oxidizing bacteria that thrives in acidic environments	Jones and Pichler (2007)
Pseudomonas arsenitoxidans	Bacteria capable of oxidizing arsenopyrite	Ilyaletdinov and Abdrashitova (1981)

electron microscopy (SEM) imaging. For samples reacted with the iron-oxidizing or mixtures of bacteria, SEM imaging revealed discrete dissolution pits on the pyrite surface, while marcasite and arsenopyrite developed rough surfaces and linear dissolution pits. Elemental sulfur deposits were also observed on the arsenopyrite surface during both abiotic control experiments and those utilizing iron-oxidizing bacteria. For samples reacted with the sulfur-oxidizing bacteria, dissolution pits were observed on all samples, similar to those seen in the abiotic control, however no sulfur deposits were observed. This is likely due to the bacteria oxidizing sulfur at the surfaces. Because iron concentrations increased linearly over the course of the reaction, they concluded that little or no iron minerals were being formed in the experimental system. Therefore, changes in the iron concentration were used to quantify dissolution rates. Analysis showed that pyrite dissolved at nearly one-sixth the rate than arsenopyrite and half the rate of marcasite. It was also observed that arsenopyrite dissolution was enhanced by the presence of both the iron-oxidizing bacteria, *F. acidarmanus*, and the mixture of *F. acidarmanus*, *T. caldus*, and L. *ferrooxidans,* while marcasite dissolution was only enhanced by the mixture. These enhanced rates resulted from the regeneration of ferric iron by the bacteria.

Arsenopyrite surface morphology changes by acidic, oxidative dissolution by *Thiobacillus ferrooxidans* in the presence of a number of salts, including phosphate, were also studied by Jones et al. (2003). Within a week's time, a layer of $Fe^{+3}PO_4$ had formed on the surface as a result of iron oxidation. This layer was not observed during abiotic control experiments. For the system containing *T. ferrooxidans*, it was also observed that this $Fe^{+3}PO_4$ layer did not prevent oxidation and dissolution of the arsenopyrite below, despite the surface coating. Because the bacteria could not have reached the arsenopyrite below the overlayer in the experimental systems, they concluded that bacteria may not need to be attached to the mineral surfaces to promote arsenopyrite dissolution.

Another study conducted by Islam et al. (2004) looked at the mobilization of arsenic from sediment samples by a mixture of native bacteria, which included Fe^{+3}-reducing and As^{+5} reducing bacteria. Results showed that the reduction of As^{+5} and Fe^{+3} by this bacteria mixture, following stimulation by acetate, was not coupled, and that Fe^{+3} was reduced first, possibly due to its higher redox potential. In addition, the native As^{+5} reducing bacteria were not obligate As^{+5} reducers, meaning that they can utilize other species as electron acceptors, including Fe^{+3}, before they utilize As^{+5}. When a culture of

anaerobic Fe^{+3}-reducing bacteria was used to observe arsenic mobilization, it was also found that arsenic was freed from sediment samples and a higher concentration of As^{+3} was measured as compared to As^{+5}, indicating that the bacteria may have reduced As in addition to Fe.

Some microbes in the aquifer may also be capable of oxidizing arsenite or reducing arsenate. These include dissimilatory arsenate-respiring prokaryotes (DARPs), heterotrophic arsenite oxidizers (HOAs), and chemoautotrophic arsenite oxidizers (CAOs) (Oremland and Stolz, 2003). Some strains are capable of oxidizing arsenite and respiring arsenate (Handley et al., 2009). The microbial arsenic cycle begins with the oxidation of As^{3+} within the aquifer to As^{5+}. This can be a result of arsenite oxidizers, or it can be triggered by human activity such as digging wells and depleting the water table, which provides both oxidants, such as oxygen and nitrogen, and additional biomass. Evidence of this microbial cycle has been found in groundwater aquifers in Bangladesh (Harvey et al., 2002). Furthermore, reclaimed water itself can contain bacterial contaminants. Therefore, it is crucial to examine the impact of both potential microbes in the injected reclaimed water and native bacteria on mineral dissolution.

3. Experimental Investigations

Although many studies exist on groundwater–arsenopyrite interactions and the subsequent fate and transport of arsenic in groundwater, no study to date has fully addressed the unique scenario ASR using reclaimed wastewater. This is in part due to the complicated nature of the interactions, as reclaimed water not only has many constituents, but also its composition will not be constant during a single ASR operation or between different ASR sites. Therefore, this study characterized the potential interactions between prevailing reclaimed water components and arsenic-bearing minerals.

The experimental approaches and procedures were provided in Neil et al. (2014). Major experiments include:

- *Aqueous phase batch reactor testing of dissolution rates.* In this set of experiments, the arsenopyrite dissolution rate were determined under different experimental conditions. Zero-order reaction kinetics were confirmed by the linear concentration evolution of arsenic in the reactor (trend lines in Figure A-3). Each batch reactor contained 250 mL of the reaction solution and 0.05 g of acid-washed FeAsS powder. Reactors were continuously stirred, and temperature was controlled at 5, 22, or $35 \pm 1°C$ using a hot water or ice bath. 2 mL samples were removed at 0, 0.5, 1, 2, 3, 4, 5, and 6 hours and filtered immediately using a 0.2 μm polytetrafluoroethylene (PTFE) membrane syringe filter and capped to prevent evaporative losses. This time frame was chosen to minimize the effect of secondary mineral precipitation on aqueous arsenic levels. Finally, samples were acidified to 2% v/v acid and arsenic concentrations were measured using ICP-MS. At least three experimental replicates were run to confirm arsenic remobilization trends.

- *Characterization of Secondary Mineral Precipitate Morphology and Mineralogy.* Changes on the arsenopyrite mineral surface were examined using polished arsenopyrite thin sections, called "coupons." Tapping mode AFM (AFM, Veeco Inc.) was used to characterize secondary mineral precipitates on arsenopyrite coupons by measuring changes in the height, amplitude and phase over the 7 day reaction period. AFM tapping mode probes were 125 μm long with phosphorus (n) doped silicon tips (nominal tip radius of 10 nm, MPP-11100−10, Bruker probes). In addition, Raman spectroscopy was conducted using an inVia Raman Microscope (Renishaw, UK) on reacted arsenopyrite in order to identify secondary mineral precipitates. Raman measurements were carried out with a 514 nm laser and a grating of 1800 lines/mm. A 20x objective and decreased power were used to limit the energy density of the laser, preventing artificial phase transformation of secondary mineral precipitates (Modesto Lopez et al., 2009).

4. Investigation Results

4.1. Arsenic Dissolution Rate

Evolution of Aqueous Arsenic Concentration

Figure A-3 shows the arsenic concentration changes with time in aqueous phase for 10 mM sodium nitrate, 10 mM sodium chloride, and wastewater under aerobic (A1, B1, and C1) and anaerobic (A2, B2, and C2) conditions. Among aerobic systems, the highest arsenic mobility was observed in the 10 mM sodium chloride system. Arsenic concentrations were similar between the wastewater and sodium nitrate systems. The only difference between the two model wastewater systems was the presence of nitrate versus chloride anions, neither of which are expected to interact significantly with arsenopyrite in the presence of dissolved oxygen according to the literature (McKibben et al., 2008). In addition, neither nitrate nor chloride compete with arsenate for Fe(III) adsorption sites (Rau et al., 2003; Youngran et al., 2007; and Guo and Chen, 2005). Therefore, differences in the arsenic mobility are not anticipated to result from changes in the oxidative dissolution of arsenopyrite or sorption of arsenic, but, more likely, from effects on secondary mineral formation and phase transformation, which further impact arsenic attenuation.

For the anaerobic system, the highest arsenic mobility was observed in the sodium nitrate system (up to 0.28 mM), while very low concentrations were observed in the 10 mM sodium chloride and wastewater systems (up to 0.12 mM and 0.08 mM, respectively). For all systems, arsenic mobility was lower under anaerobic conditions (15%, 78%, and 76% reductions for nitrate, chloride, and wastewater systems, respectively, compared to aerobic conditions), indicating the role of dissolved oxygen in the oxidative release of arsenic from arsenopyrite through reaction (1). The decreased percent reduction in the anaerobic 10 mM sodium nitrate system compared to wastewater and sodium chloride may be due to the oxidation of arsenopyrite by nitrate anions in the absence of dissolved oxygen, which is a new observation. However, more work is needed to confirm this reaction pathway.

Activaton Energy Calculations

For all aqueous systems, the activation energies for arsenic remobilization were calculated using the Arrhenius' equation. Because zero-order reaction kinetics were observed in the early stages of dissolution, the slope of the concentration evolution at each temperature (e.g., trend lines in Figure A-3) was assumed to be equal to the rate constant, k, of the reaction. A larger rate constant would therefore correlate with higher arsenic concentrations at the end of the 6-hour reaction period. The rate constant, k, is related to the temperature and activation energy in accordance with the Arrhenius' equation:

$$k = Ae^{-E_a/RT} \tag{A14}$$

Taking the natural logarithm of this equation gives a linear relationship between the rate constant and temperature, T:

$$\ln(k) = \frac{-E_a}{R}\frac{1}{T} + \ln(A) \tag{A15}$$

The rate constant k for each reaction condition was determined by calculating the slope of the best fit trend line for the concentration evolution at each temperature. The natural log of k was plotted
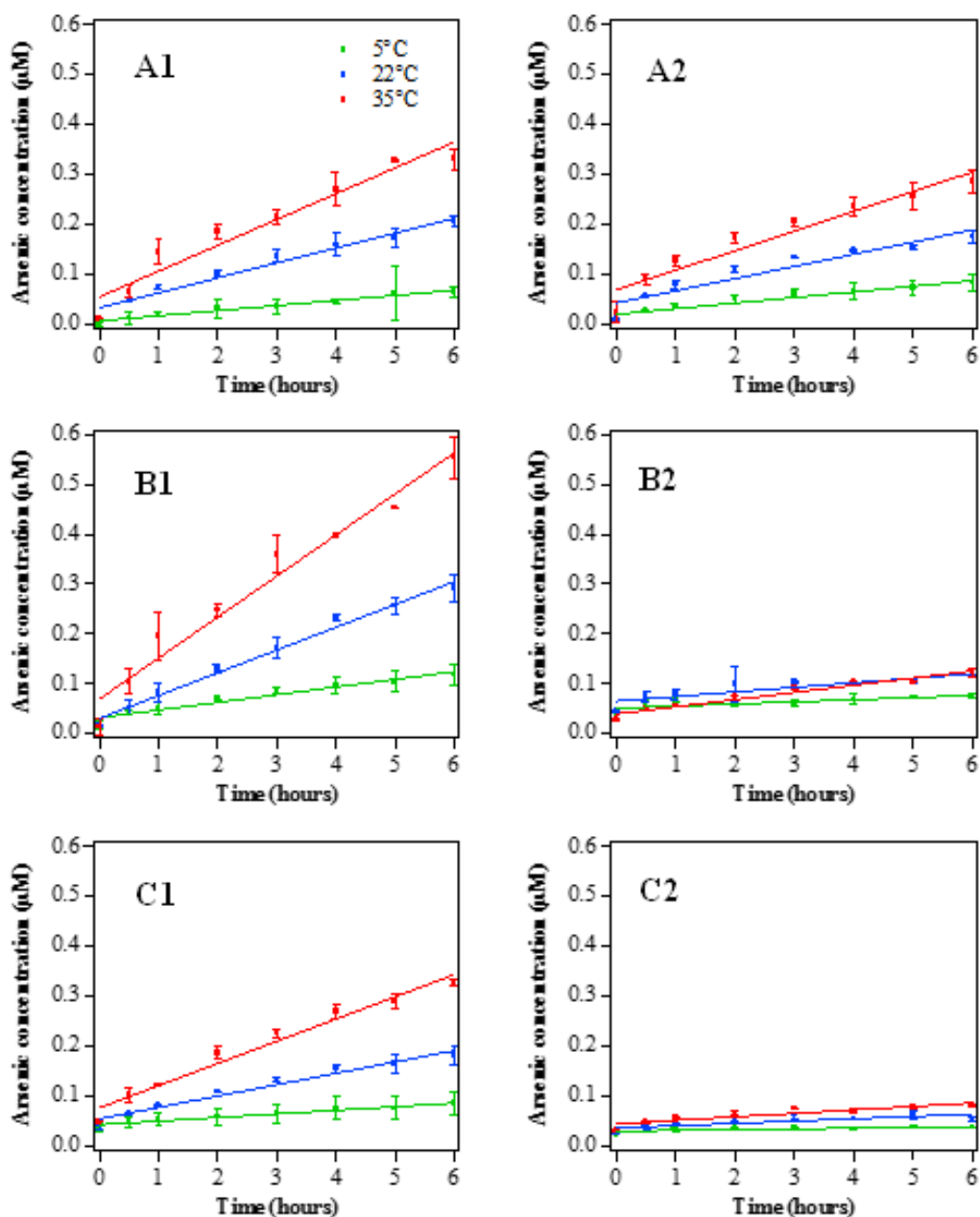
Figure A-3   Aqueous arsenic concentration in batch reactors at 5, 22, and 35°C for (A1) pH 7,
10 mM sodium nitrate, aerobic, (A2) pH 7, 10 mM sodium nitrate, anaerobic, (B1)
pH, 7 10 mM sodium chloride, aerobic, (B2) pH 7, 10 mM sodium chloride,
anaerobic, (C1) pH 7 wastewater, aerobic, (C2) pH 7 wastewater, anaerobic.
Standard deviations between replicate trials are indicated by error bars.

against the inverse of the temperature and the slope of this line was equal to the negative activation
energy, E_a, divided by the gas constant, R. For the aerobic systems, the calculated activation energies for

Table A-5.Empirically determined activation energies for arsenic mobilization from arsenopyrite.

Aqueous Media	Temperatures (°C)	Activation Energies (kJ/mol)	
		Aerobic	Anaerobic
10 mM Sodium Nitrate	5, 22, and 35	40.8 ± 3.5	31.2 ± 3.2
10 mM Sodium Chloride	5, 22, and 35	36.9 ± 2.3	28.4 ± 3.6
Wastewater	5, 22, and 35	43.6 ± 5.0	44.1 ± 6.3

Note: All reactions were carried out at pH 7.0 ± 0.2. The solid-to-liquid ratio was 250 mL: 0.05 g FeAsS powder. See Neil et al. (2014).

arsenic remobilization were 40.8 ± 3.5, 36.9 ± 2.3, and 43.6 ± 5.0 kJ/mol for 10 mM sodium nitrate, 10 mM sodium chloride, and wastewater, respectively. For the anaerobic systems, the calculated activations energies for arsenic remobilization were 31.2 ± 3.2, 28.4 ± 3.6, and 44.1 ± 6.3 kJ/mol, for 10 mM sodium nitrate, 10 mM sodium chloride, and secondary effluent samples from the wastewater treatment plant, respectively (Table A-5). The activation energies for iron release were not calculated because aqueous iron levels were below the detection limit during the 6-hour reaction period. This may result from the reprecipitation of aqueous iron as iron(III) (hydr)oxides.

The literature provides activation energies for a number of minerals related to this system, including the oxidation of arsenopyrite by dissolved oxygen (57 kJ/mol at pH 5.9) (Yu et al., 2007), and the reductive dissolution of ferrihydrite (40.7 kJ/mol) (Erbs et al., 2010), hematite (88 kJ/mol) and goethite (94 kJ/mol) (Sidhu et al., 1981). The range of observed activation energies indicates that the most likely processes occurring are the oxidation of arsenopyrite by DO or the reduction of ferrihydrite, because all measured activation energies ranged between 30 and 50 kJ/mol. Decreases in the activation energy from the aerobic to anaerobic system for sodium nitrate and sodium chloride may indicate a switching of the dominant mechanism for arsenic release from oxidation of arsenopyrite by DO to the reduction of ferrihydrite, which may take place at low reduction-oxidation potentials characteristic of anoxic environments (Pedersen et al., 2006). To confirm these hypotheses, *in situ* X-ray absorption spectroscopy (XAS) can be utilized to observe time-resolved change in iron and arsenic oxidation states and geometry for the different aqueous systems. This necessary testing was not conducted in the research.

For the wastewater system, the activation energy did not change between the aerobic and anaerobic systems. Despite the lower activation energy for 10 mM sodium nitrate and 10 mM sodium chloride in anaerobic systems, the mobility of arsenic in these systems was 3.5 times higher for nitrate and 1.5 times higher for chloride, indicating that other factors, such as the availability of reactants, prevented remobilization. To investigate these observed trends and to determine secondary mineral effects on aqueous arsenic mobilization, the differences in secondary mineral formation and phase transformation were studied between sodium nitrate, sodium chloride, and wastewater systems.

4.2. **Secondary Mineral Precipitate Morphology and Mineralogy**

Secondary Mineral Morphology and Coverage

Differences in secondary mineral precipitation between the three aqueous systems yield further insight into the observed trends in arsenic remobilization. Arsenic remobilization depends on the balance between the dissolution of existing As-bearing minerals and the precipitation of arsenic from the water. Thus the mineral phase and morphology of secondary precipitant yields a basis to assess the degree and completeness of arsenic remobilization.

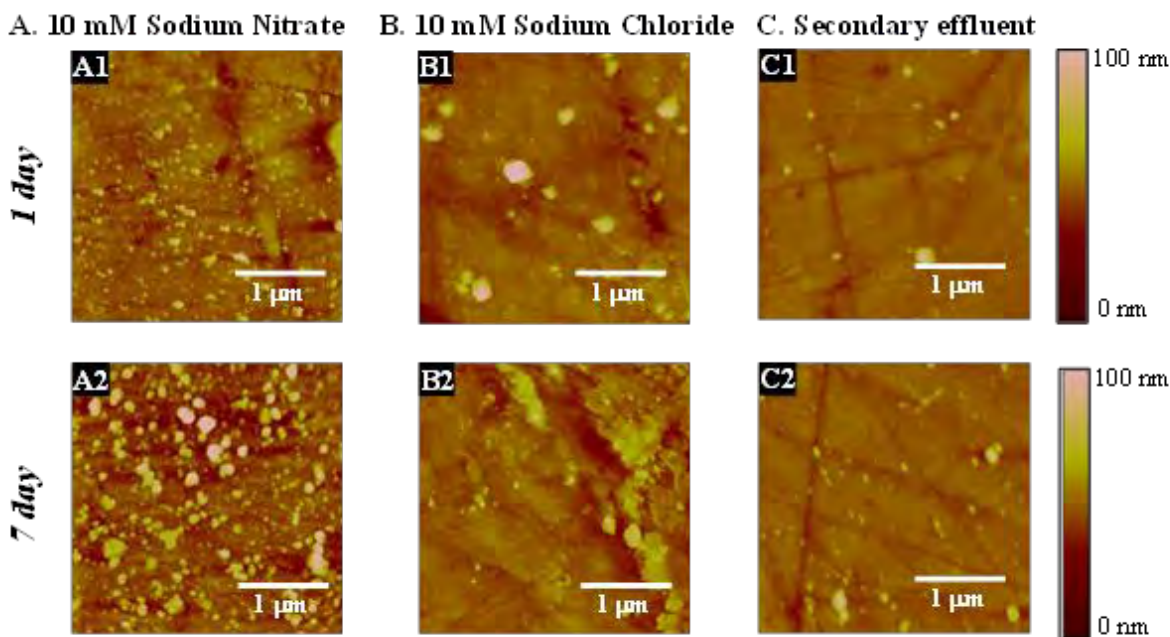A. 10 mM Sodium Nitrate   B. 10 mM Sodium Chloride   C. Secondary effluent

Figure A-4   AFM height mode images after 1 day (A1, B1, C1) and 7 days (A2, B2, C2) in the 10 mM sodium chloride, 10 mM sodium nitrate, and wastewater systems at room temperature (22°C) and under aerobic conditions. The scan size for these images is 3 microns and the height scale is 100 nm.

Figure A-4 shows the AFM height mode images after 1 day and 7 days in the 10 mM sodium chloride, 10 mM sodium nitrate, and wastewater systems at room temperature (22°C) and under aerobic conditions. Images at additional time points are provided in Figure A-5. For all time points, multiple images were taken over the entire sample surface to confirm observations. The images in Figure A-4 showed very distinct differences in precipitate morphology between the three systems. For the 10 mM sodium nitrate system, after 1 day there was a significant amount of small precipitates covering the entire surface (Figure A-4 A1). After 7 days, these precipitates grew in quantity and size, and at the end of the reaction period there was a variety of both larger and small particles, indicating continued nucleation and growth for the entire period (Figure A-4 A2). For the 10 mM sodium chloride system (Figure A-4 B), particles after 1 day were larger in size and sparse on the surface. After 7 days, these particles appeared to aggregate to form a coating on the surface. Unlike the sodium nitrate system, there was not much evidence of continued nucleation because the size and morphology of precipitates was very different between days 1 and 7. For the wastewater system (Figure A-4 C), there was little precipitation after 1 day and both the size and morphology of precipitates did not change significantly over 7 days.

Under anaerobic conditions, there was no observed precipitation on the coupons for all three systems even after 7 days (Figure A-6).
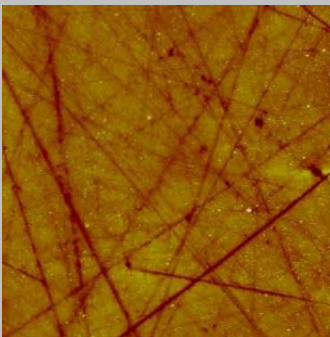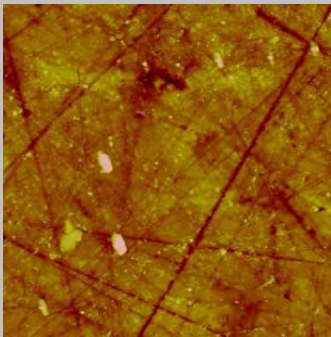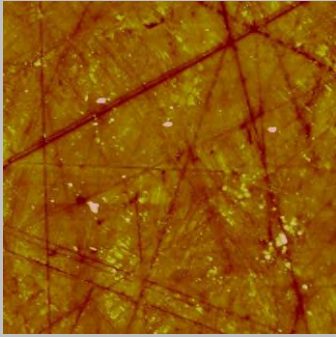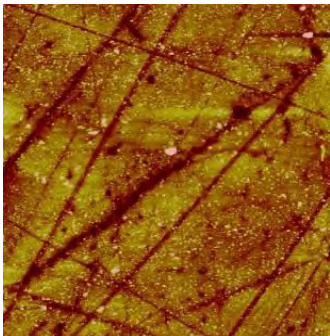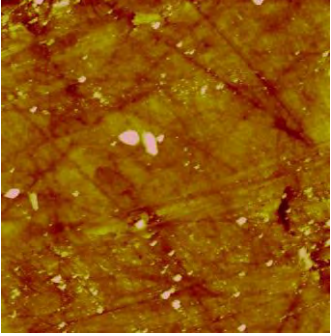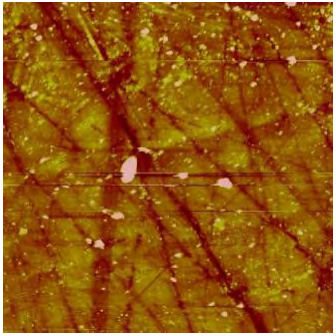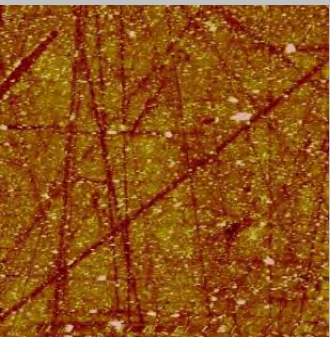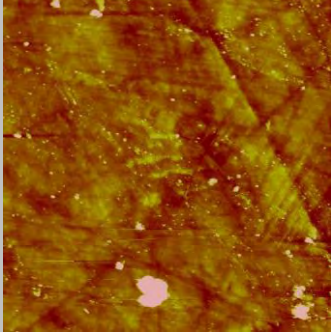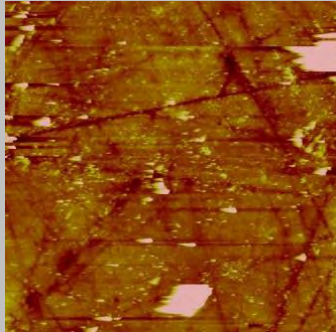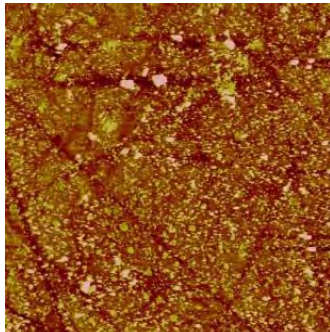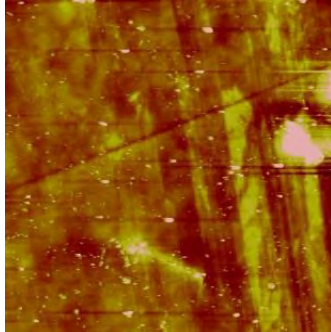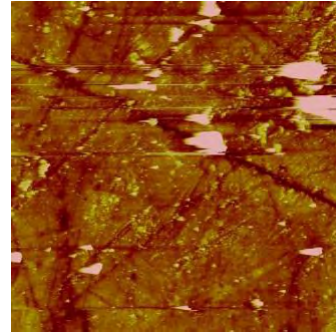
Reaction Time	10 mM sodium nitrate	10 mM sodium chloride	Wastewater
6 hours			
1 day			
4 days			
7 days			

Figure A-5   Tapping mode AFM Images of reacted FeAsS coupons in 10 mM sodium nitrate or 10 mM sodium chloride. All systems were at pH 7.0 ± 0.2, room temperature, and equilibrated with atmospheric oxygen. Images are 20 × 20 μm and the height scale is 100 nm.

Reaction System	10 mM sodium nitrate	10 mM sodium chloride	Wastewater
Anaerobic system 7 days			
Aerobic system 7 days			
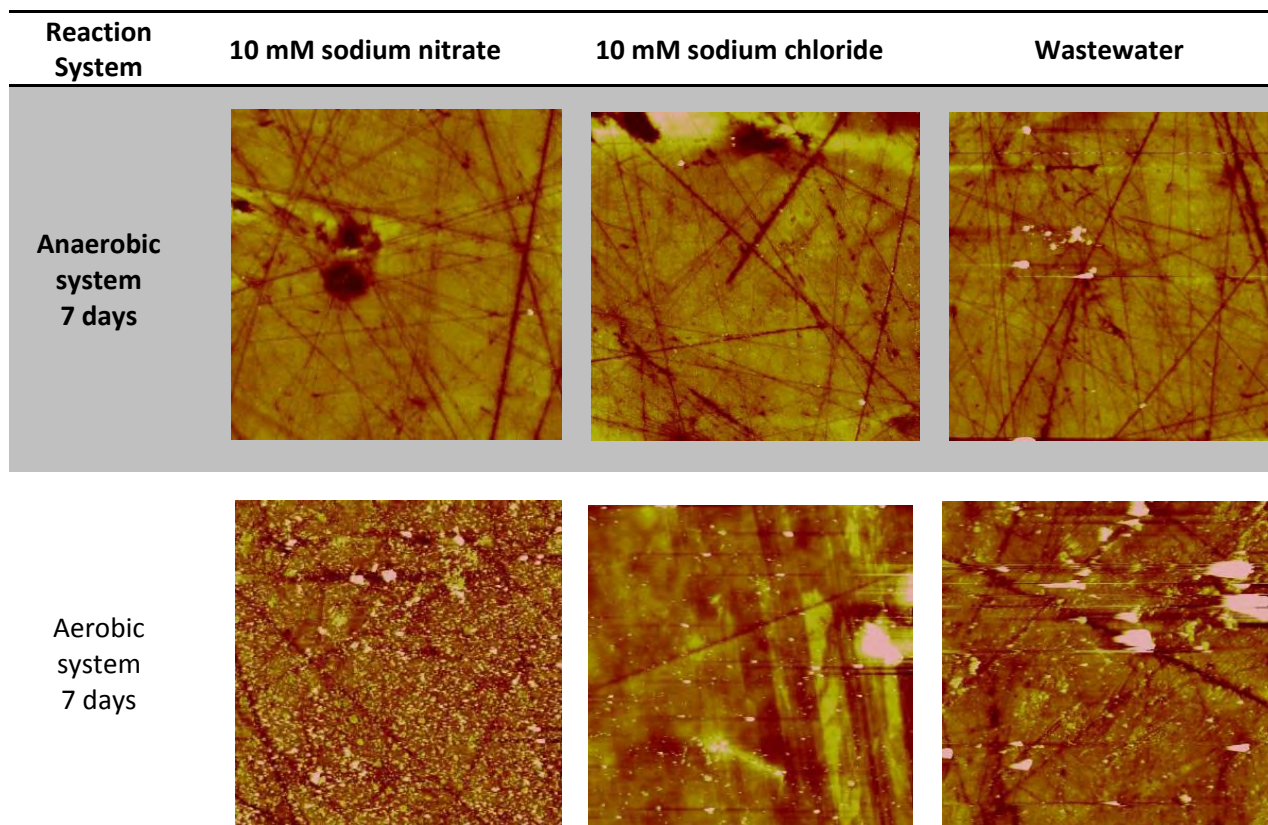
Figure A-6   Comparison between secondary mineral precipitation in the aerobic and anaerobic systems for 10 mM sodium nitrate and 10 mM sodium chloride. All systems were at pH 7.0 ± 0.2 and room temperature. Images are 20 × 20 μm and the height scale is 100 nm.

Secondary Mineral Phase Identification

Identification of secondary mineral phases in aerobic systems was accomplished using Raman spectroscopy. The characteristic spectra for different iron oxide minerals were determined by measuring standard samples on the Raman instrument (Figure A-7). For the anaerobic system, there was no precipitation in the AFM image. Neither was detectable by Raman spectroscopy.

Early in the reaction period (<1 day), there was no detectable secondary mineral precipitation on the surface for any system. In the sodium nitrate system, the characteristic peaks of maghemite (γ-Fe_2O_3), an iron(III) oxide polymorph, become detectable after 1 day of reaction (Figure A-7 B). By 7 days, the entire coupon surface in the sodium nitrate system is coated in maghemite (Figure A-7 A). For the sodium chloride system, no precipitation was detected after 1 day. After 7 days, however, the surface was covered in a non-homogeneous coating of hematite (α-Fe_2O_3) and maghemite (Figure A-7 D). The visual difference between these two mineral phases is apparent on the arsenopyrite surface (Figure A-7 C). For the wastewater system, there was no detectable precipitation over the 7-day reaction period. 6-line ferrihydrite, magnetite, and goethite standards were also considered, but the spectra did not match the reacted samples.

4.3 Water Matrix Effects on Arsenic Remobilization

Nitrate and Chloride Effects on Secondary Mineral Phase Transformation

Hematite is the most thermodynamically stable iron oxide polymorph and is the final form resulting from the transformation of less stable iron(III) (hydr)oxides (Jang et al., 2007). The occurrence of hematite in the sodium chloride system and not the sodium nitrate system after 7-days reaction time was confirmed by multiple replicates. The faster transformation of iron(III) (hydr)oxides in the presence of sodium chloride compared to sodium nitrate is a new interesting observation, and can greatly impact arsenic remobilization from arsenopyrite.

Previous research conducted into the effects of chloride and nitrate on heterogeneous and homogeneous iron(III) (hydr)oxide nucleation and growth provides insight into this phenomenon (Hu et al., 2012). Using time-resolved small angle x-ray scattering (SAXS) and grazing-incidence SAXS, Hu et al. (2012) observed that in the presence of chloride ions, Ostwald ripening was the dominant process controlling heterogeneous precipitation, whereas continuous nucleation, growth, and aggregation occurred in the nitrate system. Ostwald ripening describes the growth mechanism wherein smaller precipitates dissolve and
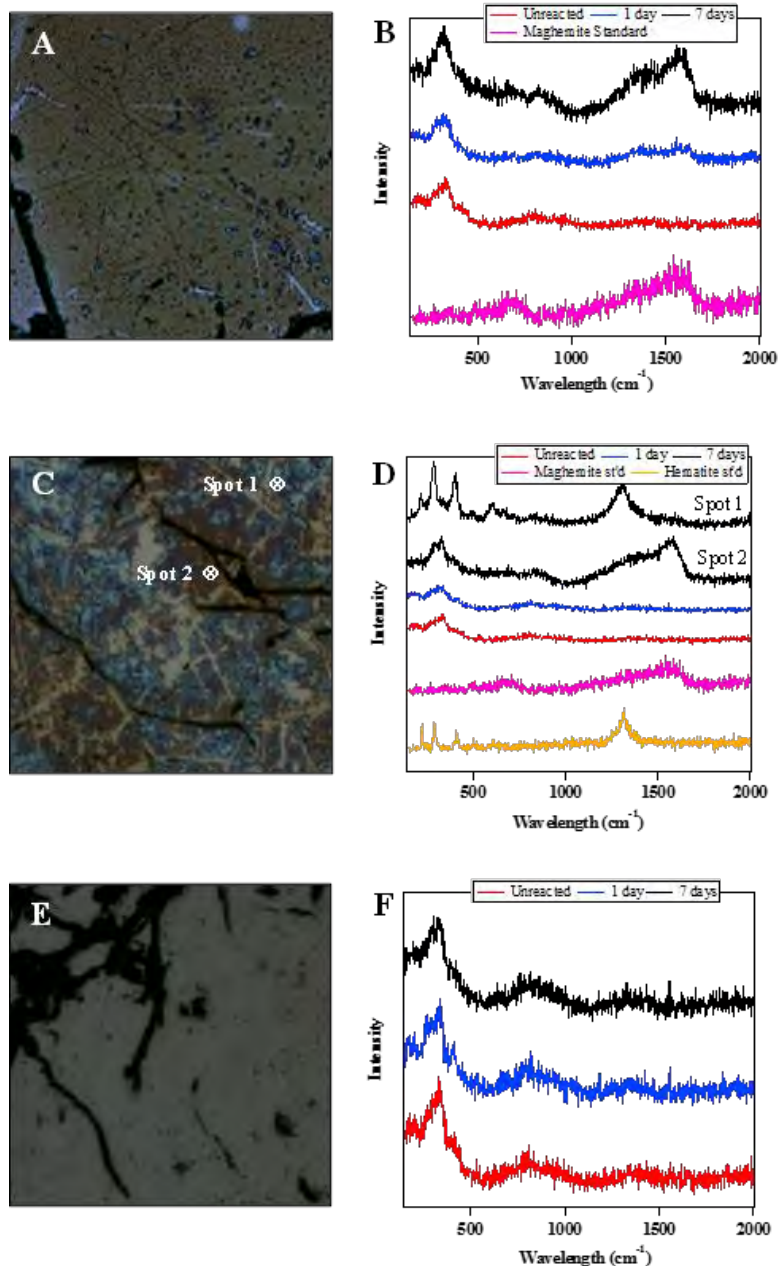
Figure A-7 Optical microscope images and Raman spectra for arsenopyrite coupons reacted in sodium nitrate (A, B), sodium chloride (C, D), and wastewater (E, F) systems. Optical microscope images for the 7-day sodium nitrate system (A) shows a uniform coating of maghemite, as indicated by the characteristic Raman peaks (B). For the sodium chloride system, after 7 days, the surface was covered in a non-homogeneous coating (C) of hematite (α-Fe2O3) and maghemite (D). No precipitation was observed in the wastewater system (E, F).

redeposit on the surface of larger precipitates, resulting in an increase in particle size while the total number of particles decreases. Ostwald ripening is a spontaneous process; the formation of larger particles with smaller surface-to-volume ratios is more stable and energetically favorable. These reported differences in the iron(III) (hydr)oxide growth mechanisms are observable in AFM images of arsenopyrite coupons after 1 and 7 days reaction time(Figure A-4). In the sodium nitrate system, small particles are always visible on the surface in addition to larger aggregates, indicating continued nucleation, growth, and aggregation. In the sodium chloride system, larger particles are visible after just 1 day. The difference in morphology is even more obvious after 7 days, with the formation of a uniform iron(III) (hydr)oxide coating. There is a lack of smaller precipitates in both the 1- and 7-day samples, indicating that primary particles may have gone through Ostwald ripening processes.

The prevalence of Ostwald ripening as a growth mechanism can also explain the faster phase transformation observed in the sodium chloride system. Ostwald ripening usually occurs in the late stages of first-order phase transformations (Slezov, 2009). During Ostwald ripening, metastable Fe^{3+}(hydr)oxide nanoparticles are dissolving and recrystallizing on the surface of larger particles to minimize surface free energies. The larger particles formed through Ostwald ripening will tend to be more thermodynamically stable than their nanoscale precursors, resulting in the phase transformation of less stable Fe^{3+} (hydr)oxide polymorphs such as ferrihydrite into more stable forms, such as maghemite and, eventually, hematite (Dubinina and Lakshtanov, 1997; Liu and Zeng, 2005).

This phenomenon will have secondary effects on arsenic motilities in the sodium nitrate and sodium chloride systems. Increased iron(III) (hydr)oxide nucleation in the sodium nitrate system leads to a large number of smaller particles. The high cumulative surface area of these precipitates can lead to more available surface sites for the sorption of aqueous arsenic anions, resulting in lower arsenic concentrations. This mechanism is consistent with observations of arsenic remobilization from arsenopyrite in the sodium nitrate system as compared to sodium chloride. With increased reaction time, iron(III) (hydr)oxide undergoes aging processes to form maghemite in the sodium nitrate system and a mixture of maghemite and hematite in the sodium chloride system. Hematite, due to its increased crystallinity, has less sorption capacity for arsenic than maghemite (Park et al., 2009). However, it is important to note that the transformation of iron(III) (hydr)oxides into more stable iron(III) oxide polymorphs can lead to the irreversible sorption of associated arsenic anions. Therefore, although these systems will have less capacity for arsenic sorption, the arsenic attenuated by the iron(III) (hydr)oxides in early stages will become strongly bound within the iron(III) oxide matrix (Peterson and Burkert, 2008). This inferred trapping mechanism can be beneficial for the long term fate and transport of arsenic in oxic or hypoxic groundwater systems where ferric iron minerals are stable.

Inhibited Secondary Mineral Precipitation in the Wastewater System

Interestingly, this research observed no precipitation in the system containing wastewater in comparison to both the sodium nitrate and sodium chloride systems. Currently, there are no studies which have reported on this apparent inhibition of Fe^{3+}(hydr)oxide precipitation. Nonetheless, studies which model arsenic remobilization during ASR operations have assumed the formation of ferrihydrite as an attenuation mechanism during arsenic transport in ASR (Willis et al., 2010).

This possibility was further examined by monitoring the reduction–oxidation potential (ORP) and pH over the 7-day reaction period for the wastewater, sodium nitrate, and sodium chloride aqueous solutions. ORP is a measure of the tendency of the solution to gain or lose electrons. A positive redox potential indicates oxidizing conditions, meaning that the aqueous solution is more likely to gain electrons from arsenopyrite, thereby becoming reduced while arsenopyrite is oxidized. Evolution trends in pH and ORP can be found in Figure A-8.
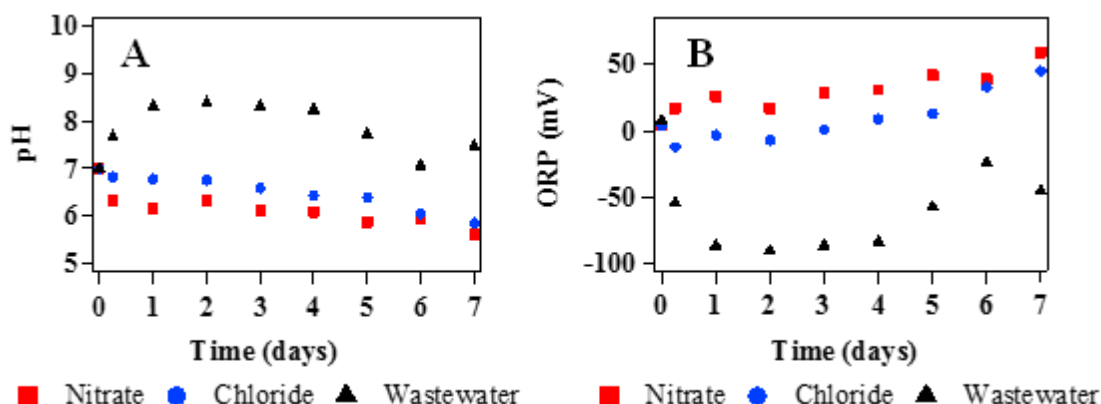
93

Figure A-8   Evolutions of pH and ORP in batch reactors over the 7-day reaction period. The pH value was not adjusted over this time. All reactors were at room temperature (22°C) and open to the atmosphere (PO_2 = 0.21 atm).

For the 10 mM sodium nitrate and sodium chloride systems, similar evolutions were observed for pH and ORP measurements. pH decreased steadily over the 7-day period. This is likely due to the continuous oxidative dissolution of arsenopyrite through reaction Eq. 1, which produces arsenous acid. For the wastewater system, the pH fluctuated between 7.0 and 8.4 over the reaction period. It is likely that the wastewater effluent from the Cincinnati Milk Creek treatment plant contains a multitude of buffering agents, such as bicarbonate ions, in addition to the metal ions. Dewettinck et al (2001) examined the buffering role of the wastewater constituents. These buffering agents may prevent decreases in pH. At a lower pH, increased arsenic remobilization would occur due to proton-promoted dissolution. Higher iron concentrations would result in higher saturation indices with regards to iron(III) (hydr)oxide precipitates. However, the higher pH in the wastewater should also contribute to higher saturation indices due to the increased hydroxide ion concentration (reaction Eq.2). Because water chemistry effects on iron(III) (hydr)oxide saturation indices are contradictory, additional factors may be contributing to the inhibited precipitation for wastewater.

The ORP values provide further insight into precipitation trends. The ORP increased over the 7-day period and was generally positive for the sodium nitrate and sodium chloride systems. In contrast, the ORP in the wastewater system fluctuated but always remained negative over the reaction period. The formation of iron(III) (hydr)oxides is contingent on the oxidation of Fe^{2+}, released through reaction eq. 1, to Fe^{3+}. The negative redox potential in the wastewater system indicates that the condition is a reducing environment for arsenopyrite. This could prevent the oxidation of Fe^{2+} and precipitation of iron(III) (hydr)oxides, a process consistent with experimental observations.

The lower ORP conditions in the wastewater system are prevalent in reclaimed wastewater. In secondary wastewater treatment, low ORP conditions are necessary to facilitate biological denitrification and phosphorus removal processes. These redox reactions are fed by the addition of dissolved organic carbon (DOC) serving as the electron donor. Although much of the DOC present in wastewater is removed prior to effluent discharge and reuse, the DOC levels can still be elevated when compared to groundwater concentrations. In the experimental investigation reported here, the wastewater samples had a non-purgeable TOC concentration of 12.42 mg/L, while concentrations in the two model systems were negligible. This factor may be the root of observed differences in precipitation, as the presence of DOC would prevent the oxidation of Fe^{2+}. However, uncertainty exists making it necessary to quantify the

94

effects of organic TOC on both arsenic remobilization from arsenopyrite and its correlation with heterogeneous and homogeneous iron(III) (hydr)oxide nucleation and growth.

5. Manage Aquifer Conditions for Reduced Arsenic Remobilization

5.1. The hydrogeological factor

In the preceding sections, the literature review and experimental investigations strongly suggest that multiple environmental factors can facilitate arsenic remobilization into groundwater, and at the same time, precipitate dissolved arsenic from the groundwater. Chemical and biologically enhanced arsenic remobilization in aquifers can occur only under specific groundwater conditions, high or low oxidation-reduction potential, dissolved oxygen presence, and low pH, as discussed in preceding sections (e.g. Table 2). The extent to which these environmental conditions evolve within a timeframe and location, depends on the geochemical compatibility of injected water and the hosting aquifer, abiotic and biotic processes that change the pH and redox conditions, and the water injection process. The resulting environmental changes also evolve in response to the local and regional groundwater flow pattern. These factors are generally location-specific and application-dependent, as potential groundwater changes can enable arsenic remobilization through the arsenic remobilization and reduction reactions in Table A-2.

Geochemical and hydrological flow simulations have been reported for a number of ASR sites (Stamos et al., 2001; Pavelic et al., 2006; Grovea and Wood, 1979; Lawrence and Upchurch, 1982; Powelson et al., 1993; Sharif et al., 2008). Literature review and analysis points to the linkage of groundwater flow regimes and the potential changes in groundwater, soil matrix, and the injected water, to the changes in groundwater chemistry, and consequently arsenic remobilization. One principal change occurring during ASR is that the injection-induced radial groundwater flow generates groundwater zoning, stratification and hence changes in pH-Eh conditions. Other major factors are the water injection and withdrawal cycle, producing groundwater table fluctuations that result in interchange of the air-filled vadose zone and upper groundwater layer.

At an ASR site, injection-withdraw or recharging operations lead to local changes in natural groundwater flow, and consequently the mixing and reactions of oxygenated injection water with native groundwater. Localized elevation of the water table, known as groundwater mounding, has been observed since 1961 as a consequence of lateral permeability restrictions to the dissipation of hydraulic head at injection facilities (Bouwer, 2002; Todd, 1961). The occurrence of groundwater stagnancy in a "bubble" and "bottle brush" of reclaimed water (Figure A-9), which form due to a lack of mixing between the injected water and groundwater, varies significantly as a result of aquifer heterogeneity, preferential flow pathways, leakage and buoyancy, and soil chemical makeups (Lowry and Anderson, 2006; Vacher et al., 2006; Clark et al., 2004). These subsurface aquifer properties contribute to variations in the water injection rate and areal extent, and can thus influence many environmental factors controlling arsenic mobility on local and micro-scales. This explains the large spatial and temporal changes often found in groundwater arsenic concentrations (Hoque et al., 2009;). In a macro-scale, however, the "bubble" and "bottle brush" concept in the ASR process (Figure A-9) prescribes two major types of macro-scale physical boundaries and geochemical domains. In these areas, the injected water interacts with native groundwater and aquifer formation (Vacher et al., 2006). Figure A-9 generalizes the ASR process and resulting mixing-replacement phenomenon – limited mixing of injected water and ambient groundwater at the perimeter and displacement of the native groundwater forming a hydraulic and geochemical bubble.

This generalization agrees with the geochemical and hydrological studies showing that zoned flow fields marked by ages and fractions of injected water prevail in the injection "bubble" as it spreads toward undisturbed aquifers (Clark et al., 2004; Ma and Spalding, 1996; Brown and Misut, 2010). On the other hand, the geochemical conditions can vary significantly at an ASR site depending upon the degree of aquifer anisotropicity, thermal and density difference between injected water and native groundwater,

and the convective flow in the frontier of the "bubble" during injection and recovery phases. These factors affect both the ASR recovery rate, and the conditions of soil-water reactions (Pavelic et al., 2006; Lowry and Anderson, 2006; Ward et al., 2008, 2007; Langevin, 2008; Minsley et al., 2011).

The macro-scale "bubble" or "bottle brush" formation coupled with micro-scale soil-water interactions sets up the basis to investigate the soil-water interactions in Table A-2 for safer and more sustainable ASR planning, design and operations. It must be noted that the spatial zoning of environmental conditions is not

Figure A-9.   ASR Bubble formation during secondary water injection

static, but subject to vertical groundwater fluctuations. ASR operations can change local groundwater flows. The injection-pumping cycles affect hydraulic communication with surface water bodies. Groundwater fluctuation introduce both oxygen and labile organic matter to shallower aquifer zones (generally <150 m), leading to the increased mobilization of arsenic in these zones as compared to deeper aquifers (Ahmed et al., 2004). The widespread pumping from these deeper aquifer strata for irrigation or other uses are found to have introduced vertical communication of frequently arsenic-contaminated shallow groundwater and have consequently eradicated deep aquifers as a arsenic-free water resource (Burgess et al., 2010).

Therefore, the vertical distribution of arsenic requires attention for investigation at ASR sites. The trend can be site specific and the causes vary. Yu et al. (2003) reported decreased arsenic concentrations with increased depth in aquifers in Bangladesh, Harvey et al. (2006) studied the geochemical profile of the Ganges Delta in South Asia. They found a maximum in arsenic concentration at 30 m depth, and hypothesized that is was correlated to the zone where older water mixes with younger, recharge water. Kinniburgh et al. (2003) and McArthur et al. (2004) observed similar bell-shaped arsenic depth profiles in their sites in Bangladesh and West Bengal, respectively. Decreased arsenic concentrations at very shallow depths (<15 m) may be due to arsenic adsorption or co-precipitation with insoluble ferrosoferric hydroxides (Kim et al., 2002).

Seasonal fluctuations in groundwater levels may also impact arsenic mobility even during non-pumping conditions and thus add complexity in characterization and mitigation. Such an impact in the Ganges Delta region was studied by Harvey et al. (2006). They observed that for the months of June through November, a uniformly elevated water table caused by heavy rainfall warranted a small groundwater gradient. After the raining season, groundwater discharge into the river and groundwater pumping during the spring for irrigation led to increased groundwater flow and a lower groundwater table. This cycle of groundwater recharge and discharge could provide a pathway for arsenic mobilizers, such as organic carbon or oxidants, to enter the aquifer. Seasonal temperature variation can also impact the reduction-oxidation potential within the groundwater (Greskowiak et al., 2006). Warmer temperatures during the summer lead to increased microbial activity, subsequently decreasing dissolved oxygen and nitrate levels and leading to a reductive potential, while during the winter, decreased microbial activity
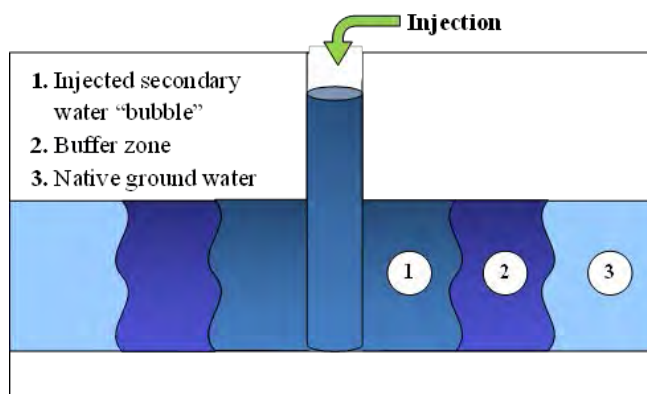
leads to increased dissolved oxygen, and a more oxidizing potential. Harvey et al. (2006) attributed these hydrological changes as the cause for observed variation of groundwater arsenic concentrations.

Additionally, the wetting and drying history of an aquifer formation can significantly affect its infiltration rate and thus the time of water residence in the vadose zone and upper groundwater layer. This occurs because frequent wetting and drying cycles lead to soil hydrophobicity. Arye et al.(2011) observed this process at an ASR site in Tel-Aviv, Israel, where reclaimed water was recharged through the use of an infiltration basin, increasing the number of wetting and drying cycles. Due to the sorption of hydrophobic substances in the reclaimed water, the soil became hydrophobic leading to the retardation of reclaimed water in the vadose zone and top soil. Hydrophobic soil also tends to sequestering organic carbon, which may be beneficial in mitigating arsenic mobilization (Spaccini et al., 2002).

5.2 The chemistry factors and geochemical processes

The experimental studies, along with the literature reviewed, indicate several geochemical conditions in control of arsenic mobility and remobilization into groundwater. Redox condition is one of the primary factors. The redox cycling of iron in the Earth's subsurface regulates the fate and transport of many elements of concern. Anthropogenic processes such as ASR can have a drastic effect on the redox potential of groundwater environments, triggering the oxidative dissolution of reduced iron minerals including arsenopyrite. In reaching a geochemical steady-state condition, arsenic released from the remobilization into groundwater is counter-balanced in attenuation processes. These include the precipitation of iron-oxyhydroxides including ferrihydrite with strong arsenic sorption capacity, and the precipitation of arsenic-containing minerals.

Formation of Iron-oxyhydroxides

As discussed in preceding sections, the breakdown of iron oxyhydroxides leads to arsenic remobilization and the formation of these iron oxyhydroxide minerals also contribute to arsenic attenuation in aquifers. The dissolution of arsenopyrite produces an abundance of aqueous iron, resulting in supersaturation with respect to a number of different iron oxyhydroxides or oxide minerals. The association of arsenic with iron oxyhydroxides or oxide minerals is well documented (McGuire et al., 2001; Dixit and Hering, 2003; Nickson et al., 1998; Bowell, 1994; Kneebone et al., 2002; Raven et al., 1998; Richmond et al., 2004; Cances et al., 2005; and references therein). Cances et al. (2005) found that of the total arsenic present in arsenic-contaminated soil samples, less than 10% was readily mobilized, 10-37% was sorbed, and more than 65% was associated with iron oxyhydroxides. This arsenic occurred primarily as As^{+5}, with very small proportions (~7%) of As^{+3}, as would be expected due to the chemical and structural affinity of these minerals to sorb As^{+5} preferentially over As^{+3}.

Dixit and Hering (2003) examined how changes in arsenic speciation impact their sorption behavior onto amorphous ferrihydrite and goethite. For arsenate, it was found that the maximum sorption density was much higher for ferrihydrite compared to the other minerals, which may be related to the amorphous structure of ferrihydrite having a higher surface area. However, the capability of ferrihydrite to sorb arsenic is extremely pH and oxidation state dependent. For example, at pH=10, goethite sorbed more arsenate than ferrihydrite. For arsenite, goethite sorbed more than ferrihydrite at both high and low concentrations. However, these results seem to conflict with previous studies which have reported decreased adsorption capacities for aged ferrihydrite, which is expected to contain some goethite, up to pH 9.129 Additional experiments showed if the water contains high levels of phosphates, As(III) will be

preferentially sorbed rather than As(V), because the phosphates will compete for As(V) sorption sites (Dixit et al., 2003).

Ferrihydrite is only thermodynamically stable at nanoscales (Navrotsky et al., 2008). Over time, it will undergo phase changes and can ultimately become one of a number of iron oxide polymorphs. Dissolution and reprecipitation of ferrihydrite in aqueous systems result in the formation of goethite, and eventually hematite, the most thermodynamically favorable bulk mineral. This characteristic results in the unique capability of ferrihydrite to irreversibly immobilize contaminants which are adsorbed during phase transformation. However, once ferrihydrite transforms into goethite or hematite, which both have crystalline structures, the adsorptive capability of the iron oxides for foreign ions decreases under circumneutral pH conditions due to the decrease in reactive surface adsorption sites (Dixit and Hering, 2003).

Arsenic-sulfide precipitation

In addition to arsenic association with iron oxyhydroxides, aqueous arsenic ions may become more permanently incorporated into aquifer minerals through the precipitation of arsenic sulfides, including orpiment and realgar (Cances et al., 2005, 2008; O'Day, 2006). This reaction will only occur in arsenic-impacted aquifer under reductive conditions, as oxidative conditions would lead to the formation of sulfate as opposed to sulfide. Acidic conditions within the aquifer, leading to a pH<4, can also trigger the transformation of arsenopyrite to realgar or orpiment (Craw et al., 2003). Furthermore, arseniosiderite $(CaFe_3(AsO_4)_3O_3 \cdot 3H_2O)$ can be formed as an oxidation product of realgar and orpiment, as well as arsenopyrite; this mineral is soluble and will not provide mitigation comparable to its precursor. Arsenic-containing minerals formed under reducing conditions where arsenic concentration was within μM level, exceeding the solubility of secondary mineral phases (O'Day et al., 2004). Arsenic precipitated from solution as realgar (As_4S_4) when sulfur concentrations were low compared to iron or orpiment (As_2S_3) when sulfur concentrations were high compared to iron. However, there was no evidence of coprecipitation of arsenic with iron-sulfide minerals. When arsenic concentrations were low, the solubility of these minerals was not exceeded and the only arsenic sequestration occurred through weak adsorption processes. Under reducing conditions, this adsorption occurred on FeS or pyrite, while under slightly reducing conditions this would occur on a variety of Fe(II, III) oxides or hydroxides. This process was not a stable means of sequestering aqueous arsenic as compared to the precipitation of arsenic-containing minerals. The importance of H_2S concentration is also noted for its role in the Fe-As-S geochemical interactions. An abundance of H_2S would increase FeS precipitation, thus creating competition for the sulfur needed for As_4S_4 or As_2S_3 formation.

Kirk et al. (2004) proposed that arsenic sulfide precipitated resulting in decreased arsenic concentrations following sulfate reduction in unconsolidated glacial aquifers. On the other hand, Zhu et al. (2008) introduced similar conditions to a sedimentary rock aquifer containing pyritic black shale and found that sulfate reduction enhanced arsenic mobilization, possibly through sulfide-arsenide exchange. Therefore, aquifer mineralogy in ASR sites is a key factor which can dictate sulfide mineral formation. Notably, ferric ions released from these minerals will form iron(III) (hydr)oxide minerals, attenuating mobilized arsenic. Groundwater and secondary injected water chemistry can greatly impact the mechanism and overall potential for concurrent arsenic sorption or co-precipitation. This investigation showed that the presence of high concentrations of chloride ions will inhibit the continued nucleation of iron(III) (hydr)oxides. In addition, the promotion of Ostwald ripening could lead to the faster phase transformation of iron(III) (hydr)oxides to maghemite and subsequently, after 7 days, to hematite. As a result, the arsenic mobility is higher in systems which contain sodium chloride rather than sodium nitrate. Lastly, it was determined that the presence of wastewater inhibits iron(III) (hydr)oxide precipitation due to a decreased ORP for this system.

5.3 Pretreatment and monitoring for enhanced reliability

The nano- to micro-scale processes controlling arsenic fate and transport have implications for ASR planning, design and operation, in order to reduce ASR environmental impact. There are no established arsenic control guidelines for the implementation of ASR design, in part due to inadequate knowledge of the soil-water interactions and controlling factors (Asano and Cotruvo, 2004). These observations on geochemical pathways in the As-Fe-S-Cl-N system have implications for the longer term fate and transport of arsenic in groundwater aquifers and should be considered when managing arsenic contamination at ASR sites. Major geochemical inferences include:

- Arsenic mobilization in groundwater is balanced between the oxidative breakdown of host minerals such as arsenopyrite and the precipitation of iron oxides and iron oxyhydroxide. The latter promotes co-precipitation or sorption of soluble arsenic in groundwater.

- Arsenic associated with stable iron oxide minerals will be trapped as long as the aqueous environment is favorable for Fe(III) (e.g., oxidative environments). High TOC content in injected water can enhance biological activities creating local reductive conditions, potentially leading to the destabilization of arsenic tapped in iron oxides or preventing arsenopyrite oxidation.

- Activation energies for arsenic mobilization in aerobic and anaerobic systems containing sodium nitrate, sodium chloride, and wastewater samples were experimentally determined. Differences in activation energies between the systems indicate that the mechanisms controlling arsenopyrite dissolution and the propensity for arsenic mobilization can vary with dissolved oxygen presence.

These considerations are the basis for developing ASR monitoring programs, modeling arsenic fate and transport, and developing pretreatment requirements for injected water. Pretreatment is often a necessary part of ASR systems (See Figure 1 in the main text). There is currently limited knowledge on how water pretreatment and water withdrawal affect arsenic mobilization. This investigation on arsenopyrite-water interactions has revealed the observations below:

- The difference in water chemistry (pH, Eh, ORP, etc.) between the injected water and native groundwater is the cause of arsenic remobilization in groundwater. Thus, pretreatment of injected water can minimize adverse geochemical reactions by reducing this difference.

- Several geochemical pathways are involved in the dissolution and precipitation of arsenic-bearing iron oxyhydroxides, and thus the arsenic mobility. The processes are facilitated by the presence of DOM, chloride ions, nitrate, sulphur and oxidants (or ORP) under a given pH-Eh condition. On the other hand, high Fe^{3+} concentrations in groundwater can lead to iron oxyhydroxide precipitation and enhanced arsenic encapsulation.

- Biological activities enhanced by DOM can lead to local environmental conditions that promote reductive iron oxide or iron oxyhydroxide dissolution.

- Injection-withdrawal operation and groundwater cycling can change the environmental conditions in the ASR formation, thus affecting the arsenic mobility. Predictive modeling of groundwater hydrology during ASR operation can help when monitoring ASR and developing injected water pretreatment requirements.

6. References

Ahmed, K. M., P. Bhattacharya, M. A. Hasan, S. H. Akhter, S. M. M. Alam, M. A. H. Bhuyian, M. B. Imam, A. A. Khan and O. Sracek, (2004). Ahmed, K. M., P. Bhattacharya, M. A. Hasan, S. H. Akhter, S. M. M. Alam, M. A. H. Bhuyian, M. B. Imam, A. A. Khan and O. Sracek, (2004). Applied Geochemistry, 2004, 19, 181-200. *Applied Geochemistry*, 2004, 19, 181-200.

Appelo, C. A. J., M. J. J. Van Der Weiden, C. Tournassat and L. Charlet, (2002). Surface complexation of ferrous iron and carbonate on ferrihydrite and the mobilization of arsenic. E*nvironmental Science & Technology*, 2002, 36, 3096-3103.

Arye, G., J. Tarchitzky and Y. Chen, (2011). Treated Wastewater Effects on Water Repellency and Soil Hydraulic Properties of Soil Aquifer Treatment Infiltration Basins. *Journal of Hydrology*, 397, 136-145.

Asano, T., and Cotruvo, J. A., (2004). Groundwater recharge with reclaimed municipal wastewater: health and regulatory considerations. *Water Research,* 2004**,** *38*, (8), 1941-1951.

Asta, M. P., J. Cama, C. Ayora, P. Acero, and G. de Giudici, (2010). Arsenopyrite dissolution rates in O_2-bearing solutions. *Chemical Geology*, **273**, 272-285.

Bahr, J., T. Grundl, G. Harrington, J. Krohelski, and M. Werner, (2002). *A review of aquifer storage recovery techniques*. Wisconsin Department of Natural Resources, 40p.

Blanchard, M., M. Alfredsson, J. Brodholt, K. Wright and C. Catlow, (2007). Arsenic incorporation into FeS_2 pyrite and its influence on dissolution: A DFT study. *Geochimica et Cosmochimica Acta*, 71, 624-630.

Bowell, R. J., (1994). Arsenic sorption by Iron oxy- hydroxides and oxides. *Applied Geochemistry*, 9, 279-286.

Bouwer, H., (2002). Artificial recharge of groundwater: hydrogeology and engineering. *Hydrogeology Journal*, 10, 121-142

Brostigen, G., and A. Kjekshus, (1970). Compounds with the Marcasite Type Crystal Structure. V. The Crystal Structures of FeS_2, $FeTe_2$, and $CoTe_2$. A*cta Chem Scandinavica*, 24, 1925-1940

Brown, C. J., K. Hatfield, M. Newman, (2006). Lessons learned from a review of 50 ASR projects from the United States, England, Australia, India, and Africa increasing freshwater supplies. In: P*roceedings of the 2006 UCOWR/NIWR Annual Conference*, Santa Fe, New Mexico, USA.

Brown, C. J., and P. E. Misut, (2010). Aquifer geochemistry at potential aquifer storage and recovery sites in coastal plain aquifers in the New York City area, USA. *Applied Geochemistry*, 25, 1431-1452.

Buckley, A. N., and G. W. Walker, (1988). The surface composition of arsenopyrite exposed to oxidizing environments. *Applied Surface Science*, **35**, 227-240.

Burgess, W. G., M.A. Hoque, H.A. Michael, C.I. Voss, G.N. Breit, and K.M. Ahmed, (2010). Vulnerability of deep groundwater in the Bengal Aquifer System to contamination by arsenic. *Nature Geoscience*, 3, 83-87.

Busbee, M.W., B.D. Kocar, S.G. Benner, (2009). Irrigation produces elevated arsenic in the underlying groundwater of a semi-arid basin in Southwestern Idaho. *Applied Geochemistry* 24, 843-859

Cances, B., F. Juillot , G. Morin , V. Laperche , L. Alvarez, O. Proux, J-L Hazemann , G. E. Brown Jr. , and G. Calas, (2005). XAS evidence of As(V) association with iron oxyhydroxides in a

contaminated soil at a former arsenical pesticide processing plant.. *Environmental Science & Technology*, 39, 7

Cances, B., F. Juillot, G. Morin, V. Laperche, D. Polya, D. J. Vaughan, J. L. Hazemann, O. Proux, G. E. Brown, Jr. and G. Calas, (2008). Changes in arsenic speciation through a contaminated soil profile: A XAS based study. *Environmental Science & Technology*, 397, 178-189.

Cheng, H.; Hu, Y.; Luo, J.; Xu, B.; Zhao, J., (2009). Geochemical processes controlling fate and transport of arsenic in acid mine drainage (AMD) and natural systems. *Journal of Hazardous Materials*, 165(1-3), 13-26.

Clark, J. F., G. B. Hudson, M. L. Davisson, G. Woodside and R. Herndon, (2004). Geochemical imaging of flow near an artificial recharge facility, Orange County, California. *Ground Water*, 42, 167-174.

Corkhill, C. L., and D. J. Vaughan, (2009). Arsenopyrite oxidation – A review. *Applied Geochemistry*, 24, 2342-2361.

Craw, D., D. Falconer, and J.H. Youngson, (2003). Environmental arsenopyrite stability and dissolution: theory, experiment, and field observations. *Chemical Geology*, **199**, 71-82.

Dewettinck, T.; Van Hege, K.; Verstraete, W., Development of a rapid pH-based biosensor to monitor and control the hygienic quality of reclaimed domestic wastewater. *Applied Microbiology and Biotechnology*, 56, (5-6), 809-815.

Dixit, S., and J. G. Hering, (2003). Comparison of Arsenic(V) and Arsenic(III) sorption onto iron oxide minerals: Implications for arsenic mobility. *Environmental Science & Technology*, **37**(18), 4182-4189.

Dubinina, E. O.; Lakshtanov, L. Z., (1997). A kinetic model of isotopic exchange in dissolution-precipitation processes. *Geochimica et Cosmochimica Acta*, 61, (11), 2265-2273.

Erbs, J. J.; Berquó, T. S.; Reinsch, B. C.; Lowry, G. V.; Banerjee, S. K.; Penn, R. L., (2010). Reductive dissolution of arsenic-bearing ferrihydrite. *Geochimica et Cosmochimica Acta,* 74(12), 3382-3395.

Fendorf, S, H. A. Michael and A. van Geen, (2010). Spatial and temporal variations of groundwater arsenic in South and Southeast Asia. *Science*, 328, 1123-1127.

Goldberg, S., and C. T. Johnston, (2001). Mechanisms of Arsenic Adsorption on Amorphous Oxides Evaluated Using Macroscopic Measurements, Vibrational Spectroscopy, and Surface Complexation Modeling. **Journal of Colloid and Interface Science**, 234, 204-216.

Gonzalez, Z, A., M. Krachler, A. K. Cheburkin, and W. Shotyk, (2006). Spatial Distribution of Natural Enrichments of Arsenic, Selenium, and Uranium in a Minerotrophic Peatland, Gola di Lago, Canton Ticino, Switzerland. *Environmental Science & Technology*, 2006, 40, 6568-6574.

Greskowiak, J., H. Prommer, G. Massmann and G. Nützmann, (2006). Modeling seasonal redox dynamics and the corresponding fate of the pharmaceutical residue phenazone during artificial recharge of groundwater. **Environmental Science & Technology**, 40, 6615-6621.

Grafe, M., M. J. Eick, P. R. Grossl, and A. M. Saunders, (2002). Adsorption of arsenate and arsenite on ferrihydrite in the presence and absence of dissolved organic carbon. *Journal of Environmental Quality*, 2002, 31, 1115-1123.

Grovea, D. B., and W. W. Wood, (1979). Prediction and Field Verification of Subsurface-Water Quality Changes During Artificial Recharge, Lubbock, Texas. *Ground Water,* 17, 250-257.

Guo, X., and F. Chen, (2005). Removal of arsenic by bead cellulose loaded with iron oxyhydroxide from groundwater. *Environmental Science & Technology*, 39 (17), 6808-6818.

Guo, H., S. Yang, X. Tang, Y. Li and Z. Shen, (2008). Groundwater geochemistry and its implications for arsenic mobilization in shallow aquifers of the Hetao Basin, Inner Mongolia. *Science of The Total Environment*, 393, 131-144.

Handley, K. M., M. Héry, and J. R. Lloyd, (2009). Redox cycling of arsenic by the hydrothermal marine bacterium *Marinobacter santoriniensis*. *Environmental Microbiology*, 11, 1601-1611.

Harvey, C. F., C. H. Swartz, A. B. M. Badruzzaman, N. Keon-Blute, W. Yu, M. A. Ali, J. Jay, R. Beckie, V. Niedan, D., P. M. O. Brabander, K. N. Ashfaque, S. Islam, H. F. Hemond, and M. F. Ahmed, (2002). Arsenic mobility and groundwater extraction in Bangladesh. *Science*, 298, 1602-1606.

Harvey, C. F., K. N. Ashfaque, W. Yu, A. B. M. Badruzzaman, M. A. Ali, P. M. Oates, H. A. Michael, R. B. Neumann, R. Beckie, S. Islam and M. F. Ahmed, (2006). Groundwater dynamics and arsenic contamination in Bangladesh. *Chemical Geology*, 228, 112-136.

Heinrich, C. A., and P.J., Eadington, (1986). Thermodynamic predictions of the hydrothermal chemistry of arsenic, and their significance for the paragenetic sequence of some cassiterite-arsenopyrite-base metal sulfide deposits. *Economic Geology*, **81**, 511-529.

Hoque, M, A. Khan, M. Shamsudduha, M. Hossain, T. Islam and S. Chowdhury, (2009). Near surface lithology and spatial variation of arsenic in the shallow groundwater: southeastern Bangladesh. *Environmental Geology*, 2009, 56, 1687-1695.

Hu, Y.; Lee, B.; Bell, C.; Jun, Y.-S., (2012). Environmentally Abundant Anions Influence the Nucleation, Growth, Ostwald Ripening, and Aggregation of Hydrous Fe(III) Oxides. *Langmuir*, 28(20), 7737-7746.

Ilyaletdinov, A., and SA Abdrashitova, (1981). Autotrophc oxidation of arsenic by *Pseudomonas arsenitoxidants*. *Mikrobiologiya*, 50, 197-205.

Islam, F. S., A. G. Gault, C. Boothman, D. A. Polya, J. M. Charnock; D. Chatterjee, and J. R. Lloyd, (2004). Role of metal-reducing bacteria in arsenic release from Bengal delta sediments. *Nature*, 430, 68-71.

Jain, A., and R. H. Loeppert, (2000). Effect of competing anions on the adsorption of arsenate and arsenite by ferrihydrite. *J. Environ. Qual.*, **29**, 1422-1430.

Jang, J.-H.; Dempsey, B. A.; Burgos, W. D., (2007). A model-based evaluation of sorptive reactivities of hydrous ferric oxide and hematite for U (VI). *Environmental Science & Technology*, 41(12), 4305-4310.

Jørgensen, B. B., (1983). The microbial sulphur cycle. *In* W.E. Krumbein ed., *Microbial Geochemistry,* Blackwell Scientific, Oxford, pp. 91-124.

Jones, G. W., and T. Pichler, (2007). The Relationship between Pyrite Stability and Arsenic Mobility During Aquifer Storage and Recovery in Southwest Central Florida. *Environmental Science & Technology*, **41**(3), 723-730.

Jones, R. A., S. F. Koval, and H. W. Nesbitt, (2003). Surface alteration of arsenophyrite (FeAsS) by *Thiobacillus ferrooxidans*. Geochimica et Cosmochimica Acta, 2003, 67, 955-965.

Jonsson, J., and D. M. Sherman, (2008). Sorption of As(III) and As(V) to siderite, greenrust (fougerite) and magnetite: Implications for arsenic release in anoxic groundwaters. *Chemical Geology*, 255, 173-181

Kneebone, P. E., P. A. O'Day, N. Jones and J. G. Hering, (2002). Deposition and fate of arsenic in iron- and arsenic-enriched reservoir sediments. *Environmental Science & Technology*, 36, 381-386.

Kim, M.-J., J. Nriagu and S. Haack, (2002). Arsenic species and chemistry in groundwater of southeast Michigan. *Environmental Pollution*, 120, 379-390.

Kinniburgh, D., P. Smedley, J. Davies, C. Milne, I. Gaus, J. Trafford, S. Burden, S. Ihtishamul Huq, N. Ahmad, K. Ahmed, A. H. Welch and K. G. Stollenwerk, (2003). The scale and causes of the ground-water arsenic problem in Bangladesh. In: Welch A, Stollenwerk KG, *edts. Arsenic in Ground Water: Geochemistry and Occurrence*. New York: Springer; pp. 211–257.

Kirk, M. F., T. R. Holm, J. Park, Q. Jin, R. A. Sanford, B. W. Fouke and C. M. Bethke, (2004). Bacterial sulfate reduction limits natural arsenic contamination in groundwater. *Geology*, 32, 953-956.

Koslides, T., and V. S. T. Ciminelli, (1992). Pressure oxidation of arsenopyrite and pyrite in alkaline solutions. *Hydrometallurgy*, **30**, 87-106.

Langevin, C. D., (2008). Modeling axisymmetric flow and transport. Ground Water, 46, 579-590.

Lawrence, F. W., and S. B. Upchurch, (1982). Identification of recharge areas using geochemical factor analysis. *Ground Water*, 1982, 20, 680-687.

Liu, B.; Zeng, H. C., (2005). Symmetric and asymmetric Ostwald ripening in the fabrication of homogeneous core-shell semiconductors. *Small*, 1, (5), 566-571.

Lowry, C. S., and M. P. Anderson, (2006). An Assessment of Aquifer Storage Recovery Using ground Water Flow Models. *Ground Water*, 44, 661-667.

Ma, L., and R. F. Spalding, (1996). Stable isotope characterization of the impacts of artificial ground water recharge. *JAWRA*, 32, 1273-1282.

Mandal, B. K., and K. T. Suzuki, (2002). Arsenic round the world: a review. *Talanta*, 58, 201-235.

Modesto Lopez, L. B.; Pasteris, J. D.; Biswas, P., Sensitivity of micro-Raman spectrum to crystallite size of electrospray-deposited and post-annealed films of iron-oxide nanoparticle suspensions. *Applied Spectroscopy*, 63(6), 627-635.

McArthur, J. M., P. Ravenscroft, S. Safiulla, and M. F. Thirlwall, (2001). Arsenic in groundwater: testing pollution mechanisms for aquifers in Bangladesh. *Water Resources Research*, **37**, 109-117.

McArthur, J. M., D. M. Banerjee, K. A. Hudson-Edwards, R. Mishra, R. Purohit, P. Ravenscroft, A. Cronin, R. J. Howarth, A. Chatterjee, T. Talukder, D. Lowry, S. Houghton and D. K. Chadha, (2004). Natural organic matter in sedimentary basins and its relation to arsenic in anoxic ground water: the example of West Bengal and its worldwide implications. *Applied Geochemistry*, 19, 1255-1293.

McGuire, M. M., K. J. Edwards, J. F. Banfield, and R. J. Hamers, (2001). Kinetics, surface chemistry, and structural evolution of microbially mediated sulfide mineral dissolution. *Geochimica et Cosmochimica Acta*, **65**, 1243-1258.

McKibben, M.; Tallant, B.; Del Angel, J., (**2008**). Kinetics of inorganic arsenopyrite oxidation in acidic aqueous solutions. *Applied Geochemistry*, **23**, (2), 121-135.

McNab Jr, W. W., M. J. Singleton, J. E. Moran and B. K. Esser, (2009). Ion exchange and trace element surface complexation reactions associated with applied recharge of low-TDS water in the San Joaquin Valley, California. *Applied Geochemistry*, 24, 129-137.

Miller, D. M., and G. S. Hansford, (1992). Batch biooxidation of a gold-bearing pyrite-arsenopyrite concentrate. *Minerals Engineering*, **5**, 613-629.

Minsley, B.J., J.B. Ajo-Franklin, A. Mukhopadhyay, and F.D. Morgan, (2011). Hydrogeophysical methods for analyzing aquifer storage and recovery systems. *Ground Water*, 49(2), 250-269.

Modesto Lopez, L. B.; Pasteris, J. D.; Biswas, P., Sensitivity of micro-Raman spectrum to crystallite size of electrospray-deposited and post-annealed films of iron-oxide nanoparticle suspensions. *Applied Spectroscopy*, 63(6), 627-635.

Navrotsky, A., L. Mazeina and J. Majzlan, (2008). Size-driven structural and thermodynamic complexity in iron oxides. *Science*, 319, 1635-1638.

Neil C., Yang YJ, Schupp D, Jun Y-S, (2014). Water chemistry impacts on arsenic mobilization from arsenopyrite dissolution and secondary mineral precipitation: Implication for managed aquifer recharge. *Environmental Science & Technology*, 48(8), 4395-4405.

Neil, C.W., Y.J. Yang, and Y-S. Jun, (2012). A critical review of the potential impact of managed aquifer recharge on mineral-water interactions responsible for arsenic mobilization in groundwater. *J. Environ. Monit.*, 14: 1772-1788.

Nesbitt, H. W., I. J. Muir and A. R. Prarr, (1995). Oxidation of arsenopyrite by air and air-saturated, distilled water, and implications for mechanism of oxidation. *Geochimica et Cosmochimica Acta*, 59, 1773-1786.

Nickson, R., J. McArthur, W. Burgess, K. M. Ahmed, P. Ravenscroft and M. Rahmann, (1998). Arsenic poisoning of Bangladesh groundwater. *Nature*, 395, 338-338.

Nimick, D. A., (1998). Arsenic Hydrogeochemistry in an Irrigated River Valley—A Reevaluation. *Ground Water*, 36, 743-753.

O'Day, P.A., D. Vlassopoulos, R. Root, and N. Rivera, (2004). The influence of sulfur and iron on dissolved arsenic concentrations in the shallow subsurface under changing redox conditions. *PNAS*, 101, 13703-13708.

O'Day, P. A., (2006). Chemistry and mineralogy of arsenic. *Elements*, 2, 77-83.

Oremland, R. S., and John F. Stolz, (2003). The ecology of arsenic. *Science*, 300, 939-944.

Overacre, R., T. Clinton, D. Pyne, S. Snyder and P. Dillon, (2006). Reclaimed water aquifer storage and recovery: Potential changes in water quality. *Proceedings of the Water Environment Federation*, 2006, 1339-1360.

Papangelakis, V. G., and G. P. Demopoulos, (1990). Acid pressure oxidation of arsenopyrite: Part II, reaction kinetics. *Canadian Metallurgical Quarterly*, **29**, 13-20.

Park, H.; Myung, N. V.; Jung, H.; Choi, H., (2009). As (V) remediation using electrochemically synthesized maghemite nanoparticles. *Journal of Nanoparticle Research*, 11(8), 1981-1989.

Pavelic, P.; Nicholson, B. C.; Dillon, P. J.; Barry, K. E., (2005). Fate of disinfection by-products in groundwater during aquifer storage and recovery with reclaimed water. *Journal of contaminant hydrology*, 77(4), 351-373.

Pavelic, P., P. J. Dillon, and B. C. Nicholson, (2006). Comparative evaluation of the fate of disinfection byproducts at eight aquifer storage and recovery sites. **Environmental Science & Technology**, 40, 501-508.

Pavelic, P., P. J. Dillon and C. T. Simmons, (2006). Multiscale characterization of a heterogeneous aquifer using an ASR operation. *Ground Water*, 44, 155-164.

Pedersen, H. D.; Postma, D.; Jakobsen, R., (2006). Release of arsenic associated with the reduction and transformation of iron oxides. **Geochimica et Cosmochimica Acta**, 70(16), 4116-4129.

Peters, S. C., and L. Burkert, (2008). The occurrence and geochemistry of arsenic in groundwaters of the Newark basin of Pennsylvania. **Applied Geochemistry**, 23, 85-98.

Postma, D.; Larsen, F.; Minh Hue, N. T.; Duc, M. T.; Viet, P. H.; Nhan, P. Q.; Jessen, S. r., Arsenic in groundwater of the Red River floodplain, Vietnam: controlling geochemical processes and reactive transport modeling. *Geochimica et Cosmochimica Acta*, 71, (21), 5054-5071.

Powelson, D. K., C. P. Gerba and M. T. Yahya, (1993) Virus transport and removal in wastewater during aquifer recharge. *Water Research*, 27, 583-590.

Randall, S. R., D. M. Sherman and K. V. Ragnarsdottir, (2001). Sorption of As(V) on green rust $(Fe_4(II)Fe_2(III)(OH)_{12}SO_43HO)$ and lepidocrocite (γ-FeOOH): surface complexation by EXAFS spectroscopy. *Geochimica et Cosmochimica Acta*, **65**, 1015-1023.

Rau, I.; Gonzalo, A.; Valiente, M., (2003). Arsenic(V) adsorption by immobilized iron mediation. Modeling of the adsorption process and influence of interfering anions. *Reactive and Functional Polymers*, 54(1-3), 85-94.

Raven, K. P., A. Jain and R. H. Loeppert, (1998). Arsenite and arsenate adsorption on ferridydrite: Kinetics, equilibrium, and adsorption envelopes. *Environmental Science & Technology*, 32, 344-349.

Reich, M., and U. Becker, (2006). First-principles calculations of the thermodynamic mixing properties of arsenic incorporation into pyrite and marcasite. *Chemical Geology*, 225, 278-290

Richmond, W. R., M. Loan, J. Morton and G. M. Parkinson, (2004). Arsenic Removal from Aqueous Solution via Ferrihydrite Crystallization Control. Environmental Science & Technology, 38, 2368-2372.

Rimstidt, J. D., J. A. Chermak, and M. P. Gagen, (1993). Rates of reaction of Galena, Sphalerite, Chalcopyrite, and Arsenopyrite with Fe(III) in acidic solutions. In C. Alpers et al. edts., *Environmental Geochemistry of Sulfide Oxidation*, ACS Symposium Series, 550, 2-13.

Ruitenberg, R., G. S. Hansford, M. A. Reuter, and A. W. Breed, (1999). The ferric leaching kinetics of arsenopyrite. *Hydrometallurgy*, **52**, 37-53.

Sadiq, M., A. Locke, G. Spiers and D. Pearson, (2002). Geochemical Behavior of Arsenic in Kelly Lake, Ontario. *Water, Air, & Soil Pollution*, 141, 299-312.

Salzsauler, K. A., N. V. Sidenko, and B. L. Sherriff, (2005). Arsenic mobility in alternation products of sulfide-rich, arsenopyrite-bearing mine wastes, Snow Lake, Manitoba, Canada. *Applied Geochemistry*, 20, 2303-2314.

Schlieker, M., J. Sch€uring, J. Hencke and H. D. Schulz, (2001). The influence of redox processes on trace element mobility in a sandy aquifer-an experimental approach. *J. Geochem. Explor.*, 73, 167–179.

Sharif, M. U., R. K. Davis, K. F. Steele, B. Kim, T. M. Kresse and J. A. Fazio, (2008). Inverse geochemical modeling of groundwater evolution with emphasis on arsenic in the Mississippi River valley alluvial aquifer, Arkansas (USA). *Journal of Hydrology*, 350, 41-55.

Sheng, Z., (2005). An aquifer storage and recovery system with reclaimed wastewater to preserve native groundwater resources in El Paso, Texas. *Journal of environmental management*, 75(4), 367-377.

Sidhu, P.; Gilkes, R.; Cornell, R.; Posner, A.; Quirk, J., (1981). Dissolution of iron oxides and oxyhydroxides in hydrochloric and perchloric acids. *Clays and Clay Minerals*, 29(6), 269-276.

Simeoni, M. A., B. D. Batts and C. McRae, (2003). Effect of groundwater fulvic acid on the adsorption of arsenate by ferrihydrite and gibbsite. *Applied Geochemistry*, 18, 1507-1515.

Slezov, V. V., (2009).Theory of the late stages of nucleation–growth processes: Ostwald ripening. In: *Kinetics of First-Order Phase Transitions*, Wiley-VCH Verlag GmbH & Co. KGaA: pp 93-169.

Smedley, P., and D.G. Kinnburgh, (2002). A review of the source, behaviour and distribution of arsenic in natural waters. *Applied Geochemistry*, 17, 517-568

Spaccini, R., A. Piccolo, P. Conte, G. Haberhauer and M. H. Gerzabek, (2002). Increased soil organic carbon sequestration through hydrophobic protection by humic substances. *Soil Biology and Biochemistry*, 34, 1839-1851.

Stamos, C., P. Martin, T. Nishikawa, and B. F. Fox, (2001). Simulation of ground-water flow in the Mojave River basin, California: U.S. Geological Survey Water-Resources Investigations Report 01–4002, 129 p.

Stollenwerk, K. G., (2003). Geochemical processes controlling transport of arsenic in groundwater: A review of adsorption. *In*, A.H. Welch and K.G. Stollenwerk, edts., *Arsenic in Ground Water: Geochemistry and Occurrence*, pp.67-100. Springer, US.

Sverjensky, D. A., and K. Fukushi, (2006). A predictive model (ETLM) for As(III) adsorption and surface speciation on oxides consistent with spectroscopic data. *Geochimica et Cosmochimica Acta*, 70, 3778-3802.

Todd, D. T., (1961). The distribution of ground water beneath an artificial recharge area. *International Association of Scientific Hydrology*, 57, 254-262

Tufano, K., J., C. Reyes, C. W. Saltikov, and S. Fendorf, (2008). Reductive processes controlling arsenic retention: Revealing the relative importance of iron and arsenic reduction. *Environmental Science & Technology*, 42, 8283-8289.

Vacher, H. L., W. C. Hutchings and D. A. Budd, (2006). Metaphors and models: The ASR bubble in the Floridan aquifer. *Ground Water*, 44, 144-154.

Vanderzalm, J., Le Gal La Salle, C.; Dillon, P., (**2006**). Fate of organic matter during aquifer storage and recovery (ASR) of reclaimed water in a carbonate aquifer. *Applied Geochemistry*, *21*, (7), 1204-1215.

Vanderzalm, J. L., P. J. Dillon, K. E. Barry, K. Miotlinski, J. K. Kirby and C. Le Gal La Salle, (2011). Arsenic mobility and impact on recovered water quality during aquifer storage and recovery using reclaimed water in a carbonate aquifer. *Applied Geochemistry*, 26, 1946-1955.

Verplanck, P. L., S. H. Mueller, R. J. Goldfarb, D. K. Nordstrom and E. K. Youcha, (2008), Geochemical controls of elevated arsenic concentrations in groundwater, Ester Dome, Fairbanks district, Alaska. *Chemical Geology*, 255(1-2), 160-172.

Violante, A., and M. Pigna, (2002). Competitive sorption of arsenate and phosphate on different clay minerals and soils. *Soil Sci. Soc. Am. J.*, 2002, **66**, 1788-1796.

Walker, F. P., M. E. Schreiber and J. D. Rimstidt, (2006). Kinetics of arsenopyrite oxidative dissolution by oxygen. *Geochimica et Cosmochimica Acta*, **70**, 1668-1676.

Wallis, I., H. Prommer, C. T. Simmons, V. Post, and P. J. Stuyfzand, (2010). Evaluation of conceptual and numerical models for arsenic mobilization and attenuation during managed aquifer recharge. **Environmental Science & Technology**, 44, 5035-5041.

Wallis, I., H. Prommer, T. Pichler, V. Post, S. B. Norton, M. D. Annable, and C. T. Simmons, (2011). Process-based reactive transport model to quantify arsenic mobility during aquifer storage and recovery of potable water. **Environmental Science & Technology**, 45, 6924-6931.

Wang, S., and Mulligan, C. N., (2006). Natural attenuation processes for remediation of arsenic contaminated soils and groundwater. *Journal of Hazardous Materials*, 138, (3), 459-470.

Ward, J. D., C. T. Simmons and P. J. Dillon, (2008). Variable-density modelling of multiple-cycle aquifer storage and recovery (ASR): importance of anisotropy and layered heterogeneity in brackish aquifers. *Journal of Hydrology*, 356, 93-105.

Ward, J.D., C.T. Simmons, and P.J. Dillon, (2007). A theoretical analysis of mixed convection in aquifer storage and recovery: how important are density effects? *Journal of Hydrology,* 343 (3–4), 169–186

Waychunas, G. A., Y.-S. Jun, P. J. Eng, S. K. Ghose, T. P. Trainor, O. B. Mark and B. K. Douglas, (2008). Anion sorption topology on hematite: comparison of arsenate and silicate. In, *Developments in Earth and Environmental Sciences*, 7, 31-65.

Wilson, L.; Amy, G.; Gerba, C.; Gordon, H.; Johnson, B.; Miller, J., (1995). Water quality changes during soil aquifer treatment of tertiary effluent. *Water Environment Research,* 67(3), 371-376.

Wolf, M., A. Kappler, J. Jiang, and R. U. Meckenstock, (2009). Effects of humic substances and quinones at low concentrations on ferrihydrite reduction by Geobacter metallireducens. *Environmental Science & Technology*, **43**, 5679-5685.

Youngran, J.; FAN, M.; Van Leeuwen, J.; Belczyk, J. F., Effect of competing solutes on arsenic (V) adsorption using iron and aluminum oxides. *Journal of Environmental Sciences*, 19, (8), 910-919.

Yu, W. H., C. M. Harvey, and C. F. Harvey, (2003), Arsenic in groundwater in Bangladesh: A geostatistical and epidemiological framework for evaluating health effects and potential remedies, *Water Resour. Res.*, 39(6), 1146, doi:10.1029/2002WR001327

Yu, Y.; Zhu, Y.; Gao, Z.; Gammons, C. H.; Li, D., (2007). Rates of Arsenopyrite Oxidation by Oxygen and Fe (III) at pH 1.8-12.6 and 15-45 C. *Environmental Science & Technology*, 41, (18), 6460-6464.

Yu, Y.; Zhu, Y., Williams-Jones, A.E., Gao, Z., Li, D., (2004). A kinetic study of the oxidation of arsenopyrite in acidic solutions: implications for the environment. *Applied Geochemistry*, 19(3), 435–444

Zheng, Y., M. Stute, A. van Geen, I. Gavrieli, R. Dhar, H. J. Simpson, P. Schlosser and K. M. Ahmed, (2004). Redox control of arsenic mobilization in Bangladesh groundwater. *Applied Geochemistry*, 19, 201-214.

Zhu, W., L. Y. Young, N. Yee, M. Serfes, E. D. Rhine and J. R. Reinfelder, (2008). Sulfide-driven arsenic mobilization from arsenopyrite and black shale pyrite. *Geochimica et Cosmochimica Acta,* 72, 5243-5250.